

FLUID SHEAR STRESS MODULATION OF EMBRYONIC STEM CELL DIFFERENTIATION

A Dissertation
Presented to
The Academic Faculty

by

Barbara A. Nsiah

In Partial Fulfillment
of the Requirements for the Degree
Doctor of Philosophy in Bioengineering in the
George W. Woodruff School of Mechanical Engineering

Georgia Institute of Technology
May 2012

FLUID SHEAR STRESS MODULATION OF EMBRYONIC STEM CELL DIFFERENTIATION

Approved by:

Dr. Todd C. McDevitt, Advisor
School of Biomedical Engineering
Georgia Institute of Technology

Dr. Robert M. Nerem
School of Mechanical Engineering
Georgia Institute of Technology

Dr. Manu O. Platt
School of Biomedical Engineering
Georgia Institute of Technology

Dr. Evan A. Zamir
School of Mechanical Engineering
Georgia Institute of Technology

Dr. Rudolph L. Gleason
School of Mechanical Engineering
Georgia Institute of Technology

Date Approved: December 13, 2011

ACKNOWLEDGMENTS

My journey through completing the Ph.D. has been met with many joyful times as well as many challenging times and through it all I had many people supporting me and pushing me. Without them I definitely would not have made it to the end and for that I am forever grateful.

I would like to thank my committee members for the mentorship, guidance, support----Dr. Todd McDevitt, Dr. Robert Nerem, Dr. Manu Platt, Dr. Rudy Gleason, and Dr. Evan Zamir. Dr. Evan Zamir's insight and expertise of developmental mechanics were very useful as well as his thought provoking scientific questions. Dr. Rudy Gleason's optimistic attitude has helped me to stay positive about my research and my results. Additionally, he has provided a great example for work life balance while having a career in academia. Dr. Manu Platt's critical questioning of my experimental design and data analysis has helped me to become a better researcher. Additionally, he has been a great mentor in helping me navigate career options after graduate school. Each committee member has been invaluable through completion of my project and for that I thank all of you.

When I initially started in the Bioengineering program I only had one advisor, Dr. Robert "Bob" Nerem, but after being here for 2 years I was fortunate enough to gain a second advisor, Dr. Todd McDevitt. Todd and

Bob have been very supportive and patient during the Ph.D. process. While Bob and Todd have contrasting advising styles, having them as advisors meant double the encouragement, support, resources, and meetings. My meetings with Todd I would hear statements such as “power through” or “I don’t doubt you can get it done” while with Bob he would usually say “my friend,” “can you get those slides to me” or “do you think you have enough time to get that done”. Between Todd’s sometimes overly optimistic attitude and Bob’s realistic optimism I have found myself somewhere in the middle, with both perspectives being necessary to get through my Ph.D. As a member of both labs I was fortunate to have two sets of resources. There were numerous times in which if I couldn’t find a reagent in the McDevitt lab I would quickly run to the Nerem lab and find what I needed and vice versa. I am thankful to the both of them for always believing in my abilities, encouraging and pushing me throughout my time here.

During my time in the Nerem lab I have had a lot of support and mentorship from senior grad students and post docs including Dr. Ann Ensley, Dr. JoSette Broiles, Dr. Stacey Schutte, Dr. Adele Doyle, Dr. Randy Ankeny, Dr. Sarah Griffiths, and Dr. Lisa McGinley. Dr. Taby Ahsan, a former post doc, provided me with invaluable guidance as a scientist and was instrumental in getting my project off the ground in its initial stages.

Even after she began her professorship at Tulane she was still open to meet with me to discuss my research during my visit to New Orleans. Casey Holliday Ankeny and I have been the youngest students in the Nerem lab since we started in fall of 2006 to now being the only grad students. She has been a great support and we have managed to do many things together including winning NSF fellowships, both being co-advised, defending our theses 5 days apart, and finally finishing our Ph.D's at the same time. We have pushed each other to ensure we both get through grad school. Julia Raykin has been very helpful throughout my time here, ranging from help with mechanics homework, matlab coding, a million quals practices, listening to my proposal presentation 3 times, setting up and washing more than 30 shear chambers, and proofreading. She also helped me have fun outside the lab with many dinner outings.

When Todd became my co-advisor, I quickly became a new member of the McDevitt lab and spent more time there than in the Nerem lab. While I was apprehensive initially, the McDevitt lab members welcomed me with open arms which made the transition a lot easier. During that time there were quite a few students---Dr. Rekha Nair, Dr. Carolyn Sargent, Dr. Rich Carpenedo, Dr. Alyssa Ngangan, Andres Bratt-Leal, and Ken Sutha. Everybody was willing to help me learn new techniques and clue me in on

Todd's expectations and advising style. The members of this lab made coming to lab and performing experiments day in and day out fun and provided constant laughter. This group of people definitely helped improve my work ethic and rigor as a researcher. Rekha the first of the McDevitt lab members to complete her Ph.D. was a great role model in showing me that with persistence and hard work I could complete my Ph.D. Carolyn was a great resource and very helpful when I first came to the McDevitt lab. She was also the resident fitness instructor in the lab which helped me get back into working out. Rich was always the person I could count on in lab meetings to critically question my experiments and objective of my project which was well needed in the early stages of my work. Alyssa Ngangan aka "Libation Queen," helped to make lab fun with her loud infectious laugh. Because she was a year ahead of me I always looked to her papers, proposal, and thesis as examples for my own work. Andres and Ken who are the same year as me have been great motivators. We have kept each other on track through reaching milestones to completing the Ph.D. We have generally done things in sort of a domino effect, I proposed and then Ken and Andres proposed. Andres defended and then within 2-3 months Ken and I will be defending. Andres was instrumental in the completion my VEGF studies as he provided me with microparticles. He has been great comic relief in the

lab with his antics, pranks, and eating abilities. Ken always has a smile on his face and always has a positive outlook. Not to mention I admire his undertaking of both an M.D. and Ph.D. degree.

A couple of years after I joined the lab we finally got a new student, Melissa Kinney. From the minute she joined the lab she fit in perfectly. She quickly joined in the usual McDevitt lab Friday happy hours and crossword challenges. Additionally, we soon had post docs come into the fold with Dr. Priya Baraniak being the first, then Dr. Ankur Singh and Dr. Krista Fridley. Priya has given great advice and mentorship on how to transition from a grad student to a post doc all while getting married and having two kids yet still keeping a smile on her face. Ankur has been very helpful with flow cytometry analysis and reminding me that I was almost done when writing my dissertation. Krista has been great at lending an ear during my frustrations about finishing up my last experiments and writing my dissertation. Between fall 2010 and fall 2011 a “large” wave of new students have joined the lab----Jenna Wilson, Anh Nquyen, Doug White, Denise Sullivan, Josh Zimmerman, Melissa Goude, and Marian Hettiaratchi. They have brought a young and vibrant perspective to the lab as they start their Ph.D. process and remind me of how far I have come in my journey to completing my Ph.D.

In the Nerem and McDevitt lab, the lab managers Steve Woodard, Marissa Cooke, and Jesse McClellan have been instrumental in ensuring I have all the materials and reagents I need to complete my experiments. Without them I would not have been able to complete my experiments in a timely manner. Each of them were always willing to do whatever it took to ensure that I had everything I needed to finish my project and for that I am very grateful.

The support staff in IBB and the ME department have been integral in ensuring that the important details got taken care of. Andrew Shaw and Aqua Asberry provided lots of help with confocal imaging and histology, respectively. Kathy Huggins kept me in touch with Dr. Nerem during his busy travels. She as well as Glenda Johnson ensured that necessary paperwork was completed. Chris Ruffin has always had his door open to answer any questions and help with paperwork for the Bioengineering program.

I have been fortunate enough to be a part of the FACES Fellows Program here at Georgia Tech. This program has provided me with numerous mentors such as Dr. Gary May, Dr. Tequilla Harris, Dr. Mitchell Walker, and Dr. Manu Platt. Through this program I have received a number of opportunities in career development especially with perspective

to preparation for potentially becoming a professor. The program has provided me with financial support for conferences and a network of fellow Ph.D. students who have served as role models. The FACES program has been integral in my completion of my Ph.D. and I am grateful that I was awarded the opportunity to participate.

My family, dad-Robert, mom-Adelaide, and brother-Rob have been constant supports while at Georgia Tech. My parents would call to check up on me and tell me to keep up the work and that they were proud of me, in addition to reminding me that I am almost done even when I was 2 to 3 years from finishing. They have instilled in me the work ethic needed to complete my Ph.D. My brother was good at letting me know that I had been in school for a long time and providing me with comical stories of his adventures in college to ease my stresses as a grad student.

TABLE OF CONTENTS

	Page
ACKNOWLEDGEMENTS	iii
LIST OF TABLES	xv
LIST OF FIGURES	xvi
LIST OF SYMBOLS AND ABBREVIATIONS	xviii
SUMMARY	xx
<u>CHAPTER</u>	
1 INTRODUCTION	1
2 BACKGROUND	5
Stem Cells	5
Embryonic Stem Cells	5
Embryonic Stem Cells and Vascular Cell Differentiation	6
Endothelial and Hematopoietic Cell Development	7
Fluid Shear Stress	8
Fluid Shear Stress and Embryonic Stem Cells	8
Fluid Shear Stress and Vascular Progenitor Cells	9
Vascular Endothelial Growth Factor	10
Vascular Endothelial Growth Factor and Development	11
Vascular Endothelial Growth Factor and Endothelial Differentiation	11
Hypoxia	12
Hypoxia Inducible Factors	12
Hypoxia and Vascular Development	13
Hypoxia and Stem Cells	14

Tissue Engineering	15
Modular Tissue Engineering	16
Pre-Vascularization of Tissue Engineered Products	16
3 GENERAL METHODS	19
ESC and EB Culture	19
Fluid Shear Stress Pre-conditioning	19
qRT-PCR	20
Whole-Mount Immunostaining of Embryoid Bodies	22
Flow Cytometry Analysis	22
Statistical Analysis	23
4 FLUID SHEAR STRESS PRE-CONDITIONING EFFECTS ON EMBRYONIC STEM CELL EMBRYOID BODY DIFFERENTIATION	24
Introduction	24
Methods	27
Histology	27
Immunofluorescence of Cell Monolayers	27
Morphometric Image Analysis	28
Cell Tracker Labeling-Mixing Study	28
Results	30
Fluid Shear Stress Effects on ESC Differentiation	30
Embryoid Body Differentiation	33
Endothelial and Hematopoietic Gene Expression	36
Embryoid Body Endothelial Protein Expression	39
Mixed Embryoid Bodies	42
Fluid Shear Pre-conditioning of pVE-cadherin GFP ESCs	44
Fluid Shear Stress Magnitude Effects on ESCs	48

	VE-cadherin Localization	53
	Embryoid Body Endothelial Gene Expression	55
	Discussion	57
	Conclusion	62
5	VEGF EFFECTS ON ENDOTHELIAL DIFFERENTIATION OF FLUID SHEAR STRESS PRE-CONDITIONED EMBRYONIC STEM CELLS	63
	Introduction	63
	Methods	65
	ESC and EB Culture	65
	Gelatin Microparticles Fabrication and VEGF Loading	65
	Immunostaining of Cryosectioned EBs	66
	Results	
	Embryoid Body Morphology	68
	Endothelial Gene Expression	72
	EB VE-cadherin Expression and Localization	75
	pVE-cadherin GFP ESCs Embryoid Body Morphology	79
	VE-cadherin Localization in pVE-cadherin GFP Embryoid Bodies	81
	GFP Expression Analysis of Single Cells from pVE-cadherin EBs	83
	Discussion	86
	Conclusion	90
6	HYPOXIA EFFECTS ON VASCULOGENESIS OF FLUID SHEAR STRESS PRE-CONDITIONED EMBRYONIC STEM CELLS	92
	Introduction	92
	Methods	94
	ESC and EB Culture	95
	LIVE/DEAD Cell Viability Assay	95

Total Protein Quantification Assays	95
VEGF Quantity Protein Analysis	96
SDS PAGE and Western Blotting	96
Results	98
Embryoid Body Morphology	98
Endothelial Gene Expression	100
VE-cadherin Protein Expression	102
Hypoxia Inducible Factor A Expression	104
VEGFA Gene and Protein Expression	106
VE-cadherin GFP Embryoid Bodies	108
Discussion	111
Conclusion	114
7 FUTURE CONSIDERATIONS	115
APPENDIX A: EMBRYOID BODIES FORMED FROM EMBRYONIC STEM CELLS CULTURED ON DIFFERENT MATRICES	123
APPENDIX B: E-CADHERIN AND VE-CADHERIN EXPRESSION IN EMBRYOID BODIES FORMED FROM PRE-CONDITIONED EMBRYONIC STEM CELLS	126
APPENDIX C: VASCULAR ENDOTHELIAL GROWTH FACTOR RELEASE FROM GELATIN MICROPARTICLES	128
APPENDIX D: MONOLAYER AND EMBRYOID BODY DIFFERENTIATION OF FLUID SHEAR STRESS PRE-CONDITIONED EMBRYONIC STEM CELLS	129
REFERENCES	131

LIST OF TABLES

	Page
Table 3.1: Primer sequences and annealing temperatures	21

LIST OF FIGURES

	Page
Figure 4.1: Fluid promotes mesodermal endothelial and hematopoietic differentiation	32
Figure 4.2: Embryoid body morphology	35
Figure 4.3: Endothelial and Hematopoietic marker gene expression.	38
Figure 4.4: Fluid shear promotes EB VE-cadherin and vWF expression	41
Figure 4.5: EBs formed from static and shear pre-conditioned ESCs	43
Figure 4.6: Fluid shear stress pre-conditioned pVE-cadherin GFP ESCs	46
Figure 4.7: EBs formed from shear pre-conditioned pVE-cadherin GFP ESCs	47
Figure 4.8: Morphology and gene expression of pre-conditioned ESCs	49
Figure 4.9: Embryoid Body Morphology	52
Figure 4.10: VE-cadherin and PECAM expression	54
Figure 4.11: Embryoid body endothelial marker gene expression	56
Figure 5.1: Day 7 Embryoid Body Morphology	71
Figure 5.2: Endothelial marker gene expression of VEGF treated EBs	74
Figure 5.3: Confocal images of VE-cadherin protein expression in day 7 VEGF treated EBs	77
Figure 5.4: VE-cadherin Expression at the periphery of day 7 VEGF treated EBs	78
Figure 5.5: VEGF Treated EB formed from pre-conditioned VE-GFP ESCs	80
Figure 5.6: GFP Localization in pVE-cadherin GFP EBs	82
Figure 5.7: Single cell VE-cadherin expression in VEGF treated pVE-cadherin GFP EBs	85
Figure 6.1: Embryoid body differentiation under hypoxic conditions	99
Figure 6.2: Embryoid body endothelial marker gene expression under hypoxia	101
Figure 6.3: Embryoid body endothelial morphogenesis	103

Figure 6.4: Hypoxia Inducible Factor A gene and protein expression	105
Figure 6.5: Hypoxia modulates VEGF-A gene and protein expression	107
Figure 6.6: VE-cadherin expression in VE-GFP EBs cultured under hypoxia	110
Figure A1: EB Morphology and Endothelial Marker Gene Expression	125
Figure B1: Embryoid Body VE-cadherin and E-cadherin Expression	127
Figure C1: VEGF Release from Gelatin Microparticles	128
Figure D1: Monolayer and EB Differentiation of Pre-conditioned ESCs	130

LIST OF SYMBOLS AND ABBREVIATIONS

ESC	embryonic stem cell
EB	embryoid body
PC	pre-conditioned
VE-cadherin	vascular endothelial cadherin
VEGF	vascular endothelial growth factor
Flk-1	VEGF receptor 2
Flt-1	VEGF receptor 1
PECAM	Platelet-endothelial cell adhesion molecule
Pax6	Paired box gene 6
AFP	alpha fetaprotein
vWF	von Willebrand Factor
HIF1 α	hypoxia inducible factor A
GAPDH	Glyceraldehyde-3-phosphate dehydrogenase
SDS	Sodium Dodecyl Sulfate
PAGE	Polyacrylamide Gel Electrophoresis
VE-GFP	pVE-cadherin
qRT-PCR	Quantitative reverse-transcriptase polymerase chain reaction
MPs	microparticles
Tal1	T-cell acute lymphocytic leukemia protein 1
Runx1	runt related transcription factor
CD45	protein tyrosine phosphatase receptor type C
CD34	cluster of differentiation molecule 34

CD41

integrin-alpha-2b

SUMMARY

Blood vessels are the primary means by which blood is transported to the body. Blood carries oxygen and nutrients which are delivered to tissues in order to maintain tissue viability and homeostasis. Endothelial cells line the vessel wall and prevent blood clot formation. Neovascularization, formation of new blood vessels or vasculature, of tissue engineered substitutes is imperative for successful implantation into sites of injury. Strategies to promote vascularization within tissue engineered constructs have focused on 1) incorporating endothelial or endothelial progenitor cells within the construct and 2) treating the constructs with angiogenic factors such as VEGF or FGF. While these strategies have shown some improvement in vascularization of tissue engineered substitutes, some challenges still remain. Diffusion of soluble angiogenic factors becomes inhibited in tissue engineered constructs which have multiple cell layers and exceed 100 μm in thickness. Additionally, since endothelial (ECs) and endothelial progenitor cells EPC are adult cell types, acquiring quantities of cells needed for regenerative medicine applications is not feasible due to diminishing availability of endothelial sources in patient populations. Stem cells have been explored as a cell source for tissue engineered substitutes for a multitude of regenerative medicine therapies due to their inherent ability to differentiate into all somatic cell types. While stem cells can give rise to a number of cell types, such as ECs, methods to better control their differentiation need to be explored. Current EC differentiation strategies require laborious and extensive culture periods, utilize large quantities of growth factors and extracellular matrix, and generally yield heterogenous populations for which only small percentage of the differentiated cells are ECs. Initial strategies to derive endothelial cells from stem cells

focused on 2D cultured in the presence of prescribed extracellular matrices and growth factors. Differentiation in vivo occurs in a 3D microenvironment, which is in contrast to the 2D in vitro microenvironment used for 2D ESC EC differentiation strategies. In order to recapitulate 3D ESC differentiation in vivo 3D aggregates or embryoid bodies (EBs) have been employed in vitro. EBs can give rise to endoderm, endoderm, and mesoderm cell, including ECs. Additionally, EBs recapitulate aspects of embryogenesis, such as vasculogenesis and angiogenesis. Thus, the *objective* of this project was to examine the effects of pre-conditioning ESCs with fluid shear stress on EB endothelial differentiation and vasculogenesis. The overall *hypothesis* of this research is that exposing ESCs to in vivo vasculogenic cues will promote EB endothelial differentiation and vasculogenesis.

In the developing embryo fluid shear stress is an instructive cue for endothelial differentiation and vasculogenesis and has been explored as a means to differentiate ESCs into ECs. Fluid shear stress can be applied to ESCs in a homogeneous manner in comparison to the use of cytokines and growth factors to promote ESC differentiation. The application of fluid shear stress at different magnitudes and profiles promotes stem cells to differentiate to ECs and hematopoietic cells. While the acute effects of fluid shear stress on ESC-EC differentiation are well characterized, the extended effects of fluid shear stress on ESC-EC differentiation are unknown. To examine the effects of fluid shear stress on ESCs, shear pre-conditioned (0, 5, or 15 dyn/cm²) ESCs were differentiated as EBs and then analyzed for endothelial and hematopoietic genes throughout EB differentiation. Additionally, expression of endothelial and hematopoietic proteins and changes in EB morphology were investigated. Endothelial gene expression

analysis displayed differences in endothelial gene expression profile in EBs formed from shear pre-conditioned ESCs and EBs formed from statically cultured ESCs. Most notably, EBs formed from shear pre-conditioned ESCs developed a homogeneous morphology which was significantly different from the morphology observed in EBs formed from statically cultured ESCs. Moreover, EBs formed from shear pre-conditioned ESCs developed a central cluster of endothelial-like cells which expressed VE-cadherin and were observed throughout EB differentiation. Presence of endothelial-like cells within EBs formed from ESCs pre-conditioned with shear could be detected by centrally located dark regions observed through phase microscopy. Overall, the results suggest that shear pre-conditioning ESCs prior to EB formation affected the organization and localization of endothelial-like cells within EBs and yielded populations of EBs which contained endothelial-like cells.

During embryogenesis VEGF is important for endothelial differentiation, vasculogenesis, and angiogenesis. This angiogenic factor stimulates proliferation and migration of cells expressing VEGF receptors. Because of its importance in endothelial specification *in vivo*, VEGF has been consistently used to promote ESC EC differentiation. Thus, in order to modulate differentiation and expansion of the endothelial-like clusters in EBs formed from shear pre-conditioned ESCs, EBs were treated with VEGF. VEGF was delivered to EBs solubly or via release from microparticles. Diffusion of growth factors into the EB microenvironment is limited due to tight cell junctions on the outer layer of the EB. Therefore, microparticles which released VEGF were incorporated within the EB microenvironment to circumvent diffusion limitations. Soluble VEGF treatment of EBs formed from shear pre-

conditioned ESCs yielded EBs which were smaller in size in comparison to similar EBs which were not treated with VEGF. Moreover, VEGF soluble treatment induced endothelial-like cells to localize to the outer layer of EBs formed from shear pre-conditioned ESCs unlike untreated EBs which developed a cluster of endothelial-like cells at the center of EBs. Endothelial-like cells clustered at the center of the EBs even in the presence of microparticles. Endothelial marker gene expression analysis revealed significant increases in expression of *Flk-1*, *Flt-1*, *PECAM*, and *VE-cadherin* in shear pre-conditioned EBs treated with soluble VEGF compared to shear pre-conditioned EBs not treated with VEGF, indicating that pre-conditioning ESCs with shear prior to VEGF treatment promotes endothelial differentiation. Few differences in endothelial gene expression were detected between EBs treated with VEGF releasing microparticles and unloaded microparticles. VEGF treatment of EBs formed from ESCs cultured statically caused no change in EB endothelial marker gene expression. Altogether these results, demonstrated that preconditioning ESCs with fluid shear stress elicited unique endothelial differential profile in the presence of VEGF. Additionally, soluble treatment of VEGF elicited endothelial-like cells to organized on the outer layers of EBs..

Oxygen gradients during embryogenesis regulate patterning and development of the vasculature. Additionally, oxygen regulates endogenous production of angiogenic factors such as VEGF and transcription factor hypoxia inducible growth factors. Therefore, the effects of low oxygen on vasculogenesis within EBs formed from shear pre-conditioned ESCs were investigated. EBs formed from pre-conditioned ESCs were cultured for 7 days under normoxic (21% O₂) or under hypoxic (3% O₂) conditions. Hypoxia culture of EBs elicited different EB morphology compared to EBs cultured

under normoxia, but low oxygen did not have any adverse effects on cell viability as demonstrated by LIVE/Dead staining. Following 4 days of hypoxia culture EBs expressed similar levels of *Flk-1*, *Flt-1*, *VE-cadherin*, and *PECAM* compared to EBs cultured under normoxia. After 7 days of hypoxia culture, endothelial marker genes were expressed at higher levels in all EB groups as compared to EBs cultured under normoxia. At day 7, endothelial-like cells in shear pre-conditioned EBs cultured under hypoxia organized into primitive vascular networks. VEGF-A EB production results demonstrated that shear pre-conditioned EBs cultured under hypoxia produced the largest quantity of VEGF-A as compared to EBs cultured under normoxia as well as hypoxia EBs formed from statically cultured ESCs. Gene expression analysis hypoxia inducible factor-1 α (HIF1 α), a transcription factor regulated by oxygen levels, revealed no drastic changes in EB expression, however by day 7, HIF1 α was expressed at similarly low levels in hypoxia EBs formed from statically cultured ESCs and hypoxia EBs formed from shear pre-conditioned EBs. These studies demonstrated that hypoxia modulated EB endothelial differentiation, vasculogenesis, and angiogenic factor production. Moreover, shear pre-conditioning ESCs prior to EB formation in conjunction with hypoxia may be a method to promote and control vasculogenesis within EBs.

In conclusion, this work has developed a method to pre-vascularize pluripotent stem cell aggregates which could be used for a multitude of tissue engineered substitutes for regenerative medicine applications. A pluripotent stem cell aggregate which has primitive vasculature surrounded by cells which can be differentiated into cardiomyocytes, osteocytes, or beta-islets is an ideal template for developing cardiac, bone, or pancreatic tissues respectively. Furthermore, these studies have revealed that

priming ESCs with fluid shear stress prior to EB formation has subsequent effects on EB endothelial differentiation, endothelial cell-like organization and localization, angiogenic factor production, and vasculogenesis. Future work will continue to explore strategies to engineer pre-vascularized EBs into tissues resembling in vivo organs. Pre-vascularization of pluripotent stem cell aggregates have great utility in modular tissue engineering approaches for regenerative medicine applications.

CHAPTER 1

INTRODUCTION

Tissue engineered products have been developed for a multitude of diseases and injuries ranging from cardiovascular [1, 2], spinal [3], pancreatic [4], skin [5] and orthopedic [6]. Many advancements in the field of tissue engineering have been made, few tissue engineering products have been approved by the FDA [5, 7], however major challenges still exist in order to create more engineered tissues that translate into the clinic. One such challenge is vascularization of tissue engineered products, without proper vascularization tissue engineered products will not integrate with surrounding host tissue or remain viable. Researchers have investigated different strategies to promote vasculogenesis within tissue engineered products. These strategies include adding angiogenic factors [8-10] and incorporating vascular cells such as endothelial cells or endothelial progenitor cells[11-13]. While these strategies have shown some promise, promoting vasculogenesis in tissue engineered products with complex architecture, multiple cell layers, and sizes that exceed optimal diffusion of nutrients have not been successful [14].

During embryonic development, vasculogenesis occurs in a well organized pattern that is spatially and temporally controlled by various cues and signals, such as fluid shear stress, hypoxia, and VEGF [15-19]. Fluid shear stress regulates cardiovascular gene and protein expression patterns in the embryo [17, 20]. Additionally, fluid shear stress imparted by blood flow is vital to the maturation and stabilization of the

primitive embryonic vasculature [21] and regulates arterial and venous specification, patterning of embryonic vessels [22] and eventual vessel size [23]. During embryogenesis, vasculogenesis and angiogenesis occur and diffusion of oxygen is inhibited due to embryo growth, causing an oxygen gradient throughout the embryo [18]. Hypoxia mediates temporal and spatial expression of VEGF receptors, Flk-1 and Flt-1[24], and VEGF which are required for differentiation and organization of the vascular system [25]. In vivo, fluid shear stress, hypoxia, and VEGF are vital for the proper development of the vasculature system demonstrating the instructive potential of these cues and signals for development of vasculature in vitro.

Embryonic development can be recapitulated in vitro in 3D aggregates of embryonic stem cells(ESCs) called embryoid bodies(EBs). EBs can spontaneously differentiate and give rise to cells from all three germ layers: ectoderm, mesoderm, and endoderm[26-29]. Additionally, many morphogenic and developmental events, such as vasculogenesis can occur [30, 31]. However because differentiation is spontaneous there is great heterogeneity in EB populations in terms of the morphogenic events that the EBs are undergoing [32]. EBs can serve as an ideal template for a multitude of tissue engineered products due to their potential to give rise to cells of various tissues and ability to develop vascular networks. Therefore, the *objective of this work is to study the effects of fluid shear stress preconditioning of embryonic stem cells (ESCs) on embryoid body endothelial differentiation and vasculogenesis.* The *central hypothesis* is that exposing ESCs to fluid shear stress prior to EB differentiation will promote EB endothelial differentiation and vasculogenesis. The hypothesis was tested using the following three specific aims:

Specific Aim 1: Evaluate the effects of preconditioning ESCs with fluid shear stress on subsequent embryoid body cardiovascular differentiation and morphogenesis. The working hypothesis is that fluid shear stress preconditioning alters ESC endothelial differentiation and morphogenesis. A parallel plate flow chamber was used to apply varying magnitudes (5 and 15 dyn/cm²) of fluid shear stress to ESCs. ESCs preconditioned with and without fluid shear stress were afterwards differentiated as EBs. Endothelial gene and protein expression was assessed after fluid shear stress preconditioning and during embryoid body culture, using qRT-PCR, immunostaining, and flow cytometry.

Specific Aim 2: Examine the effects of vascular endothelial growth factor (VEGF) on endothelial differentiation, endothelial-like cell organization, and vasculogenesis within embryoid bodies containing shear preconditioned ESCs. The working hypothesis was that treating EBs with angiogenic factors will promote endothelial differentiation and endothelial-like cell organization within EBs. VEGF was delivered to EBs solubly or by incorporating VEGF loaded gelatin microparticles within the EBs. Vasculogenesis and endothelial-cell like organization were assessed through immunofluorescence of endothelial proteins and analyzed by confocal microscopy. Quantitative real time PCR analysis of endothelial genes and western blots and flow cytometry analysis of endothelial proteins of single cells dissociated from EB samples were performed and compared to untreated EBs.

Specific Aim 3: Investigate the effects of hypoxia on vasculogenesis in EBs formed from shear pre-conditioned ESCs. The working hypothesis was that hypoxia would promote formation of vascular networks in EBs formed from shear pre-conditioned

ESCs. Following shear pre-conditioning, ESCs were differentiated as EBs under hypoxic conditions (1% O₂) or normoxic conditions (21% O₂) for 7 days. Viability was assessed throughout EB differentiation and endothelial differentiation was assessed using qRT-PCR, flow cytometry, and western blot. Formation of vascular networks was assessed by whole-mount immunostaining of EBs for endothelial markers VE-cadherin and PECAM through confocal microscopy. Additionally, expression of hypoxia inducible factors was assessed through western blot and qRT-PCR.

This work is **innovative** because it demonstrates that physical forces have prolonged effects on stem cell fate and differentiation potential. Exposing pluripotent stem cells to fluid shear stress effects how they respond to environmental cues such as oxygen levels and VEGF. Altogether this work will add to the knowledge base and understanding of the role of fluid shear stress on ESC differentiation within EBs. This research provides insight into new strategies to promote ESC endothelial differentiation. The **expected outcome** of this work is to gain a better understanding how physical forces effect ESC stem cell fate, behavior, and morphogenesis.

CHAPTER 2

BACKGROUND

Stem Cells

The significant discovery of stem cells almost 5 decades ago has created major advancements in regenerative medicine, cellular therapeutics, developmental biology, and stem cell biology. Resident adult stem cells were initially identified in the bone marrow [33, 34], and then later discovered in brain [35, 36], fat [37], muscle [38], and skin [39] tissues. While several isolation, expansion, and differentiation protocols have been established for adult stem cells [39-41], they cannot be expanded to the quantities required for regenerative medicine applications. Moreover, stem cells from adult tissues possess limited potency since their differentiation potential is limited by the tissue from which they were isolated.

Embryonic Stem Cells

Embryonic stem cells (ESCs) are derived from the inner cell mass of a blastocyst stage embryo [42, 43]. Due to their unique ability to give rise to cells comprising the three germ lineages: ectoderm, endoderm, mesoderm, [26-28, 44, 45]. ESCs have been examined as a potential cell source for a wide variety of cells including but not limited to cardiomyocytes [46], neural cells [47], pancreatic cells [48], blood cells [49] and endothelial cells [50]. In order to obtain somatic cells from ESCs various differentiation strategies have been employed such as culturing ESCs in the presence of different cytokines, growth factors, and extracellular matrices [27]. However, ESCs can also be differentiated as 3D aggregates termed embryoid bodies (EBs). EBs recapitulate aspects

of embryogenesis and allow for spontaneous differentiation in the three germ layers [26, 32]. ESCs within EBs differentiate in response to stimuli such as cell-matrix interaction [51], cell-cell adhesions, cytokines [52], and growth factors [53], which are all microenvironmental stimuli present during embryonic development. Because the EB microenvironment parallels the in vivo embryonic microenvironment more than 2D culture, ESC EB differentiation may be more effective in deriving somatic cells.

Embryonic Stem Cells and Vascular Cell Differentiation

Directed differentiation culturing methods have been established to derive endothelial cells (ECs) from ESCs [45, 50, 54-57]. The culturing methods generally involve the use of VEGF, collagen IV and collagen I, selection of Flk-1 positive cells, and multiple passaging procedures [50, 54-56]. The derivation of ECs from ESCs requires long culturing periods, large quantities of growth factors and extracellular matrix, which typically results in low cell yields.

ESCs have the ability to differentiate into vascular cells in 3D culture. EBs have been used to study vasculogenesis and angiogenesis [30, 31, 57, 58]. EBs recapitulate vasculogenesis and angiogenesis with the presence of immature hematopoietic cells and endothelial cells [30, 31]. EBs which have been differentiated for 7 days contained populations of CD41 (hematopoietic) positive cells surrounded by channels and lumen lined with VE-Cadherin positive cells [31]. Although endothelial and hematopoietic differentiation can occur in EBs, the percentage of ESCs within the embryoid body which differentiate into endothelial and hematopoietic cells is less than 10% [31] and there is heterogeneity between EBs in terms of endothelial and hematopoietic differentiation

potential due to the complex nature of the EB microenvironment (matrix, cytokines, and growth factors). The challenges associated with differentiating ESCs into vascular cells motivate the need to develop new methods to direct and enhance vascular cell differentiation.

Endothelial and Hematopoietic Cell Development

Endothelial and hematopoietic cells originate from mesoderm via a common precursor known as the hemangioblast [59, 60]. The hemangioblast is most notably defined by its expression of Flk-1 and SCL/Tal-1 genes [61, 62]. During early embryogenesis aggregates of hemangioblasts, in the extraembryonic yolk sac, mature and form blood islands which consists of an inner core of blood cells and an outer layer of endothelial cells[63]. The organization of hematopoietic and endothelial cells into blood islands initiates the onset of vascular development and expansion as blood island cells migrate, divide, and create connections to form the yolk sac vasculature[58]. Endothelial cells that develop from hemangioblast lose SCL/Tal-1 expression while hematopoietic cells lose Flk-1 expression. By day 8 of development, aortic endothelial cells, expressing VE-Cadherin, CD34, PECAM, and Flk-1, have organized to form vessels [64]. Hematopoietic cells, characterized by the expression of SCL/Tal-1, c-kit, Runx1, CD41, and CD45 [65], are confined to the vascular lumen [64].

Fluid Shear Stress

Fluid shear stress has been well studied and characterized in the vascular system . Within the vascular system shear stress spans a large range magnitudes and regimes (oscillatory, laminar, steady, tubrulent) and varies both spatially and temporally. Endothelial cells (ECs) which line the vasculature experience these shear stresses and respond to this physical force [66]. In vitro fluid shear studies have revealed that fluid shear stress modulates endothelial cell processes such as proliferation [67], cytoskeleton arrangement [68, 69], integrin expression [70], alignment [71], nitric oxide production, calcium signaling [72], as well as endothelial adhesion molecules such as vascular endothelial-cadherin (VE-cadherin) [73]. Somatic [71, 74] and stem cells [75-78] have been subjected to fluid shear stress at varying magnitudes and regimes in vitro using a number of bioreactor systems [71, 77, 79] for in vitro culture maintenance and cell generation as well as examination of fluid shear on cell phenotype. In vitro fluid shear stress has been used as a method to recapitulate the in vivo fluid shear stress forces and study their cellular behavior in response to changes in this physical force.

Fluid Shear Stress and Embryonic Stem Cells

Embryonic stem cells have the ability to respond to fluid shear stress by changes in gene expression and cell proliferation [80]. Many researchers have demonstrated that fluid shear stress induces ESCs to differentiate towards vascular cells (endothelial cells and smooth muscle cells) [81-84]. ESCs exposed to pulsatile flow with resulting wall shear stresses of -0.98 to 2.2 dynes/cm² demonstrated some endothelial function with the protein expression of PECAM1 and alignment in the direction of the pulsatile flow [84]. Flk-1+ ESCs cultured under fluid shear stress of 1.5 and 5 dynes/cm² display

significantly increased gene expression of endothelial specific markers such as Flk-1, Flt-1, PECAM1, and VE-Cadherin [81]. Laminar shear stress of 10 dynes/cm² increases smooth muscle cell and endothelial cell protein expression in ESCs. ESCs exposed to 24 hrs of laminar shear stress had increased protein expression of smooth muscle actin, monocyte enhancer factor-2c, and alpha sarcomeric actin, Flk-1, eNOS[83]. Shear stress also induces ESCs to form tube-like structures in Matrigel™ or collagen I more readily than ESCs which have been cultured under static conditions [81, 83]. While such studies aimed to assess the effects of fluid shear stress on ESC endothelial differentiation, they are incomplete since these studies do not examine the prolonged effects of fluid shear stress pre-conditioning on ESC endothelial differentiation potential. Additionally, the majority of these studies focus on magnitudes lower than 15 dynes/cm².

Fluid Shear Stress and Vascular Progenitor Cells

Fluid shear stress elicits phenotypic changes in ESC-derived endothelial cells, vascular progenitor cells, and hematopoietic progenitor cells [85-89]. ESC-derived endothelial cells respond similarly to fluid shear stress as mature endothelial cells respond to fluid shear stress with respect to changes in morphology, gene expression and protein expression. ESC-derived endothelial cells elongate and orient in the direction of flow as do endothelial cells [86, 87]. In addition, shear stress induces similar changes in expression of monocyte chemotactic protein-1(MCP1), tissue plasminogen activator (tPA), matrix metalloproteinase-1 (MMP1), cyclooxygenase-2 (COX2), SOD2, and transforming growth factor β 1 (TGF β 1) in ESC-derived endothelial cells and mature endothelial cells. Furthermore, shear stress modulates gene transcription and expression

of CD31, ICAM1, and VE-Cadherin similarly in both cell types [87]. Zeng et al. determined that laminar flow increases proliferation of vascular progenitor cells(Sca1+ ESCs) and mRNA expression of PECAM1 (CD31), prominin1 (CD133),VE-Cadherin (CD144), VEGF receptor 1(Flt-1), and VEGF receptor 2(Flk-1) [85]. Hematopoietic progenitor or cKit+CD41+ ESCs show increased expression of Runx1, Myb, and Kruppel-like factor 2 (Klf2) and had increased frequency of colony formation after exposure to fluid shear stress. These genes are associated with hematopoietic differentiation, vasculogenesis, and endothelial differentiation [89]. Daley et al. also demonstrated that shear stress can restore the hematopoietic progenitor cell population in mice embryos which lack the ability to initiate a heartbeat. Overall, ESC-derived endothelial cells and vascular progenitor cells and endothelial cells respond similarly to fluid shear stress.

Vascular Endothelial Growth Factor

Vascular endothelial growth factor (VEGF), a member of the platelet-derived growth factor family, (mouse 22-24kDa, human 45kDa), stimulates vasculogenesis and angiogenesis in response to low oxygen supply [90]. During embryonic development VEGF plays a major role in the creation of new blood vessels or vasculogenesis [15]. Additionally, VEGF stimulates growth of blood vessels from pre-existing vessel, angiogenesis, following blood vessel damage[91]. Because VEGF has a primary role in vasculature development in vivo, VEGF has been used to differentiated stem cells to vascular cells and promote vasculogenesis in vitro[50, 92, 93].

Vascular Endothelial Growth Factor and Development

During development VEGF is imperative for proper development of the vascular system. In vivo, loss of a single VEGF allele is lethal in mouse embryos because it leads to impaired angiogenesis and blood island formation [94]. When VEGF null ESCs are implanted into a blastocyst the developing embryo has defects in initial vasculature development as there is reduced yolk sac blood supply. This leads to impairment in other developing organs such as unsegmented branchial arches and forelimbs, delayed development of the heart, and reduced number of nucleated blood cells within the yolk sac [95]. The detrimental effects which are caused by lack of VEGF during development clearly demonstrate the important role of VEGF in the initial development of the cardiovascular system, which supplies blood and nutrients to ensure proper formation of all organs and tissues.

Vascular Endothelial Growth Factor and Endothelial Differentiation

Angiogenesis and vasculogenesis each occur through migration and organization of endothelial cells (ECs). Endothelial cells which express VEGF receptors, Flk-1 and Flt-1, produce VEGF [96] and respond to VEGF in a number of ways including survival, proliferation, migration, and angiogenesis [94, 97-99]. Therefore, VEGF has been used to derive ECs from stem cells. Established ESC EC differentiation protocols all require VEGF treatment of ESCs in order to promote Flk-1 expression of ESCs and to continue to promote Flk-1+ ESCs to acquire EC phenotype [50, 54, 55]. Not only has VEGF been employed in 2D culture of ESCs, embryoid bodies treated with varying concentrations of VEGF (5-50ng/mL) yielded cells which expressed endothelial markers

CD31, VE-cadherin and vWF [50, 54]. These cells were able to form lumenized vessels in vitro and form networks of vessels containing host blood cells when implanted in infarcted rat hearts [92]. Additionally, VEGF can promote ESC differentiation towards hematopoietic cells [100, 101]. VEGF stimulation of ESC monolayers induces formation of sac-like structures which consisted of endothelial and hematopoietic like cells [102]. Implanted hematopoietic stem cell survival is regulated by VEGF, VEGF gene ablation results in inability to home and implant at engraftment sites [103]. VEGF is critical for development, maintenance, and function of vascular cells.

Hypoxia

Low oxygen or hypoxic conditions are present throughout many physiological environments, disease pathologies, and during embryonic development [19, 104-107]. While cells are generally maintained and cultured at 21% oxygen (normoxic) in vitro, in vivo cells develop and function at oxygen levels are generally ranging from 1-10% (hypoxic) [19]. Oxygen levels play a very important role in many cellular processes including but not limited to metabolism, differentiation, proliferation, and tissue morphogenesis, [19, 108-110]. More specifically oxygen levels play a critical role in vascular development and differentiation during embryogenesis [19, 24, 111].

Hypoxia Inducible Factors

Hypoxia inducible factors (HIFs) are transcription factors which are responsible for coordinating multiple processes which maintain homeostasis of O₂ levels within mammals [112, 113]. HIFs are heterodimeric complexes which are made up of an alpha and beta subunit. Under hypoxia HIF heterodimer complexes are stabilized and regulate

at least 180 genes) including VEGF, Flk-1, Flt-1, and Oct-4 [24, 112]. HIFs regulate transcription by binding to hypoxia response elements located on the promoter regions of their target genes [114, 115]. The HIF family is comprised of HIF-1, HIF-2, and HIF-3 each having an alpha and beta subunit [116]. The alpha subunits are regulated by hypoxia, however the beta subunits are largely unresponsive to changes in O₂ levels and affect O₂ independent pathways [19, 116]. HIF-1 α is universally expressed while HIF-2 α is generally expressed to vasculature of early developing embryos, endothelial cells, neural crest derivative cells, lung type II pneumocytes, liver parenchyma, and kidney intestinal cells [117, 118]. HIF2 α has been reported to regulate stem cell pluripotency and proliferation under hypoxic conditions [119, 120]. Hypoxia mediates a multitude of cellular responses through stabilization of a family of transcription factors called HIFs, which are key regulators of many genes which play roles in a multitude of cellular processes.

Hypoxia and Vascular Development

Oxygen levels regulate the development of a number of tissues including, but not limited to the tracheal, cardiovascular, placental, and skeletal systems (Simon, 2008 #123). Prior to the development of the circulatory system embryonic oxygen levels are approximately 3% O₂ [114, 121]. Low oxygen tension is imperative for proper morphogenesis and function of the cardiovascular system in the early embryo [122]. During cardiovascular development, the most critical and first system to develop within the embryo, vascular endothelial growth factor (VEGF) is produced by oxygen deprived cells [123, 124]. Lee et al. discovered spatial and temporal co-localization of HIF1 α and

VEGF along with PECAM expressing cells forming vasculature and proliferating in hypoxic regions of the embryo [125]. Oxygen gradients within the embryo are critical for proper development and patterning of the vascular and cardiovascular systems.

Hypoxia and Stem Cells

Low oxygen effects have been examined in a variety stem cell populations including pluripotent [111, 120, 126], mesenchymal [127-129], glioma [130] and hematopoietic [128]. Hypoxia regulates proliferation and differentiation [119, 131], as well as alters expression of genes responsible for survival, angiogenesis, and vasculogenesis [24, 120]. Furthermore, hypoxia pretreatment of stem cells has been explored as a means to improve stem cell survival and engraftment after transplantation into a number of diseased models [127, 132].

In pluripotent stem cells hypoxia (1-5% O₂) downregulates the expression of pluripotency marker Oct4, while significantly upregulating angiogenic and vasculogenic markers VEGF and angiopoietin-like proteins. Additionally, 50% hESCs cultured under 5% O₂ became CD34⁺ positive, an endothelial progenitor cell marker. Implantation of these CD34⁺ into a MI rodent model, resulted in improved fractional shortening and systolic function and reduced fibrosis scar tissue [111]. When 3D aggregates of ESCs were cultured under hypoxia, an increased percentage of cells expressed Flk-1 and Flt-1 earlier during EB differentiation as compared to ESCs cultured under normoxia, as well as increases in CD31⁺ (PECAM) expressing cells were observed. Furthermore, hypoxia promoted development and maturation of vasculature and angiogenic outgrowth within EBs [24]. Hypoxia pre-treatment of neuronal-differentiating ESCs resulted in a 50%

reduction in apoptosis and caspase-3 activation, increased expression of HIF-1 α , and increased cell survival when transplanted into a rat ischemic brain model [132]. Low oxygen tension environments are more favorable than normoxic oxygen levels in maintaining proliferative and pluripotent stem cell populations [119, 131]. ESCs cultured at 20% oxygen tension displayed reduced expression of pluripotency genes Sox2, Nanog, and Oct4 compared to ESCs cultured at 5% oxygen. Additionally, ESCs expressed HIF1 α , HIF2 α , and HIF3 α and spatial expression of HIFs within the cell was regulated by duration at low oxygen tension [119]. Overall, hypoxia is a key regulator of stem cell survival, proliferation, vascular cell differentiation and vasculogenesis.

Tissue Engineering

In the early 1980s E. Bell et al. reconstructed skin [133] and thyroid gland [134] tissue from living cells and matrix materials. Prior to this development, allogenic living tissue replacements were stored in tissue banks or tissue replacements were produced from synthetic materials. As the field of tissue engineering has evolved focus has been put on developing off the shelf replacement tissues which mimic native tissue characteristics [135], which has led to an increased understanding of developmental biology and tissue formation. Additionally, great importance has been placed on the tissue engineering triad which is the concept that tissue replacements must consist of cells, extracellular matrices, and signals[136, 137]. The need for off the shelf availability of tissue engineered products has rendered stem cells, which are highly proliferative, expandable, and easily isolated a desirable cell source option for many tissue engineered products. While tissue engineering has made many strides some major challenges still

remain such as vascularization of tissue replacements in vitro as well as rapid vascularization in vivo of large and complex engineered tissues [138].

Modular Tissue Engineering

Modular tissue engineering has been employed to develop large tissues which better mimic the complex architecture of native tissues. This strategy involves creating smaller tissues which have similar structural and biological features and then assembling them into a larger tissue via stacking[139, 140], directed assembly[141], or random aggregation[142, 143]. This approach has been utilized to vascularize tissue engineered constructs. McGuiagan and colleagues demonstrated blood perfusion through sub mm sized tissue by assembling endothelial cell-laden collagen gel rod modules into a larger tissue construct. The endothelial cells organized to form vascular networks which were nonthrombogenic and remained viable [144, 145]. Modular tissue engineering approaches represent a promising method to vascularize large tissue engineered constructs.

Pre-Vascularization of Tissue Engineered Products

While researchers have developed to engineered tissues such as bone [6], heart [8, 10], pancreas [9], kidney [146, 147] and the spinal cord [3], in the lab setting, translation to clinical use has been unsuccessful due to the lack of sufficient vascularization upon implantation in animal in vivo models. The formation of blood vessels upon implantation is imperative to ensure nutrients and oxygen delivery to

implanted tissues as well as proper integration of the implanted tissue into surrounding host tissue. In order to vascularization of implanted tissues researchers have attempted to pre-vascularize engineered tissues prior to implantation in hopes that these engineered tissues will more rapidly develop vasculature and integrate with surrounding host tissue.

Approaches to pre-vascularize engineered tissues and promote rapid vascularization upon implantation include addition of vascular cells within the tissues [11-13] and incorporating angiogenic factors within the tissues [8-10]. These approaches have not been successful for tissues with complex architecture and multiple layers of matrix and cells. In addition, generating blood vessels in vitro requires the addition of multiple angiogenic factors at varying concentrations along with variations in exposure times to these factors. Additionally, many engineered tissues are larger than 200 μm , which is the length scale at which diffusion of molecules through tissues is limited.

Various endothelial cell types, progenitor (EPCs), umbilical vein (HUVEC), and adult, have been utilized to pre-vascularize a multitude of tissue engineered constructs such as bone, cardiac, and dermal constructs. Federovich et al. co-cultured EPCs and multipotent stromal cells and found that EPCs assembled into early blood vessels and contributed to multipotent stromal cell osteogenic differentiation [6]. When HUVECs were co-cultured with fibroblasts in fibrin gels for a week and then implanted into dorsal surface of immune-deficient mice, accelerated vascularization with the presence of HUVEC lined vessels containing red blood cells and significantly larger number and area of perfused lumens compared to non pre-vascularized constructs [11]. Furthermore, HUVEC prevascularization of fibroblast cell sheets promoted in vivo neovascularization

and network formation [13]. ECs and neural progenitor cells cultured in a PLGA and PEG scaffold induced significant increase in functional vessel formation when implanted into an injured rat spinal cord model [3]. While these studies report some success in vascularization by incorporating endothelial cells within engineered tissues, this approach is still not sufficient for development of vasculature within large tissues which will be used in the clinic and require using cell types which cannot be easily isolated and expanded. Therefore, more vascularization approaches need to be explored which utilize modular tissue engineering approaches and cells which can be easily isolated, expanded and have application in a multitude of regenerative medicine applications.

CHAPTER 3

GENERAL METHODS

ESC and EB Culture

D3 and D3 pVE-cadherin GFP murine embryonic stem cells were cultured on 0.1% gelatin-coated tissue-culture polystyrene cultureware (Corning) in Dulbecco's Modified Eagle Medium (DMEM, Mediatech) containing 15% fetal bovine serum (FBS, Hyclone), 1X non-essential amino acids, 2 mM L-glutamine, 100mg/mL streptomycin, 0.25 mg/ml amphotericin, 100 U/mL penicillin, 10^3 U/mL leukemia inhibitory factor (LIF, Millipore), and 0.1 mM β -mercaptoethanol. ESCs were fed every 2 days and passaged using 0.05% trypsin-EDTA (Mediatech) every 2-3 days before reaching 70-80% confluency. EBs were formed from single-cell suspension of 2×10^6 cells in 10 mL of differentiation media (DMEM with FBS and supplements except LIF) and were maintained in a 100 mm petri dish on a rotary orbital shaker (Lab-Line Lab Rotator, Barnstead) at 40 rpm (Carpenedo, 2007 #2). Rotary orbital shakers were calibrated every day to ensure constant speed throughout the period of EB suspension culture. EBs were re-fed every 2 days by gravity-induced sedimentation in a 15ml conical tube and exchanging approximately 90% of the media.

Fluid Shear Pre-conditioning

ESCs were seeded onto 28.5 cm^2 glass slides pre-coated with rat tail collagen IV (20ug/ml solution; BD Biosciences) at a density of 20,000 cells/ cm^2 and cultured for 48hrs under static conditions to allow the ESCs to form a confluent monolayer. The confluent monolayer of ESCs was then subjected to either 0 dynes/ cm^2 (static) in a 150

mm petri dish or 5 dynes/cm² (shear) fluid flow for 48 hrs using a parallel plate flow chamber connected to a peristaltic pump [71]. During pre-conditioning, ESCs were cultured in differentiation media consisting of Alpha MEM (Mediatech), 10% FBS, 100 U/mL penicillin streptomycin, and 0.1 mM β -mercaptoethanol. Alpha MEM is commonly used for ESC EC differentiation [54, 148, 149].

Quantitative reverse-transcriptase polymerase chain reaction (qRT-PCR)

Total RNA was extracted from samples using an RNeasy Mini Kit (Qiagen). The quantity and quality of RNA was determined using a Nanodrop® Spectrophotometer ND1000 reading at 280 nm and the ratio between the absorbance at 260 nm and 280 nm, respectively. Samples with ratios between 1.7 and 2.0 were used to synthesize complementary DNA (cDNA) from 1 μ g of total RNA using an iScript cDNA synthesis kit (Bio-Rad) on a thermocycler (Bio-Rad) with the following parameters: 25°C for 5 min, 42°C for 30 min, 85°C for 5 min, and store at 4°C. Quantitative PCR was performed using SYBR green technology on a MyIQ cycler (Bio-Rad); amplification was performed using a two-step cycling program run at the appropriate annealing temperatures for each primer set (40 cycles, 1min). Primer sequences (Invitrogen) (Table 4.1) were designed using Beacon Designer software, validated using appropriate cell controls for target genes, *Flk-1* (vascular endothelial growth factor receptor 2), *Flt-1* (vascular endothelial growth factor receptor 2), *VE-cadherin* (vascular endothelial cadherin), *PECAM* (platelet-endothelial cell adhesion molecule), *Runx1* (runt related transcription factor), and *Tall* (T-cell acute lymphocytic leukemia protein 1), *AFP* (alpha fetoprotein), *Pax6* (Paired box gene 6), *Nkx2.5* (cardiac specific homeobox protein), *Mef2c* (Myocyte-specific enhance

factor 2C), *GATA4* (global transcription factor 4), *VEGFA* (vascular endothelial growth factor A), and *HIF1 α* (hypoxia inducible factor 1 alpha. Primer sequences and annealing temperatures are listed in Table 1. The concentrations of the specific genes were calculated using a standard curve of known gene quantities and normalized to housekeeping gene, Glyceraldehyde-3-phosphate dehydrogenase (*GAPDH*), expression levels. Relative fold changes (Chapters 5 and 6) were quantified relative to PC Static or PC Shear samples by using the Pfaffl method for quantification [150]

Table 3.1: Primer Sequences and Annealing Temperatures

Gene	Forward	Reverse	Temp
<i>Flk-1</i>	GGC GGT GGT GAC AGT ATC	TGA CAG AGG CGA TGA ATG G	64.3°C
<i>Flt-1</i>	ATC GGC AGA CCA ATA CAA TC	TGC TCT CTT AGT TGC TTT ACC	60.5°C
<i>VE-cadherin</i>	TGA ACC GCC AGA ATG CTA AG	CCA CAA TGA GGG CAG TAA GG	57.9°C
<i>PECAM</i>	CTC CTT CAC CAT CAA CAG	TTA TAC ACC ATC GCA TCG	60.5°C
<i>Runx1</i>	CAC CTC TTC CTC TGT CCA C	CGG AGC CGT TGA GAG TCG	64.3°C
<i>Tal1</i>	CTC ACG GCA AGC TAA GTA ACT G	TGG GGC ATA TTT AGA GAG ACC TAC	60.5°C
<i>AFP</i>	CAC ACC CGC TTC CCT CAT CC	TTC TTC TCC GTC ACG CAC TGG	60.5°C
<i>Pax6</i>	ACGGCATGTATGATAAACTAAG	GCTGAAGTCGCATCTGAG	58.0°C
<i>Nkx2.5</i>	CAA GTG CTC TCC TGC TTT CC	GGC TTT GTC CAG CTC CAC T	64.3°C
<i>Mef2c</i>	CCC AAT CTT CTG CCA CTG	GGT TGC CGT ATC CAT TCC	56.1°C
<i>GATA4</i>	TGC TTT GAT GCT GGA TTT AAT TTC G	CGG GTG TGC GGA ACT GTC	58.0°C
<i>HIF1α</i>	GAGGTGGATATGTCTGGGTTG	AGGGAGAAAATCAAGTCGTGC	57.9°C
<i>VEGFA</i>	TGCACCCACGACAGAAGG	GCACACAGGACGGCTTGA	56.5°C
<i>GAPDH</i>	GCC TTC CGT GTT CCT ACC	GCC TGC TTC ACC ACC TTC	60.5°C

Whole-Mount Immunostaining of Embryoid Bodies

EBs were washed in PBS (without Ca^{2+} and Mg^{2+}) then fixed in 4% paraformaldehyde for 1 hour at 4°C. Following fixation, EBs were washed 3 times in blocking buffer containing PBS (with Ca^{2+} and Mg^{2+}) 2% donkey serum and 0.1% Tween-20. EBs were permeabilized with 1.5% Triton X-100 for 30 minutes and additionally fixed in 4% paraformaldehyde in blocking buffer for 15 minutes. EBs were incubated in blocking buffer for 1-3 hours at 4°C and incubated in the following primary antibodies from Santa Cruz Biotechnology: goat anti-VE-cadherin (CD144) (1:200), rabbit anti-PECAM (CD31) (1:200), or rabbit anti-vWF (1:200) diluted in blocking buffer overnight at 4°C. Following the overnight incubation, EBs were washed 3 times (15 minutes each) with blocking buffer and then incubated with a donkey anti-goat AlexaFluorTM 488 or donkey anti-rabbit AlexaFluor546TM (Invitrogen) secondary antibodies (1:200) and Hoechst (1:100) for 4 hours at 4°C. EBs were then washed 3 times (15 minutes each) with blocking buffer and then imaged the following day using a Zeiss LSM 510 NLO Multiphoton confocal microscope.

Flow Cytometry Analysis

EBs were washed in PBS (without Ca^{2+} and Mg^{2+}) and then dissociated by incubating EBs with 0.05% trypsin-EDTA (Mediatech) for either 15 minutes (day 2 and 4 EBs) or 30 minutes (day 7 EBs) at 37°C. Dissociated cells were then quenched with ESC media to inactivate trypsin and then centrifuged for 5 min at 1000 rpm. Following

dissociation, cells were then rinsed with cold PBS (with Ca^{2+} and Mg^{2+}) containing 0.1% BSA, passed through a 35 μm strainer and then analyzed for pVE-cadherin GFP expression using an Accuri C6 flow cytometer. Undifferentiated D3s and pVE-cadherin GFP D3s were used as negative controls. Approximately 27,000-33,000 events were recorded from 6 independent samples from each experimental group.

Statistical Analysis

Experimental treatments were investigated with a minimum of 3 independent replicates in independent experiments and presented as mean \pm standard error of multiple samples. Statistical analysis was performed using SYSTAT 12 software (Systat Software Inc.). Comparisons across time points between experimental groups were made using a two-way analysis of variance (ANOVA) followed by post-hoc Tukey-Kramer test to determine significant ($p < 0.05$) differences between different groups. Paired t-tests were employed to determine statistical significance ($p < 0.05$) between static and shear pre-conditioning regimens.

CHAPTER 4

FLUID SHEAR STRESS PRE-CONDITIONING EFFECTS ON EMBRYONIC STEM CELL EMBRYOID BODY DIFFERENTIATION

Introduction

Embryonic stem cells (ESCs) are an attractive cell source for numerous regenerative medicine and cell therapy applications because of their inherent abilities to differentiate into all somatic cell types[26, 27]. However, one major challenge in utility of these cells for such applications is efficient derivation methods to generate the desired homogeneous populations of differentiated cell types. In the case of vascularization for replacement tissues and as a lining for vascular grafts, a source of endothelial cells (ECs) is imperative, due to the lack of autologous endothelial cell sources, limited expansion capabilities and loss of phenotype in vitro. Lack of vascularization in engineered tissues leads to inability to integrate with host tissue and to cell and tissue death of engineered constructs. In the case of vascular grafts ECs provides a nonthrombogenic layer to prevent blood clots. Thus the critical multi-factorial role that ECs play in vascularization illustrates the need to develop methods to derive endothelial cells from ESCs.

*Modified from:

B. Nsiah, T. Ahsan, R. Nerem, and T. McDevitt Fluid Shear Stress Pre-conditioning Promotes Endothelial Morphogenesis of Embryonic Stem Cells within Embryoid Bodies

Current protocols to derive ECs from ESC monolayers require long culture periods, large concentrations of growth factors and cytokines, labor intensive cell sorting

and generally result in a heterogeneous mixture of differentiated cell types with a low percentage of the cells becoming mature endothelial cells [54]. Embryoid body (EB), 3D aggregates of ESCs, differentiation has been employed because EBs recapitulate in vivo morphogenic events, such as development of mesodermal endothelial cells and vasculogenesis [26, 30-32, 58]. While endothelial differentiation occurs within EBs, there is variability from EB to EB in terms of endothelial differentiation efficiency and endothelial morphogenesis [30, 58]. In order to improve homogeneity and efficiency of differentiated cell populations in 2D ESC EC differentiation protocols, researchers have examined the use of mechanical forces such as fluid shear stress to derive ECs from ESCs. Studies have revealed that ESCs respond to fluid shear stress by alterations in self renewal abilities [151], cell proliferation, and endothelial and hematopoietic gene expression [80, 84]. Fluid shear stress at varying magnitudes (1-15 dynes/cm²) and profiles (steady, pulsatile, laminar) have been employed to promote stem and progenitor cells to differentiate towards various cardiovascular cell types including endothelial cells, hematopoietic cells, and smooth muscle cells [84, 85, 89].

Fluid shear stress has been examined because it mimics the physiological forces ECs experience in the body. Fluid shear stress plays a role in EC phenotype, function, and homeostasis during development of vasculature and in fully developed vessels. This physical force is critical for the development of the cardiovascular system, which is the first functioning physiological system to be established within the embryo [16, 17]. Gene and protein expression patterns which develop in the embryonic cardiovascular system are regulated by fluid shear stress, and disruption of fluid flow can lead to abnormal cardiogenesis and irregular expression patterns of genes related to vasoconstriction and

vasodilation in the cardiac system [17, 20]. In vivo, fluid shear stress is vital for the proper development of the cardiac, vascular, and hematopoietic system, demonstrating the instructive potential of this physical force in the morphogenesis of various cardiovascular cell types.

Recent studies have demonstrated that fluid shear stress has induced increased expression of endothelial genes in a variety of stem and progenitor cell populations. However, it is still unclear how this physical force modulates further endothelial differentiation and morphogenesis. Therefore, the objective of this study was to examine the prolonged effects of fluid shear stress on ESC endothelial differentiation and morphogenesis by exposing ESCs to 0, 5, or 15 dyn/cm² for 48 hrs and then further culturing them as embryoid bodies. Several days after exposure to fluid shear stress, ESC expressed VE-cadherin and localized to the center of EBs. Additionally, fluid shear stress pre-conditioning of ESCs induced EB morphogenic events, had prolonged effects on endothelial differentiation, and generated a population of EBs undergoing endothelial differentiation. The presence of endothelial like cells within EBs formed from shear pre-conditioned ESCs demonstrate that exposing ESCs to fluid shear stress prior to EB differentiation may be a method to modulate endothelial differentiation within EBs.

Methods

Histology

EB samples were prepared for histology after being fixed in 10% formalin for 30 minutes at room temperature, washed 3 times with PBS, and resuspended in 200-400ul histogel (ThermoScientific). Histogel-embedded EB samples were dehydrated through a graded series of alcohol solutions (70-100%) and xylene rinses before being infiltrated and embedded in paraffin. Histological samples were sectioned at 5 μm using a microtome (Microm HM 355S), affixed to Superfrost Plus (VWR) glass slides, and de-paraffinized prior to histological staining. Samples were stained with hematoxylin and eosin (H&E) using a Leica AutoStainer XL.

Immunofluorescence of Cell Monolayers

ESC monolayers were washed with PBS (with Ca^{2+} and Mg^{2+}) 3 times prior to fixation in 4% paraformaldehyde for 10 minutes at room temperature. Following fixation, adherent cells were washed with PBS 3x and blocked and permeabilized with PBS (with Ca^{2+} and Mg^{2+}) containing 2% donkey serum and 0.05% Triton X-100 at room temperature for 45 minutes. Monolayers were then rinsed twice with PBS and incubated in goat anti- Oct-4 (Santa Cruz Biotechnology) primary antibody diluted in PBS (1:200) containing 2% donkey serum overnight at 4°C. The samples were rinsed 3 times in PBS before incubation in a donkey anti-goat AlexaFluor™ 488 (Invitrogen) secondary antibody (1:200) and Hoescht (1:100) diluted in PBS (with Ca^{2+} and Mg^{2+}) containing 2% donkey serum for 1 hour at room temperature. Monolayers were rinsed 3 times in

PBS (with Ca^{2+} and Mg^{2+}) cover slipped using Fluoro-Gel™ mounting media and imaged shortly thereafter using a Zeiss LSM 510 NLO multiphoton confocal microscope.

Morphometric Image Analysis

Phase images of EBs were acquired on days 2, 4, 7, and 10 during the course of EB differentiation with a Nikon TE 2000 inverted microscope (Nikon Inc.) equipped with a SpotFLEX camera (Diagnostic Instruments, Inc.). A minimum of three fields of EBs per sample were analyzed using ImageJ image analysis software such that the cross-sectional area of shear and static pre-conditioned EB samples was measured for a minimum of 100 EBs from independent samples (n=6). The percentage of EBs with dark, centrally located foci was determined by counting the number of such EBs relative to the total number in the same field. Only EBs which contained a dark or optically opaque, centrally located foci that constituted $\geq 10\%$ of the EB cross-sectional area were counted as an EB with a dark region.

Cell Tracker Labeling-Mixing Study

Following preconditioning ESCs were labeled with either CellTracker™ Green CMFDA or CellTracker™ Red CMTPX (Invitrogen, Molecular Probes). Cells were incubated for 30 minutes in 10uM CellTracker™ diluted in serum free differentiation medium at 37°C. Next cells were incubated in differentiation medium for 30 minutes at 37°C and then rinsed with PBS. Cells were then trypsanized and cultured as EBs in a 100mm² petri dishes on a rotary orbital shaker (Lab-Line Lab Rotator, Barnstead) at 40RPM. Embryoid bodies(EBs) were formed by combining 1E6 cells labeled red and

1E6 cell labeled green into a single-cell suspension of 2E6 cells in 10mL differentiation media(DMEM and supplements w/o LIF). Static Green/Static Red EBs were formed from ESCs not preconditioned with shear labeled green and red, Shear Green/Shear Red EBs were comprised of shear preconditioned ESCs labeled green and red. Mixed EBs or Static Green/Shear Red EBs contained ESCs not preconditioned with shear labeled green and ESCs preconditioned with shear labeled red.

Results

Fluid Shear Stress Effects on ESC Differentiation

Following 2 days of culture on collagen IV and an additional 2 days (Fig. 4.1A) of culture at either 0 dyn/cm² (Fig. 4.1B) or 5 dyn/cm² (Fig. 4.1C), ESC populations did not exhibit morphological differences. Both ESC populations largely retained their undifferentiated stem cell phenotype, with the majority of static pre-conditioned ESCs and shear pre-conditioned ESCs expressing Oct4 (Fig. 4. 1D&E). Immediately after fluid shear pre-conditioning, endothelial and mesoderm gene, *Flk-1*, was approximately 3-fold ($p=0.005$) higher in shear pre-conditioned ESCs compared to ESCs cultured at 0 dyn/cm² (Fig. 1F). *Flt-1* (*VEGFR1*) expression (Fig. 4.1G) was comparable in static and shear pre-conditioned ESCs. ESCs pre-conditioned at 5 dyn/cm² expressed higher levels of *VE-cadherin* ($p=0.041$) (Fig. 1H), *PECAM* ($p=0.02$) (Fig. 4.1I), and the hematopoietic transcription factor *Runx1* ($p=0.002$) (Fig. 4.1J), as compared to ESCs not subjected to fluid shear stress. *Tal1* (*Scl*), a hematopoietic gene (Fig. 1K) was not different in ESCs pre-conditioned at 5 dyn/cm² compared to ESCs pre-conditioned at 0 dyn/cm². There were no significant differences in the expression of cardiac genes *GATA4*, *Nkx2.5*, or *Mef2c* between static and shear pre-conditioned ESCs (Fig. 4.1L-N). Static and shear pre-conditioned ESCs also expressed similarly low levels of endoderm gene, *AFP* (Fig. 4.1O) and ectoderm gene, *Pax6* (Fig. 4.1P), suggesting that fluid shear stress pre-conditioning does not significantly affect endoderm and ectoderm differentiation. Although the majority of ESCs subjected to static and shear conditions largely retained pluripotent characteristics, the significant differences in endothelial and hematopoietic gene expression suggests that fluid shear stress initiated endothelial and hematopoietic

differentiation. While fluid shear stress was sufficient to initiate vascular differentiation, it is still unclear if this initial physical modulation is sufficient for vascular differentiation commitment and induces extended effects on ESC EB differentiation.

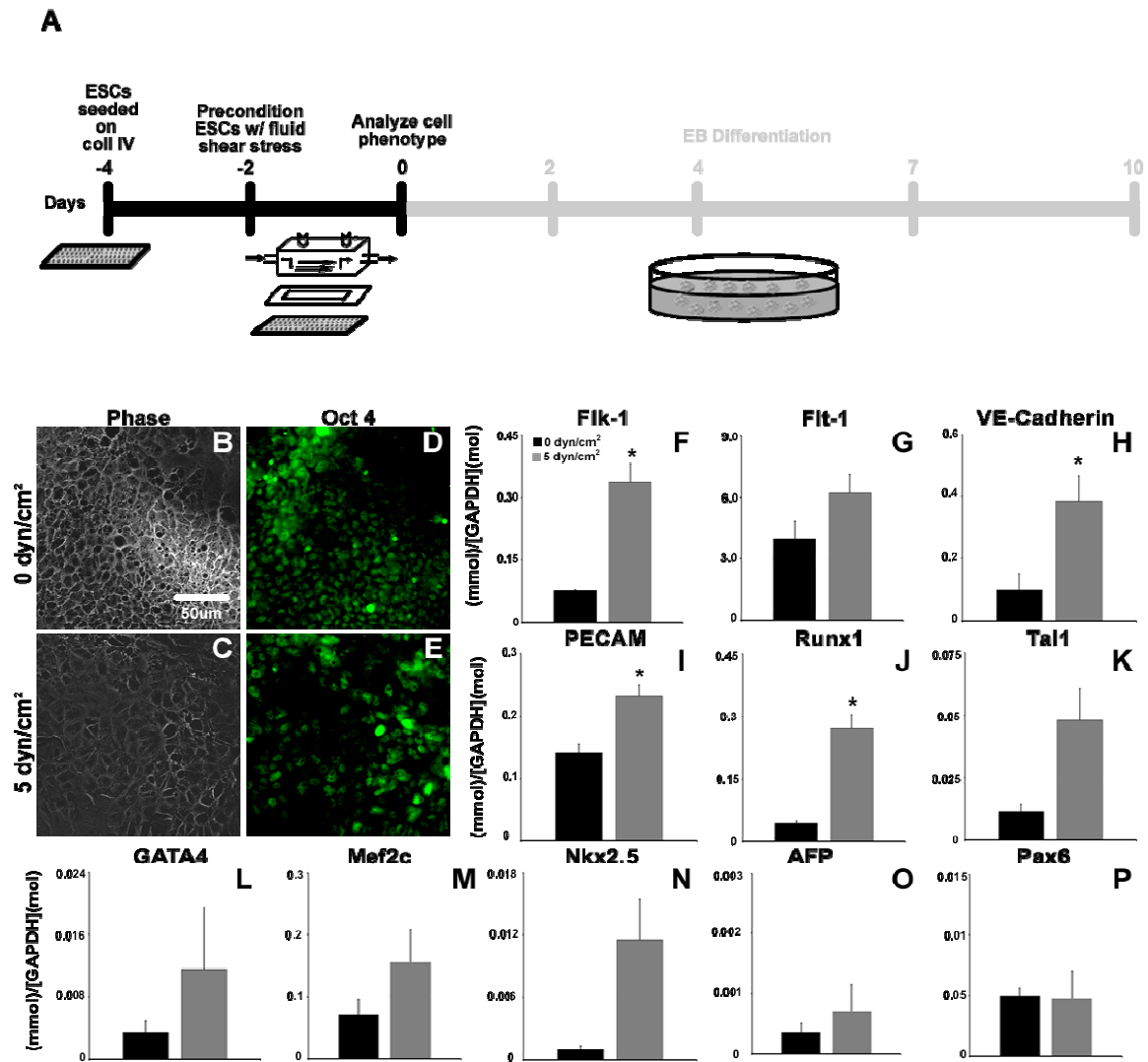


Figure 4.1: Fluid shear promotes mesodermal endothelial and hematopoietic differentiation. Fluid shear pre-conditioning experimental design and morphology, protein and gene expression of fluid shear pre-conditioned ESCs. ESCs were cultured on collagen IV and sheared for 48hrs (A). Phase images show no distinct differences in morphology between ESCs cultured at 0 dyn/cm² (static; B) and 5 dyn/cm² (C). Corresponding Oct4 stained fields illustrate that ESCs cultured at 0 dyn/cm² (D) and 5 dyn/cm² (E) contain populations of cells positive for Oct4. ESCs cultured at 5 dyn/cm² expressed significantly more Flk-1 (D), VE-cadherin (I), PECAM (J), and Runx1 (F) gene than ESCs cultured at 0 dyn/cm². Flt-1 (E) gene expression was similar in ESCs cultured at 0 dyn/cm² and 5 dyn/cm² and Tal1(K) gene expression was higher in ESCs cultured at 5 dyn/cm² than in ESCs cultured at 0 dyn/cm². GATA44 (L), Mef2c (M), Nkx2.5 (N), AFP (O), and Pax6 (P) expression levels were not significantly difference between static and shear pre-conditioned ESCs. (n=4; *=p<0.05).

Embryoid Body Differentiation

Following the 2 different pre-conditioning regimens (+/- shear), single-cell suspensions of the respective ESC populations were differentiated as EBs for up to 10 days using rotary orbital suspension culture (Fig. 4. 2A). Previous results from our group [77] [152] and others [153, 154] have indicated that continuous rotary orbital shaking promotes more homogeneous populations of EBs than static suspension cultures. On the second day of EB culture, EBs formed from ESCs pre-conditioned under static (Fig. 4.2 B) or shear (Fig. 4.2F) conditions appeared similar in gross morphology. After 4 days of culture, morphological differences became evident, as dark foci appeared in EBs formed from ESCs pre-conditioned at 5 dyn/cm² (Fig. 4.2G), while EBs formed from ESCs pre-conditioned at 0 dyn/cm² (Fig. 4.2C) were devoid of any such dark regions. Differences in EB morphology were more apparent on day 7 (Fig. 4.2D) with the presence of centrally located dark regions within EBs formed from shear pre-conditioned ESCs (Fig. 4. 2H). After 10 days of EB differentiation the differences in EB morphology between static and shear pre-conditioned ESCs were not detected (Fig. 4.2E, I). Significantly ($p < 0.001$) more EBs formed from shear pre-conditioned ESCs ($68.9 \pm 12.4\%$) contained dark regions compared to EBs formed from statically pre-conditioned ESCs ($6.1 \pm 6.4\%$) (Fig. 4.2K). However, at the same time point, the cross sectional area of (Fig. 4. 2J) EBs formed from ESCs pre-conditioned under static and shear were approximately $10,270.0 \pm 2,550.0$ and $10,120.0 \pm 2,210.0 \text{ } \mu\text{m}^2$, respectively. The similarity in EB size between EB groups suggested that the differences in morphogenic events between EB groups were independent of EB size. High magnification images of EBs containing statically pre-conditioned ESCs revealed uniform EB morphology (Fig. 4.2L) and histological analysis

demonstrated no distinct cellular organization (Fig. 4. 2N). However, EBs formed from shear pre-conditioned ESCs contained an optically opaque dark foci (Fig. 4.2M) centrally located within the EB that was similar in size to the cluster of cells observed through histological analysis (Fig. 4.2O). The striking difference in morphology between EBs containing shear pre-conditioned and statically cultured ESCs observed several days following pre-conditioning suggests that initial physical modulation of ESCs induced extended effects on EB morphogenesis.

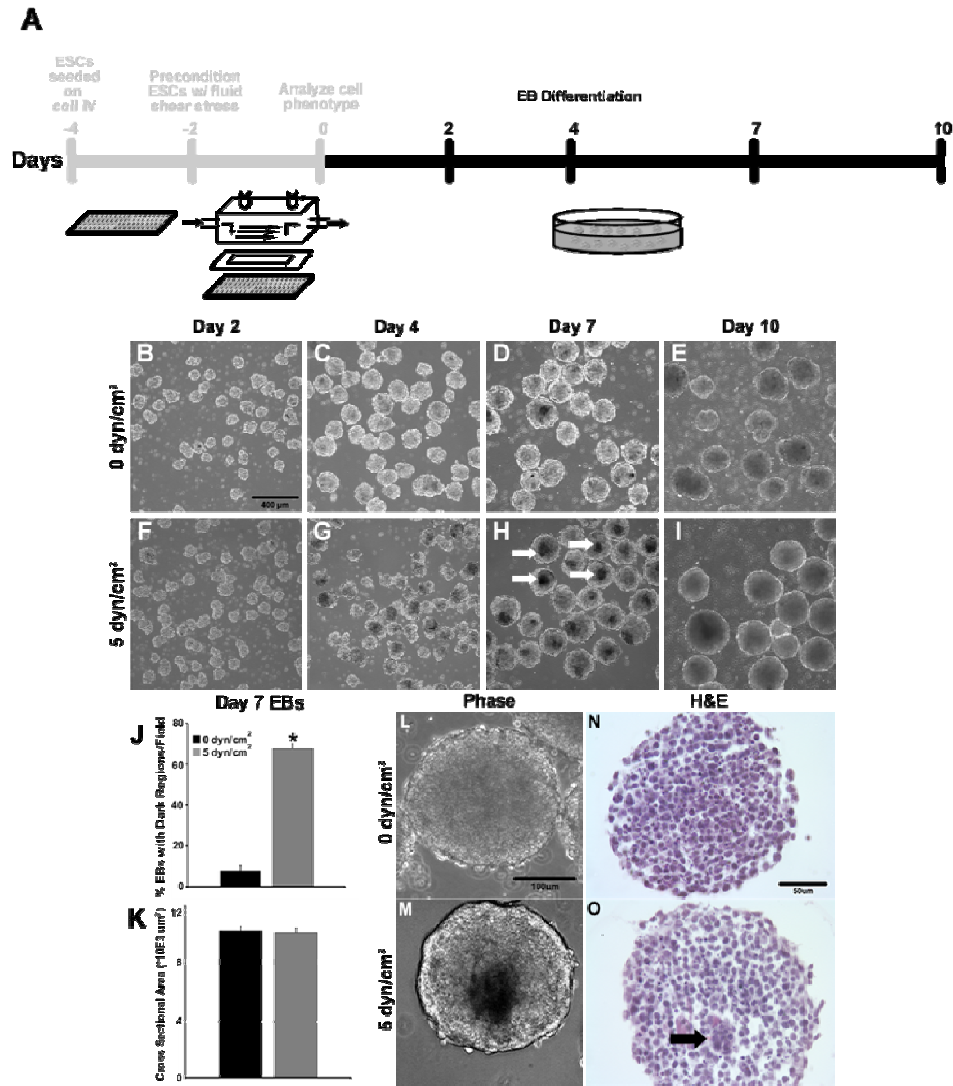


Figure 4.2. Embryoid body morphology. Shear and static pre-conditioned ESCs were differentiated as embryoid bodies for 10 days (A). Phase images of embryoid bodies formed from ESCs pre-conditioned at either 0 dyn/cm² (static) (B, C, D, and E) or 5 dyn/cm² (shear) (F, G, H, and I) at days 2, 4, 7, and 10 of differentiation. At day 7 significantly more EBs formed from shear pre-conditioned ESCs contain a dark foci (indicated by white arrows) compared to EBs formed from statically pre-conditioned ESCs (J). EBs formed from ESCs pre-conditioned at 0 dyn/cm² and 5 dyn/cm² have similar cross sectional areas (K), (n=6; Pairwise t-test *(p<0.05). High magnification phase images of day 7 EBs formed from 0 dyn/cm² (L) and 5 dyn/cm² (M) fluid shear stress pre-conditioned ESCs illustrate the difference in optical opacity of the dark foci compared to the other regions of the EB. Day 7 EBs stained with hematoxylin and eosin (H&E) (N and O). The arrow indicates a tightly packed cluster of cells which is centrally located within a day 7 shear pre-conditioned EB.

Endothelial and Hematopoietic Gene Expression

To examine the subsequent effects of fluid shear stress pre-conditioning on cardiovascular differentiation within EBs, the temporal gene expression patterns of endothelial and hematopoietic differentiation markers were assessed. *Flk-1*, which was higher in shear pre-conditioned ESCs immediately following shear pre-conditioning (i.e. day 0, Fig. 4.1F), remained elevated in EBs formed from shear pre-conditioned ESCs at days 2 ($p=0.001$) and 4 ($p=0.009$). However by day 7 and 10, *Flk-1* gene levels were similar between EB groups (Fig. 4.3A). While *Flt-1* gene levels were initially similar (day 0, 2, and 4) (Fig. 4.1G, 4.3B) in both populations, by day 7, shear pre-conditioned EBs expressed ($p=0.047$) elevated *Flt-1* expression compared to static pre-conditioned EBs (Fig. 4B). *Runx1* levels, which were higher in shear pre-conditioned ESCs prior to EB formation (i.e. day 0 Fig. 4.1J), were also higher in shear pre-conditioned EBs compared to static pre-conditioned EBs at day 4 ($p=0.03$) and day 7 ($p=0.001$) and similar at day 10 (Fig. 4.3C). *VE-cadherin* expression levels were greater in shear pre-conditioned ESCs (day 0, Fig. 4.1H) and higher at day 7 in EBs formed from shear pre-conditioned ($p=0.012$) ESCs when compared to EBs formed from statically pre-conditioned ESCs (Fig. 4.3D). While *PECAM* expression levels were initially higher in shear pre-conditioned ESCs (i.e. day 0, Fig. 4.1I), on day 2, *PECAM* expression levels were ($p=0.014$) lower in shear pre-conditioned EBs. However, *PECAM* expression was higher on day 7 ($p=0.01$) and day 10 ($p=0.02$) (Fig. 4.3E) in shear pre-conditioned EBs when compared to static pre-conditioned EBs. No differences in *Tall* gene expression were detected between static and shear pre-conditioned ESCs (i.e. day 0, Fig. 4.1K) or pre-conditioned EB groups until day 10 when static pre-conditioned EBs expressed

($p=0.001$) more *Tall* than shear pre-conditioned EBs (Fig. 4.3F). Following 7 days of EB differentiation, the time point at which distinct differences in EB morphology between shear and static pre-conditioned EBs were observed, 3 of the 4 endothelial genes examined, *Flt-1*, *VE-cadherin*, and *PECAM* were higher in shear pre-conditioned EBs. The differences in endothelial marker gene expression observed in EBs formed from statically cultured ESCs and shear pre-conditioned ESCs indicates fluid shear pre-conditioning had extended effects on ESC endothelial differentiation profile.

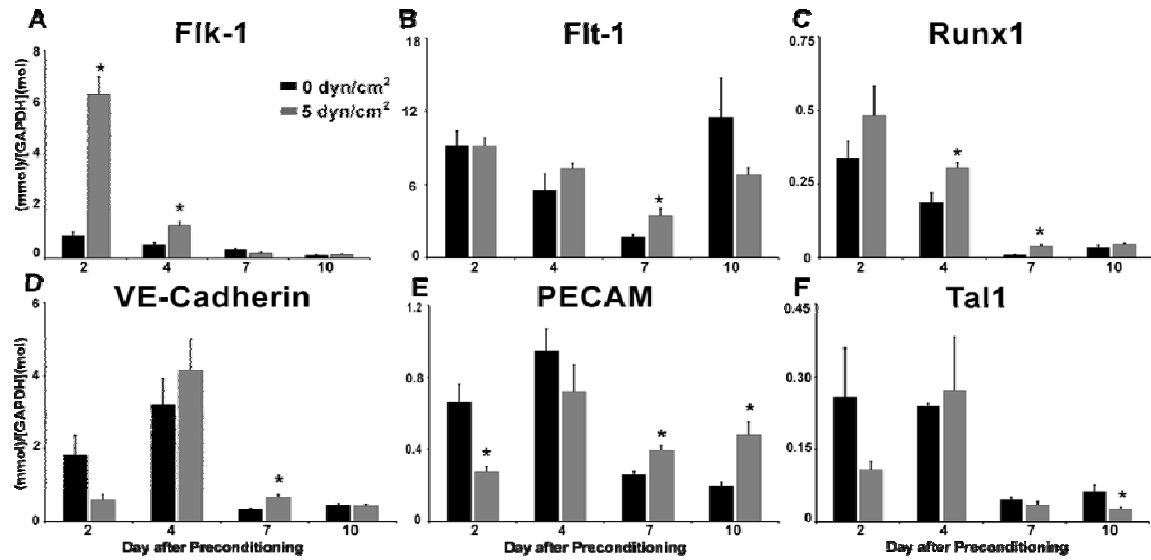


Figure 4.3: Endothelial and Hematopoietic marker gene expression. EBs formed from shear pre-conditioned ESCs exhibited greater expression of Flk-1 (A) on days 2 and 4 than EBs formed from 0 dyn/cm² pre-conditioned ESCs. However, on day 7 EBs formed from static pre-conditioned ESCs exhibited greater expression of Flk-1 than EBs formed from shear pre-conditioned ESCs. On day 7, EBs formed from shear pre-conditioned ESCs exhibited greater expression of Flt-1 (B), VE-cadherin (D), and PECAM (E) than EBs formed from 0 dyn/cm² pre-conditioned ESCs. Runx1 (C) and Tal1 (F) expression in EBs formed from fluid shear pre-conditioned ESCs decreases over time (n=3; *=p<0.05 compared to EBs formed from statically pre-conditioned ESCs at similar time point).

Embryoid Body Endothelial Protein Expression

To assess persistent effects of fluid shear stress pre-conditioning on ESC endothelial and hematopoietic differentiation within EBs endothelial and hematopoietic protein expression was analyzed. The presence of endothelial cells within EBs was analyzed by immunofluorescence staining of VE-cadherin, vWF, and PECAM. EBs formed from ESCs cultured under static conditions (0 dyn/cm²) did not appear to contain VE-cadherin positive cells at any of the time points examined (days 2, 4, 7, 10; Fig. 4.4A-D). However EBs containing shear pre-conditioned ESCs stained positively for VE-cadherin at all time points examined and the VE-cadherin positive cells remained centrally clustered within the EBs throughout differentiation (Fig. 4. 4E-H). Co-localization of the dark regions and VE-cadherin⁺ cell clusters was analyzed in day 7 EBs formed from static (Fig. 4.4I-K) and shear pre-conditioned groups. The dark regions observed by phase contrast microscopy in day 7 EBs containing shear pre-conditioned ESCs, overlapped with similar size VE-cadherin positive cell clusters (Fig. 4.4O-Q). Day 7 EBs formed from statically cultured ESCs were not positive for vWF (Fig. 4.4L-N). However, the VE-cadherin⁺ cell clusters within day 7 EBs formed from shear pre-conditioned ESCs exhibited co-localized staining for vWF expression, a more mature endothelial marker (Fig. 4.4R-T). While vWF was detected at day 7, vWF was not detected at days 2 or 4, suggesting that the VE-cadherin positive ESCs were differentiating into mature endothelial cells within the EB. Day 7 EBs formed from ESCs not pre-conditioned with shear lacked vWF expression (Fig. 6. 4L-M). PECAM, CD45 CD34, and CD41 expression was not detected in EBs formed from shear or static pre-conditioned ESCs. These results reveal that fluid shear stress pre-conditioning

promoted VE-cadherin protein expression in ESCs which led to specific VE-cadherin positive cell clustering at the center of EBs. Additionally, the EB microenvironment promoted further differentiation of endothelial like cells, as VE-Cadherin⁺ cells developed expression of a more mature endothelial marker protein vWF. Moreover, the expression of endothelial proteins VE-cadherin and vWF along with significantly higher expression of endothelial genes *VE-cadherin*, *PECAM*, and *Flt-1* on day 7 of EB differentiation reveals that fluid shear stress pre-conditioning promoted EB endothelial differentiation and morphogenesis.

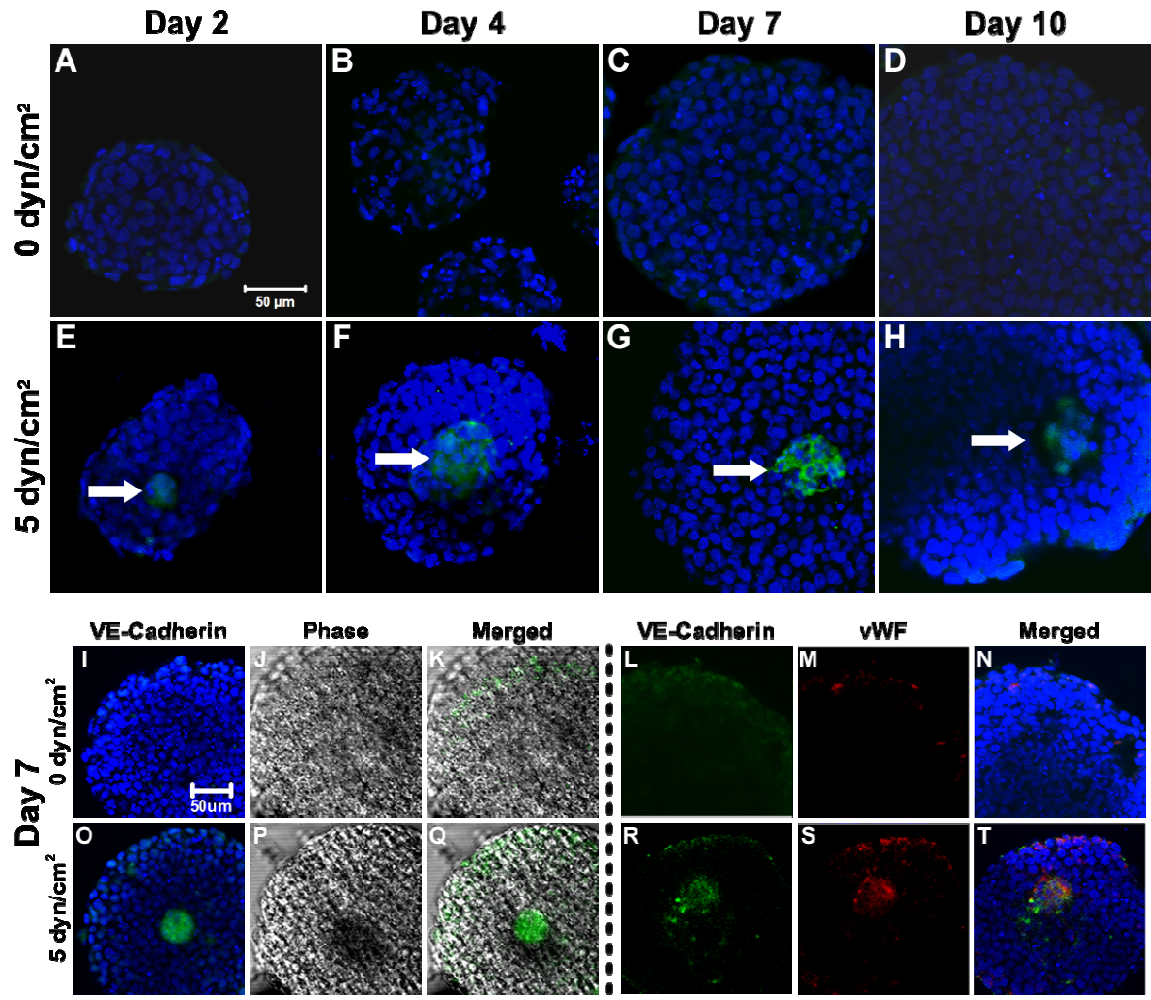


Figure 4.4: EB VE-cadherin and vWF expression. Embryoid bodies formed from ESCs pre-conditioned at 0 dyn/cm² do not contain VE-cadherin positive cells on days 2 (A), 4 (B), 7 (C), and 10 (D). However, embryoid bodies formed from ESCs pre-conditioned with 5 dyn/cm² fluid shear stress on day 2 (E), 4(F), 7 (G), and 10 (H) contain clusters of VE-cadherin positive cells. White arrows indicate clusters of VE-cadherin positive cells. Day 7 EBs formed from ESCs pre-conditioned at 0 dyn/cm² are negative for VE-cadherin (I, K, L) and vWF (M, N), and lack a dark region (J). Conversely, day 7 EBs formed from ESCs pre-conditioned at 5 dyn/cm² exhibits co-localization of VE-cadherin positive cell clusters (O) with the dark foci (P, Q) within the EB. Additionally, merged confocal microscopy images demonstrate that VE-cadherin positive cell clusters (J) are also positive for vWF (K) demonstrating these cluster of cells are endothelial-like (T).

Mixed Embryoid Bodies

To investigate cellular organization and segregation of different cell phenotypes within EBs, static and shear pre-conditioned ESCs were labeled with either CellTracker™ Red or Green after pre-conditioning and prior to EB formation. Three groups of EBs were formed; 1) EBs containing green and red static pre-conditioned ESCs, 2) EBs containing green and red shear pre-conditioned ESCs, and 3) EBs containing green static pre-conditioned ESCs and red shear pre-conditioned ESCs. EBs formed from static pre-conditioned ESCs labeled green and red did not exhibit any distinct cellular organization with red and green cells dispersed randomly throughout the EB at day 2 and 7 (Fig. 4.5A, D). However, day 2 and 7 EBs containing shear pre-conditioned ESCs labeled green and red contained clusters of cells centrally located within the EB composed of red and green cells (Fig. 4.5B, E). The cellular organization, location and size of labeled shear pre-conditioned ESCs within EBs was similar to that of the VE-cadherin⁺ cell clusters and dark regions previously observed. When green labeled static pre-conditioned ESCs and red labeled shear pre-conditioned ESCs were mixed to form EBs, clusters of cells centrally located within the EBs were observed (Fig. 4.5C, F). But, at day 2 these clusters only contained shear pre-conditioned ESCs labeled red, with static pre-conditioned ESCs labeled green located on the periphery of the EB. The same cellular organization persisted after 7 days of EB differentiation. These observations illustrate how different cell phenotypes, static pre-conditioned ESCs and shear pre-conditioned ESCs, spatially organized and segregated within EBs and confirmed that fluid shear stress promotes a distinct ESC phenotype.

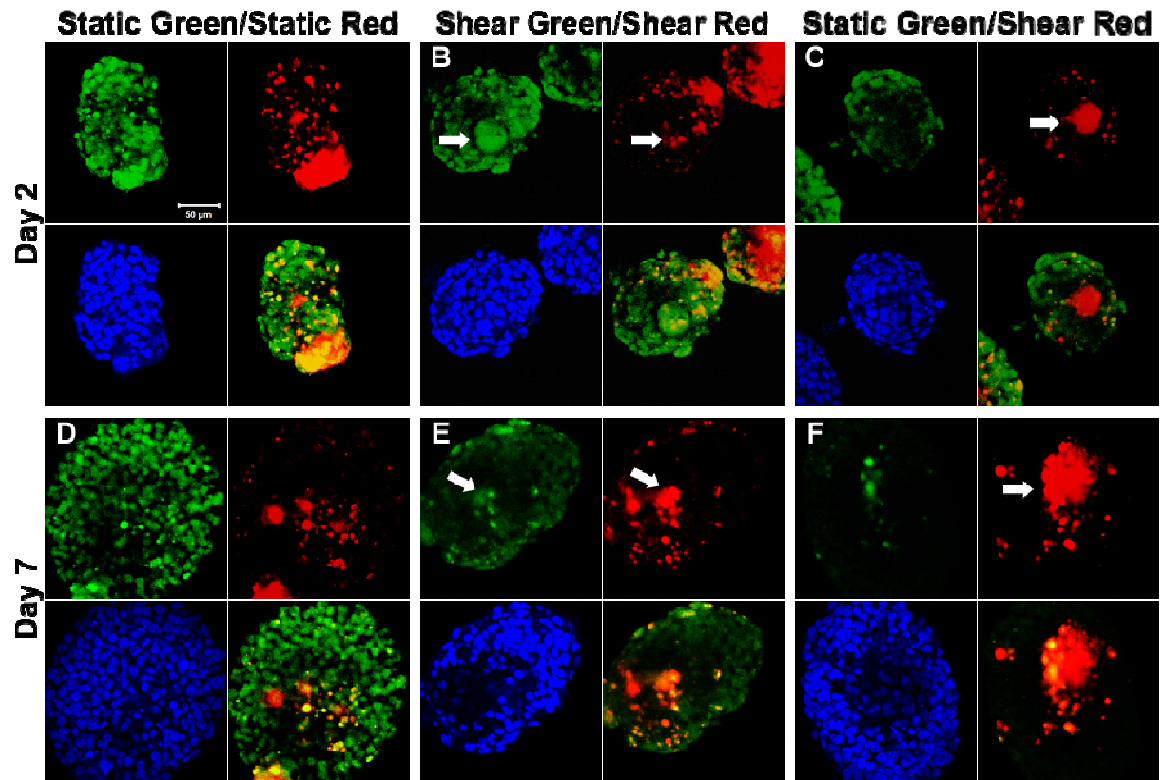


Figure 4.5: EBs formed from static and shear pre-conditioned ESCs. Day 2 EBs were formed from static ESCs labeled green and red(A). EBs containing shear pre-conditioned ESCs labeled green and shear pre-conditioned ESCs labeled red contain a cluster of red and green cells centrally located within the EB by day 2(B). However, day 2 EBs formed from ESCs not pre-conditioned with shear labeled green and shear pre-conditioned ESCs labeled red contained a cluster of red cells centrally located within the EB (C). Red and Green ESCs were randomly distributed throughout day 7 EBs containing static ESCs labeled green and red (D). Day 7 EBs comprised of green and red shear pre-conditioned ESCs had a cluster of red and green cells in the center of the EB (E). In addition, EBs formed from green static ESCs and red shear pre-conditioned ESCs had a cluster of red cells centrally located within the EB, on day 7(F).

Fluid Shear Pre-conditioning of pVE-cadherin GFP ESCs

In order to track VE-cadherin expression in ESCs after fluid shear stress pre-conditioning and during EB differentiation, pVE-cadherin GFP ESCs (VE-GFP ESCs) were cultured with or without shear for 48 hrs and then cultured as EBs for 7 days. Using VE-GFP ESCs allowed for real time visualization of VE-cadherin expression after shear pre-conditioning and during EB differentiation. Moreover, GFP as a readout for VE-cadherin expression allowed for direct detection of VE-cadherin positive cells rather than indirect detection of VE-cadherin⁺ cells (immunofluorescence, i.e. primary and secondary antibody coupling). Initial GFP expression was assessed in undifferentiated VE-GFP ESCs using fluorescence microscopy and flow cytometry. Undifferentiated VE-GFP ESCs displayed no detectable levels of GFP expression (Fig. 4.6A). Following the two pre-conditioning regimens, GFP⁺ ESCs were not observed in monolayers of ESCs pre-conditioned statically (Fig. 4.6B); however, GFP⁺ ESCs were visible through fluorescence microscopy in shear pre-conditioned populations (Fig. 4.6C). Flow cytometry analysis of GFP expression revealed $2.0\% \pm 0.1\%$, $21.6\% \pm 3.1\%$, and $23.4\% \pm 4.3\%$ of undifferentiated, statically pre-conditioned, and shear pre-conditioned VE-GFP ESCs were GFP (VE-cadherin) positive, respectively (Fig. 4.6D-F). While no differences in the percentage of GFP⁺ cells between shear and statically pre-conditioned groups was detected, the GFP mean fluorescence intensity was significantly higher ($p=0.015$) in shear pre-conditioned VE-GFP ESCs (1146 ± 119 fluorescence intensity) compared to statically pre-conditioned VE-GFP ESCs (964 ± 82 fluorescence intensity) (Fig. 4.6G). Furthermore, there was a larger shift in GFP mean peak fluorescence intensity between undifferentiated and shear pre-conditioned VE-GFP ESCs compared to

the shift in GFP mean peak fluorescence intensity between undifferentiated and statically pre-conditioned VE-GFP ESCs (Fig. 4.6H-I). Day 7 EBs formed from statically pre-conditioned VE-GFP ESCs were devoid of dark regions and GFP+ cell clusters (Fig. 4.7A,B), which paralleled day 7 EBs formed from statically pre-conditioned ESCs (Fig. 4.7F). Throughout EB differentiation, GFP+ cells were not observed in statically pre-conditioned VE-GFP EBs (Fig. 4.7C-E). However, EBs formed from shear pre-conditioned VE-GFP ESCs exhibited dark regions at day 7 (Fig. 4.7F) which co-localized with the dark regions at the center of the EBs (Fig. 4.7G), similar to those observed previously with non-transfected shear pre-conditioned ESCs (Fig. 4.7G). Furthermore, GFP+ cell clusters were observed in EBs formed from shear pre-conditioned VE-GFP ESCs (Fig. 4.7H-J) at all time points examined. The dark regions and GFP+ cell clusters observed in EBs formed from shear pre-conditioned VE-GFP ESCs confirmed the observations reported in the fluid shear stress pre-conditioning ESC studies.

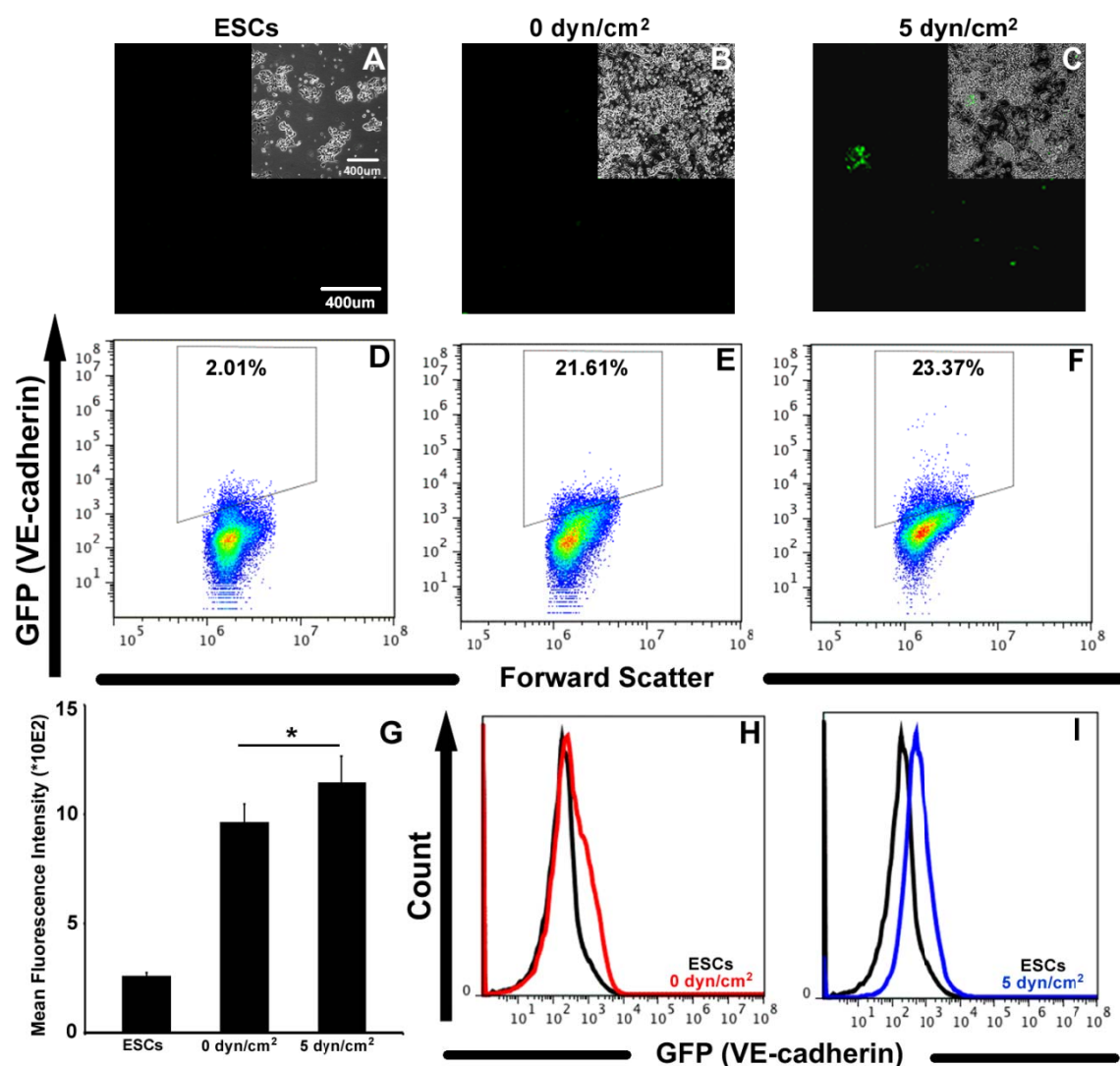


Figure 4.6: Fluid shear stress pre-conditioned pVE-cadherin GFP ESCs. GFP positive cells in monolayers of undifferentiated (A) and statically pre-conditioned pVE-cadherin GFP ESCs (B) were not detected through fluorescence microscopy, while monolayers of shear pre-conditioned pVE-cadherin GFP ESCs (C) contained populations of GFP positive cells. Single cell analysis of GFP expression, using at 2% gate on undifferentiated pVE-cadherin GFP ESCs (D), revealed no significant difference in the percentage of GFP positive cells between static (E) and shear (F) pre-conditioned pVE-cadherin GFP ESCs. Significant differences were observed in GFP mean fluorescence intensity (G) between pre-conditioned regimens. There was no noticeable shift in GFP mean fluorescence intensity between undifferentiated pVE-cadherin GFP ESCs and pVE-cadherin GFP ESCs pre-conditioned at 0 dyn/cm² (H), however there was a marked shift in GFP mean fluorescence intensity between undifferentiated pVE-cadherin GFP ESCs and pVE-cadherin GFP ESCs pre-conditioned at 5 dyn/cm² (I).

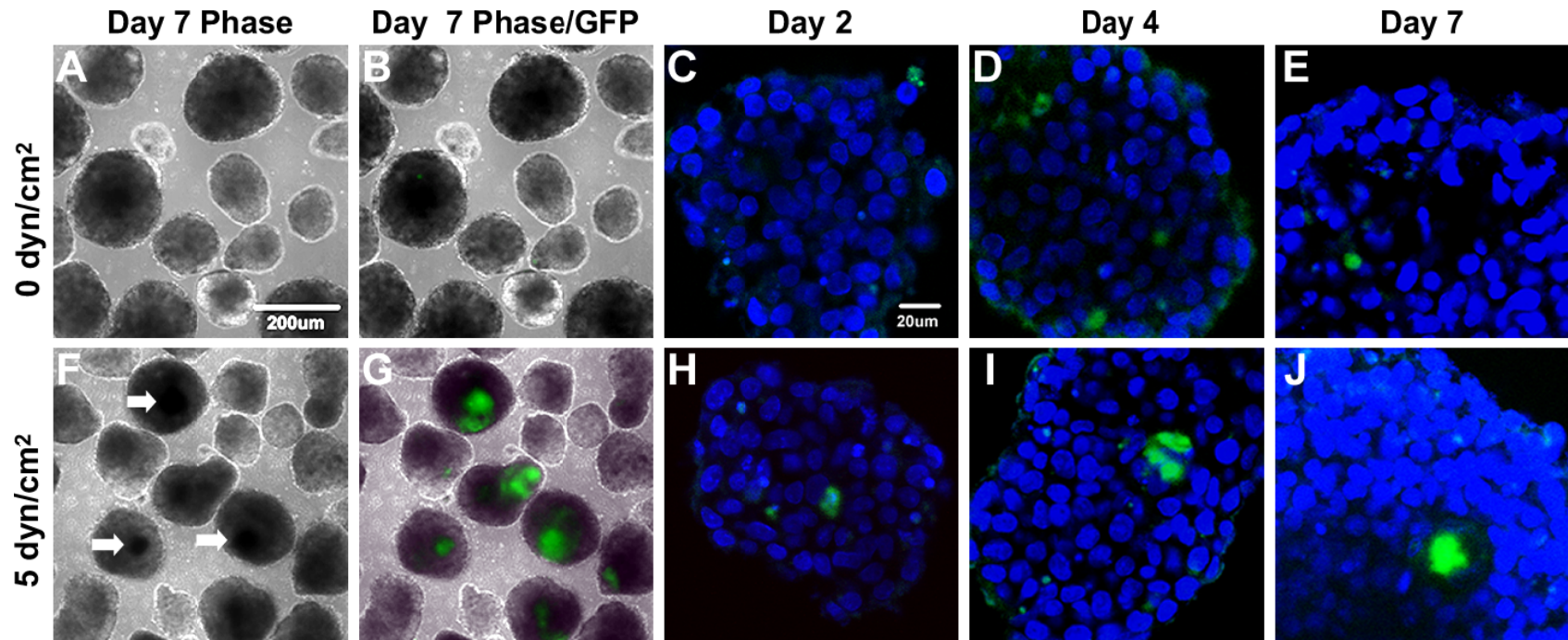


Figure 4.7: EBs formed from shear pre-conditioned pVE-cadherin GFP ESCs. EBs formed from static pre-conditioned pVE-cadherin GFP ESCs did not develop dark foci (A) and lack GFP positive cell clusters (B). Additionally, GFP positive cell clusters were not detected at day 2(C), 4(D), and 7(E) in EBs formed from static pre-conditioned pVE-cadherin GFP ESCs, using confocal microscopy. Following 7 days of EB differentiation shear pre-conditioned pVE-cadherin GFP EBs developed dark foci (F) which colocalized with GFP expressing cells (G). GFP positive cell clusters were observed at day 2 (H), 4 (I), and 7 (J) in shear pre-conditioned pVE-cadherin GFP EBs.

Fluid Shear Stress Magnitude Effects on ESCs

Following 48 hours of fluid shear stress stimulation, ESC morphology and differentiation were examined. ESCs cultured under static, 5 dyn/cm², and 15 dyne/cm² (Fig. 4.8 A-C) displayed no distinct differences in morphology. Flk-1, a mesoderm gene and VEGF receptor gene expressed by endothelial cells was higher in ESCs exposed to 5 and 15 dyn/cm² compared to ESCs cultured statically (Fig. 4.8D). However, fluid shear stress decreased Pax6, an ectoderm gene (Fig. 4.8E). Fluid shear stress had no effect on AFP expression as all ESC groups expressed similarly low levels of AFP, a marker for endoderm differentiation (Fig. 4.8F). Vascular endothelial cadherin, a cadherin exclusively expressed on endothelial cells, was increased in shear pre-conditioned ESCs ($p < 0.05$) (Fig. 4.8G). However, Flt-1, VEGF receptor 1, was only higher ($p < 0.05$) in ESCs pre-conditioned at 5 dyn/cm² compared to ESCs cultured statically (Fig. 4.8H). PECAM expression was not different between statically cultured or shear pre-conditioned ESCs. Overall the data suggested that exposing ESCs to fluid shear initiates mesodermal endothelial differentiation. In general, there were few differences in gene expression between the two shear regimens suggesting that the fluid shear stress physical stimulation, irrespective of fluid shear stress magnitude promotes an endothelial phenotype in ESCs.

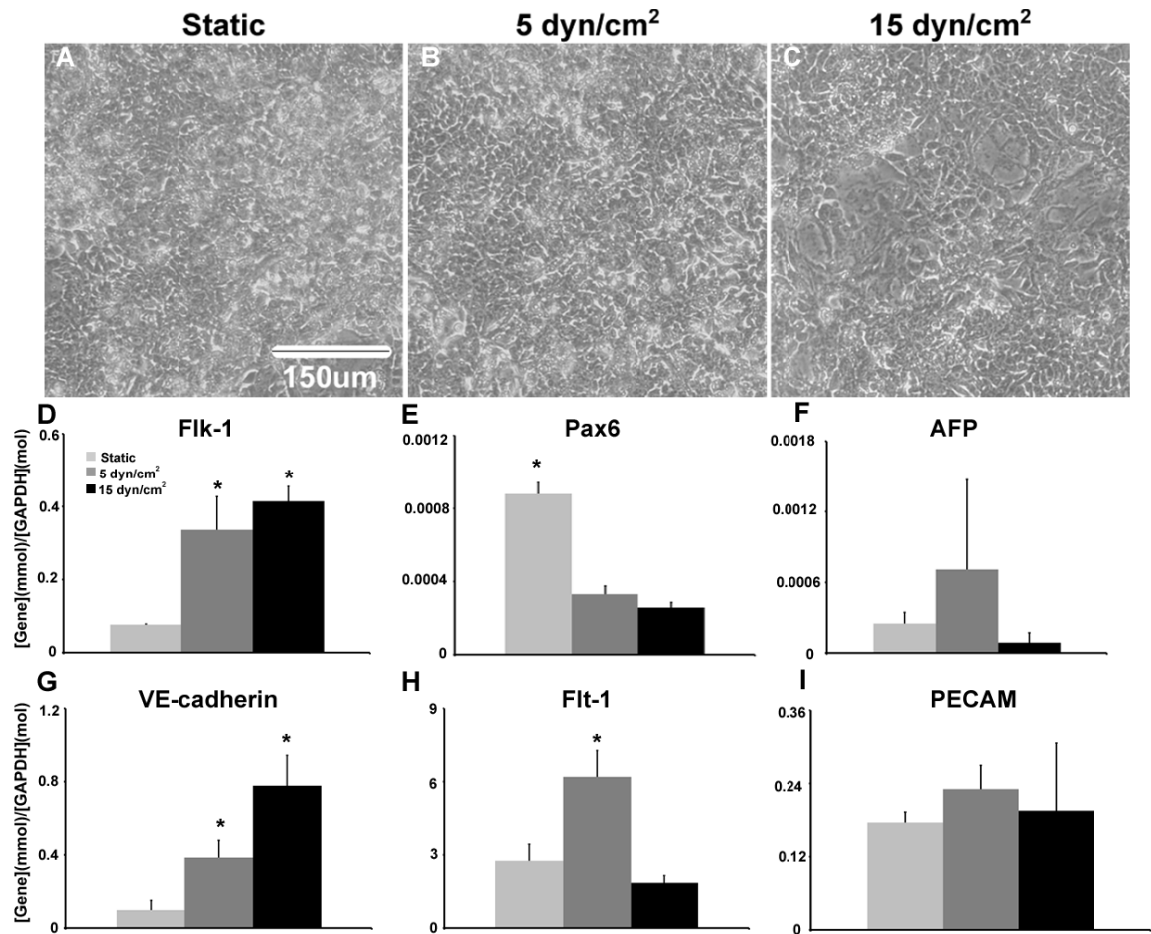


Figure 4.8. Morphology and gene expression of pre-conditioned ESCs. Phase images of ESCs cultured statically (A), and at 5 (B) and 15 (C) dyn/cm² demonstrated no significant difference in morphology. Mesoderm and endothelial gene Flk-1 (D) was higher in ESCs cultured at 5 and 15 dyn/cm². Fluid shear stress decreased expression of ectoderm gene Pax6 (E). Endoderm gene AFP is expressed at similarly low levels in static and shear groups (F). VE-cadherin (G) was expressed significantly higher in ESCs cultured at 5 and 15 dyn/cm². ESCs exposed to 5 dyn/cm² expressed higher levels of Flt-1 (H) compared to ESCs cultured under static conditions. PECAM was expressed at similar levels in all ESC groups (I). (n=3-6, *=p<0.05 compared to all groups)

Following the 3 different pre-conditioning regimens (static, 5 dyn/cm², 15 dyn/cm²), single-cell suspensions of the respective ESC populations were differentiated as EBs for up to 10 days using rotary orbital suspension culture (Fig. 4.9A). On the second day of EB culture, ESCs pre-conditioned at 0, 5, and 15 dyn/cm² yielded significantly different amounts of EBs (0 dyn/cm² - $2,716 \pm 196$, 5 dyn/cm² - $4,6377 \pm 510$, 15 dyn/cm² - $7,167 \pm 440$ EBs per plate) (Fig. 4.9A). While the EB cross sectional area for 0, 5, and 15 dyn/cm² was $8,44.8 \pm 265.5$, $6,643.3 \pm 156.8$, $11,686.5 \pm 327.5$ μm^2 , respectively (Fig. 4.9B-E). The differences in EB yield and cross sectional area after 2 days of EB culture between EB groups suggests that fluid shear stress affects subsequent aggregation kinetics of ESCs. After 4 days of culture, morphological differences became evident, as dark foci appeared in EBs formed from ESCs pre-conditioned at 5 and 15 dyn/cm² (Fig. 4.9G,H), while EBs formed from ESCs pre-conditioned at 0 dyn/cm² (Fig. 4.9F) were devoid of any such dark regions ($8.3 \pm 2.4\%$). Differences in EB morphology became more apparent on day 7 (Fig. 4.9I) with the presence of dark regions within EBs formed from shear pre-conditioned ESCs (Fig. 4.9J,K). While both EB groups formed from shear pre-conditioned ESCs developed dark regions, the spatial patterning of the dark regions between groups was distinctly different. EBs formed from ESCs pre-conditioned at 5 dyn/cm² ($67.7 \pm 2.4\%$) developed dark regions which localized to the center of the EB while EBs formed from ESCs pre-conditioned at 15 dyn/cm² ($66.6 \pm 2.4\%$) developed dark regions that varied in shape and location within EBs, yielding a more morphologically heterogeneous EB population (Fig. 4.9 J,K). By day 10, all EB groups looked distinctly different from one another (Fig. 4.9L-N), with dark regions only observed in EBs formed from ESCs pre-conditioned at 5 dyn/cm². Quantitative analysis

of the percentage of day 7 EBs which developed dark regions in pre-conditioned EB groups illustrated that EBs formed from statically cultured ESCs developed less dark regions compared to EBs formed from shear pre-conditioned ESCs (Fig. 4.9 M). The significant difference in morphology between EBs containing shear pre-conditioned and statically cultured ESCs observed 7 days following pre-conditioning suggested that the exposure to fluid shear stress exerted subsequent effects on ESC clustering, organization, and morphogenesis within EBs.

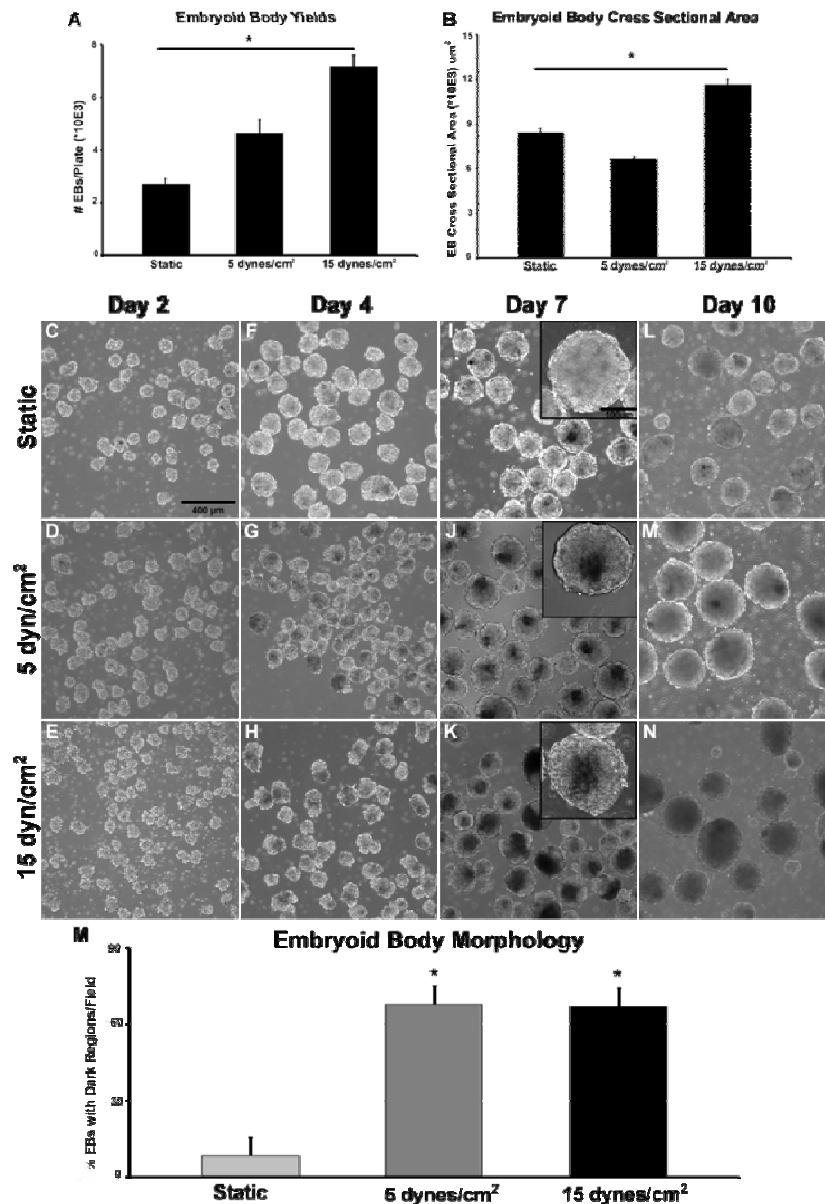


Figure 4.9. Embryoid Body Morphology. After 2 days of EB differentiation statically cultured ESCs formed fewer EBs compared to ESCs exposed to shear (A) ($n=3-6$, $^*p<0.05$). Day 2 embryoid body size was largest in ESCs pre-conditioned at 15 dyn/cm^2 (B) ($n=4$ (total of 110-118 EBs), $^*p<0.05$). Phase images of EBs formed from ESCs cultured at 0 dyn/cm^2 (C, F, I, L), 5 dyn/cm^2 (D, G, J, M), and 15 dyn/cm^2 (E, H, K, N) exhibited distinct differences in EB morphology at day 7 and 10 of EB culture with the presence of dark regions in 5 and 15 dyn/cm^2 groups (scale bar= $400\mu\text{m}$, inset scale bar= $100\mu\text{m}$). Following 7 days of EB culture, EBs formed from statically pre-conditioned ESCs did not develop dark regions while EBs formed from shear pre-conditioned ESCs developed significantly more dark regions (D) ($n=9$ fields from 3 independent replicates, $^*p<0.05$ compared to Static).

VE-cadherin Localization

Endothelial morphogenesis and differentiation were assessed at day 7 by examining expression of endothelial adhesion molecules vascular endothelial cadherin (VE-cadherin) and platelet endothelial cell adhesion molecule (PECAM). VE-cadherin was not detected in the static EBs (Fig. 4.10E); however VE-cadherin positive cell clusters were detected in EBs formed from ESCs cultured at 5 (Fig. 4.10F) and 15 dyn/cm²(Fig. 4.10G). More interestingly, the VE-cadherin⁺ cell clusters observed at the center of the EBs co-localized with the dark regions observed in the phase images. VE-cadherin positive cell clusters were only observed at the center of the EB in a circular pattern. PECAM expression was not detected in any of the EBs. The correlation between EB morphology and VE-cadherin⁺ cellular organization within shear pre-conditioned EBs at day 7 indicated that these EBs underwent endothelial morphogenesis and that fluid shear stress pre-conditioning of ESCs had prolonged effects on endothelial differentiation within EBs.

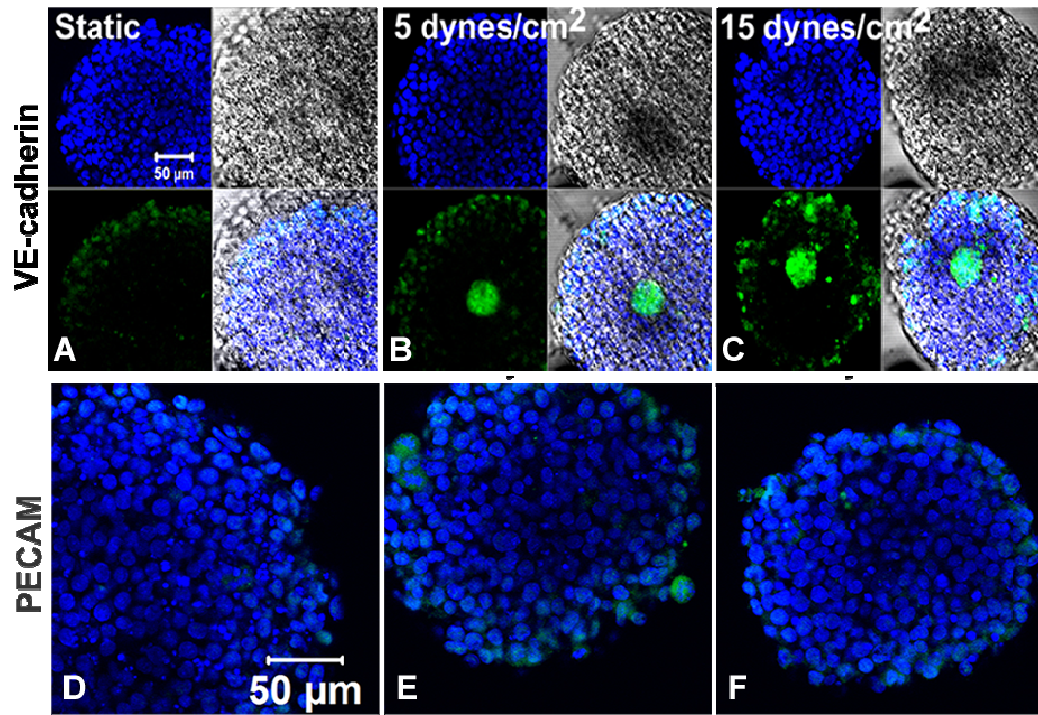


Figure 4.10: VE-cadherin and PECAM expression. VE-cadherin expression was not detected in EBs containing statically cultured ESCs (A), however EBs formed from ESCs cultured at 5 (B) and 15 (C) dyn/cm² contain clusters of VE-cadherin positive cells. These VE-cadherin positive cell clusters co-localize with the dark regions observed through phase microscopy. PECAM was not detected in EBs formed from statically cultured ESCs(D). While few PECAM positive cells were detected in EBs formed from ESCs culture 5 (E), or 15(E) dyn/cm² (Blue=Nuclei, Green=VE-cadherin or PECAM, scale bars=50μm).

Embryoid Body Endothelial Gene Expression

Immediately after exposure to fluid shear stress, ESCs expressed significantly higher levels of endothelial genes. Therefore in order to examine if exposure to fluid shear stress had extended effects on endothelial differentiation, genes *Flk-1*, *Flt-1*, *VE-cadherin*, and *PECAM* were analyzed during EB differentiation of shear pre-conditioned ESCs. *Flk-1* levels in EBs containing ESCs pre-conditioned at 5 dyn/cm² was highest at day 2 compared to the other time points examined and then progressively decreased from day 2 to day 10 (Fig. 4.11 A). ESCs cultured statically and at 15 dyn/cm² did not display any significant changes in *Flk-1* expression during EB culture. EBs formed from ESCs cultured under static conditions expressed higher levels of *Flt-1* on day 2 compared to day 7. While EBs formed from ESCs exposed to 5 dyn/cm² shear stress expressed decreased levels of *Flt-1* on day 7 compared to all other time points examined (Fig. 4.11-B). *VE-cadherin* expression peaked at day 4 in EBs groups formed from statically cultured ESCs and ESCs exposed to 5 dyn/cm² shear stress (Fig. 4.11C). *PECAM* gene expression remained relatively low in EB groups and was not altered between EB groups or across time points (Fig. 4.11D). Lack of PECAM gene expression changes correlated with low levels of PECAM protein expression observed in day 7 EB groups. The changes and differences in endothelial gene expression profile of EBs formed from shear pre-conditioned ESCs indicated that fluid shear stress has prolonged effects on EB endothelial differentiation profile and modulates EB temporal endothelial marker gene expression. However, in general no significant differences were detected between EB groups in gene expression at similar time points.

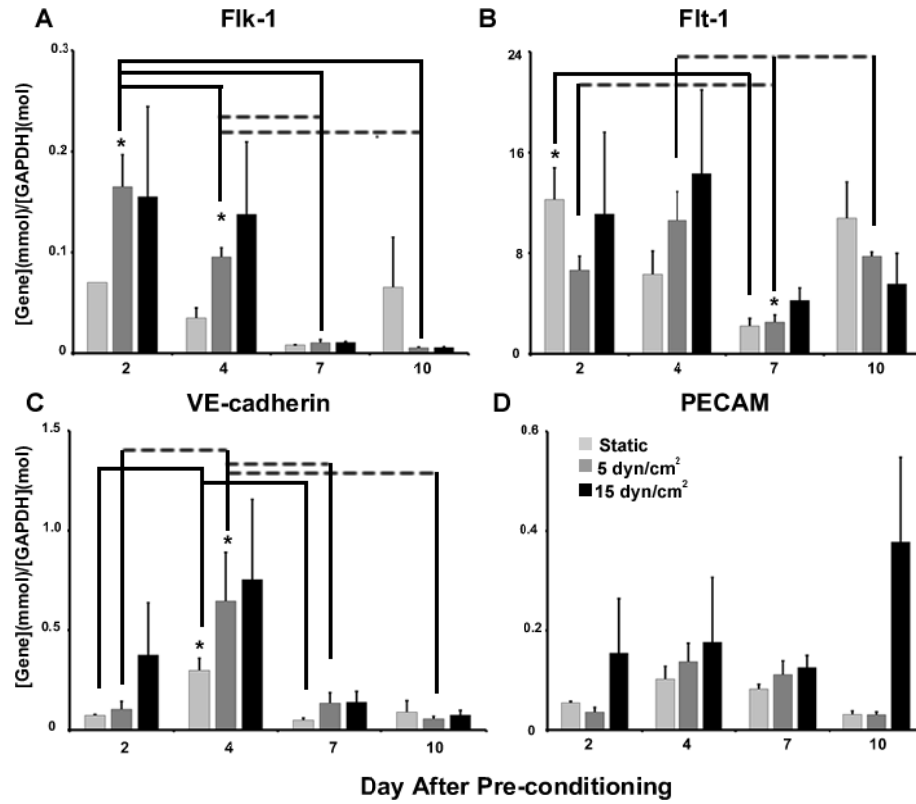


Figure 4.11: Embryoid body endothelial marker gene expression. *Flk-1* (A) expression levels were highest at day 2 compared to day 4, 7, and 10 in EBs formed from 5 dyn/cm² shear pre-conditioned ESCs. *Flt-1* (B) was highest in EBs formed from statically cultured ESCs at day 2. Day 7 EBs formed from 5 dyn/cm² shear pre-conditioned EBs expressed significantly lower *Flt-1* compared to day 2, 4, and 10. *VE-cadherin* (C) expression peaked at day 4 in EBs formed from statically cultured ESCs and EBs formed from ESCs pre-conditioned at 5 dyn/cm². PECAM (D) expression was not significantly altered throughout EB differentiation. (n=3-4, *=p<0.05 compared to samples linked by bars)

Discussion

In this study, the extended effects of fluid shear stress pre-conditioning on ESCs endothelial differentiation and morphogenesis within EBs were assessed. Immediately following fluid shear stress exposure, ESCs expressed elevated levels of endothelial genes while still retaining pluripotent characteristics. Centrally organized clusters of VE-cadherin⁺ cells were observed as early as 2 days following initial formation of EBs from shear pre-conditioned ESCs. The central clusters of cells, observed in EBs formed from shear pre-conditioned ESCs, which were clearly distinguishable by phase contrast microscopy alone at day 7, persisted for up to 10 days of differentiation in suspension culture. Moreover, EBs formed from shear pre-conditioned ESCs expressed significantly more endothelial genes on day 7 than EBs formed from static pre-conditioned ESCs. GFP⁺ cell cluster formation in EBs formed from shear pre-conditioned VE-GFP ESCs verifies the results observed in EBs formed from shear pre-conditioned ESCs. The results revealed that fluid shear stress increased expression of endothelial markers Flk-1, PECAM, and VE-cadherin, which leads to increased endothelial differentiation, as well as endothelial cell patterning, and morphogenesis of ESCs within EBs. More specifically this study demonstrates fluid shear stress stimulation of ESCs during early differentiation has persistent effects on ESC EC differentiation and morphogenesis.

Recent studies have examined acute effects of fluid shear stress on ESC differentiation. However, ESC differentiation profile and morphogenesis within EBs days after fluid shear exposure have not been examined [81, 85, 148]. Previous studies examining the effects of fluid shear stress on ESC monolayers have reported increases in endothelial genes and proteins, such as Flk-1, Flt-1, PECAM, and VE-cadherin, and

ability to form tubular structures and uptake acetylated LDL [80, 84, 148]. In such studies, varying manners and magnitudes of fluid shear stress have been examined, including pulsatile and laminar at magnitudes ranging from 0.98 to 10 dynes/cm² [84, 85]. While initial studies were performed examining 5 and 15 dyn/cm², gene expression, protein expression and EB morphogenesis results were similar. However for the studies reported herein, 5 dyn/cm² was investigated further because this magnitude is more representative of the physiological shear stress embryonic stem cells experience in the embryo since the wall shear stress in the dorsal aorta at day 10.5 of development in the mouse embryo is 5 dyn/cm² [89]. An increase in the expression of Runx1 in shear-preconditioned ESCs parallels the results of a recent study in which mouse ESC Flk-1+ cells isolated from EBs cultured for 3.25 days and sheared at 5 dyn/cm² for 30 hours demonstrated an increased expression of Runx1 and CD41 [89]. In addition, ESC-derived endothelial cells, vascular progenitor cells, and hematopoietic progenitor cells have been reported to exhibit changes in morphology and increased expression of endothelial, vascular, and hematopoietic genes in response to fluid shear stress exposure [85-87, 89, 155]. In contrast to previous studies which focused primarily on examining the phenotype effects of fluid shear stress on stem cells immediately following the application of shear stress, this study examined the temporal response of fluid shear preconditioned ESCs undergoing differentiation as EBs and the downstream effects of fluid shear stress on ESC differentiation.

Endothelial and hematopoietic cells originate from mesoderm via a common precursor, the hemangioblast [59, 60]. The hemangioblast is defined by its expression of Flk-1, SCL/Tal-1, CD34, and CD133, [61, 62, 156]. During early embryogenesis,

aggregates of hemangioblasts in the extraembryonic yolk sac(primitive hematopoiesis) and aorta-gonad-mesonphros (definitive hematopoiesis) mature and form blood islands, which consist of an inner core of blood cells and an outer layer of endothelial cells [63, 157]. The organization of hematopoietic and endothelial cells into blood islands initiates the onset of vascular development and expansion, whereby blood island cells migrate, divide, and create connections to form the yolk sac vasculature [58]. The striking similarities in morphology between the dark regions observed in EBs formed from shear pre-conditioned ESCs and blood islands, which appear dark in contrast to other parts of the developing embryo, develop at the center of the embryo and are comprised of endothelial cells, suggests that EBs formed from shear pre-conditioned ESCs may be recapitulating yolk sac hematopoiesis [30, 156, 158]. In the developing embryo blood islands develop in the center of the embryo, are optically opaque and darker in contrast compared to other regions of the embryo [157, 159]. Moreover, the co-expression of VE-cadherin and vWF, a prothrombotic glycoprotein synthesized and secreted by vascular endothelial cells for platelet adhesion to sites of vascular damage [160], indicates that the cluster of cells are becoming mature endothelial cells. The endothelial maturation of fluid shear stress pre-conditioned ESCs at the center of EBs suggests that the EB microenvironment supports ESC endothelial differentiation and subsequent maturation.

The organization of VE-cadherin+ cells within EBs formed from shear pre-conditioned ESCs illustrates cadherin mediated selective cell adhesion and indicates that these cells are differentiating into endothelial cells. Cadherins play an important role in selective cell adhesion, tissue organization, segregation and morphogenesis [161, 162].

In vitro, cadherins played a role in the reorganization of single cells dissociated from chick embryonic liver, kidney and skin when implanted back into the chick embryo, to form liver, kidney, and skin tissue having a similar architecture and morphology as found in the naturally developing embryo [163]. VE-cadherin, a cadherin specifically expressed at the intercellular junctions of endothelial cells [164] is essential for vascular morphogenesis [165, 166]. Vascular formation during embryogenesis is imperative for the development of the cardiovascular system, which supplies oxygen and nutrients to all developing tissues. Therefore, lack of VE-cadherin would lead to impaired tissue morphogenesis of developing organs, vasculogenesis and angiogenesis within the embryo [165]. The presence of VE-cadherin⁺ cells at the core of EBs is analogous to previous in vitro studies in which VE-cadherin⁺ cell clusters were observed in day 6 EBs cultured with an angiogenic growth factor mixture [55], suggesting that fluid shear stress pre-conditioning accelerated the kinetics of vascular differentiation of ESCs similar to angiogenic factors.

The maturation of VE-cadherin⁺ ESCs following fluid shear pre-conditioning during EB culture suggests that the EB microenvironment promotes endothelial differentiation. One such microenvironment property which may have played a role in endothelial maturation and differentiation is hypoxia. EBs which exceed 200µm in diameter generally develop necrotic cores due to lack of oxygen and nutrient transport[167]. By day 7 EBs formed from shear pre-conditioned ESCs had diameters which suggest oxygen gradients were present within the EB. Hypoxia has been reported to promote ESC vascular differentiation, endothelial expansion, and angiogenesis within EBs [24, 111]. Additionally, hypoxia mediates temporal expression of VEGF receptors,

Flk-1 and Flt-1 [24]. During embryogenesis, hematopoiesis and angiogenesis occur as diffusion of oxygen is inhibited due to embryo growth, causing an oxygen gradient, throughout the embryo, [18] which regulates, Flk-1, Flt-1, and VEGF, genes required for differentiation and organization of the cardiovascular system [25].

The differences in EB yield and size between statically cultured and shear pre-conditioned ESCs indicated differences in aggregation kinetics during EB formation. Undifferentiated ESC aggregation during EB formation is mediated by E-cadherin binding [75], while ESCs which lack E-cadherin fail to aggregate [153]. Several studies have demonstrated that when cells expression different cadherin subtypes are cultured in suspension form aggregates with cells expressing similar cadherins [168, 169]. Additionally, differences in EB cross sectional area may have been attributed to increased proliferation of fluid shear pre-conditioned ESCs [81, 85].

The findings of this study reveal that fluid shear stress has subsequent effects on ESC endothelial differentiation and primitive vascularization within EBs. The results illustrate that pre-conditioning ESCs with fluid shear stress prior to EB formation enhanced endothelial differentiation within EBs and yielded approximately 70% of EBs containing cells undergoing endothelial differentiation. In addition, fluid shear stress induced ESCs to express an endothelial specific cadherin which appeared to promote subsequent specific cell adhesion and organization, and vascular morphogenesis within EBs. Furthermore, the morphogenic events and gene expression patterns observed in EBs formed from shear pre-conditioned ESCs 7 days following physical stimulation provides evidence that physical modulation of ESCs during early differentiation has extended effects on the differentiation path of ESCs.

Conclusion

The findings of this study revealed that fluid shear stress has subsequent effects on ESC endothelial differentiation and localization and patterning of VE-cadherin positive cells in EBs. Applying different magnitudes of fluid shear to ESCs prior to EB formation elicited differences in EB morphology but only subtle differences in endothelial marker gene expression profile. However, major differences were observed between shear pre-conditioned ESCs and ESCs cultured statically. ESCs pre-conditioned with shear underwent distinctly different morphogenic events within EBs compared to ESCs cultured statically. Additionally, pre-conditioning ESCs prior to EB formation led to a unique endothelial gene expression profile when compared to statically culturing ESCs. Furthermore, dark centrally located regions, only observed in EBs formed shear pre-conditioned EBs, correlated with the organization of endothelial-like cells at the center of the EB. Altogether, the results demonstrate that exposing ESCs to shear promotes spatial localization and organization of endothelial-like cells within EBs.

CHAPTER 5

VEGF EFFECTS ON ENDOTHELIAL DIFFERENTIATION OF FLUID SHEAR STRESS PRE-CONDITIONED EMBRYONIC STEM CELLS

Introduction

Pluripotent embryonic stem cells (ESCs) represent an attractive cell source for regenerative medicine and tissue engineering applications due to their inherent ability to differentiate into numerous cell types needed for therapies to replace a variety of damaged tissues. For cardiovascular applications, endothelial cells (ECs) are needed to line the vascular grafts and to provide vascularization in tissue engineered substitutes. Acquiring, isolating, and expanding the quantities of endothelial and endothelial progenitor cells required for tissue engineering applications is difficult due to loss of phenotype in vitro and decrease in quantities found in vivo [170, 171]. Challenges in isolation and expansion of autologous EC sources demonstrate the need for new potential cell sources for ECs.

Established protocols to derive endothelial cells from embryonic stem cell (ESC) monolayers require extensive culture periods and labor intensive cell sorting methods. Additionally, these methods use large quantities of VEGF and extracellular matrix, only yielding heterogeneous populations with few cells expressing markers for endothelial differentiation such as, Flk-1 and VE-cadherin [54, 149]. In order to overcome the challenges of using chemical cues to derive ECs from ESCs, physical cues have been investigated as an alternative method. Fluid shear stress, which is experienced by

endothelial cells *in vivo*, has been utilized to promote endothelial differentiation of a multitude of stem and progenitor cell populations [81, 88, 148, 172].

EBs can give rise to cells of the 3 germ layers including, endothelial cells [32, 58, 173]. However, without directed differentiation strategies such as growth factor stimulation, endothelial differentiation within EBs is heterogeneous and inefficient [58, 173]. In order to more efficiently direct endothelial differentiation within EBs, researchers have used growth factors such as VEGF [45, 55]. Soluble delivery of growth factors has led to inefficient EB differentiation because soluble delivery of molecules generally only affects the cells at the periphery of the EB due to diffusion barriers at the exterior of the EB [174, 175]. The EB outer layer of tight cell-cell contacts is a great limitation in using growth factors to direct and control EB differentiation. To overcome diffusion limits at the exterior of EBs, the McDevitt laboratory has developed a method to deliver growth factors at the interior of the EB through use of microparticles or micropsheres which have the ability to bind and release morphogens [174]. Microparticles can be made of adhesive extracellular matrix with which cells can potentially bind and interact. Therefore, during EB formation microparticles can be incorporated within the EB structure by allowing ESCs and microparticles to aggregate together. Once the microparticles are within the EB they can locally release growth factors and potentially affect ESC differentiation within the EB.

Previous studies in chapters 3 and 4 have revealed that pre-conditioning ESCs prior to EB differentiation elicits clustering of endothelial like cells (VE-cadherin⁺) at the center of EBs. Thus, this study aimed to further direct endothelial differentiation in EBs by pre-conditioning ESCs with fluid shear stress prior to EB formation and then treating

these EBs with VEGF. Two methods of VEGF delivery were examined 1) soluble and 2) via microparticles. VEGF was delivered via microparticles to allow for VEGF release within the interior of the EB in contrast to soluble delivery which relies on free diffusion of factors from the outside of the EB into the interior of the EB. The effects of VEGF stimulation on directing EB endothelial differentiation, endothelial morphogenesis, and cell patterning within EBs were analyzed and compared in EBs formed from statically cultured ESCs and EBs formed from shear pre-conditioned ESCs.

Methods

ESC and EB Culture

D3 and D3 pVE-cadherin GFP ESCs as previously described in Chapter 3. EBs treated with soluble VEGF were fed with differentiation media supplemented with 50ng/ml VEGF (R&D) and maintained on a rotary orbital shaker (Chapter 3). EBs which contained gelatin microparticles (MPs) were formed by placing $\approx 2 \times 10^6$ cells and $\approx 666,000$ gelatin MPs (1 MP:3 cells) in 10mL of differentiation media on a rotary orbital shaker.

Gelatin Microparticle Fabrication and VEGF Loading

Gelatin microparticles (MPs) were fabricated using an adaptation of a previously published protocol [176]. 2mL of a 10% w/v solution of gelatin B (Sigma Aldrich) in deionized water as heated to 55C and then added drop-wise to 60mL of corn oil and homogenized for 5min at 5000RPM in order to create a water-in-oil emulsion. Following

homogenization the solution was cooled for 10 min at 4°C. The MPs were then retrieved through centrifugation at 200xg and washed in 25mL acetone 3 times. Next the MPs were crosslinked at room temperature with 5mM glutaraldehyde, 0.1% w/v Tween 20 solution in deionized water under agitation. Following 15 hours of crosslinking, the MPs were centrifuged and treated with 25mL of 25mM glycine in deionized water to block residual aldehyde groups. MPs were washed 3 times in 25mL deionized water. Prior to use for EB incorporation, gelatin MPs were loaded with VEGF by adding 125ng of VEGF to 1mg ($\approx 2.5 \times 10^6$ MPs) of MPs briefly centrifuged (15-30s) and then incubated at 4°C for 4-6 hours. Unloaded gelatin MPs (-VEGF MPs) and VEGF loaded gelatin MPs (+VEGF MPs) were used for experiments.

Immunostaining of Cryosectioned EBs

EB samples were prepared for cryofixation after being fixed in 10% formalin for 30 minutes at room temperature, washed 3 times with PBS, and resuspended in 200-400ul Histogel. Histogel-embedded EB samples were soaked in 30% sucrose at 4°C overnight followed by infiltration with sucrose and OCT solutions under vacuum at -20inHg pressure. Optimal sucrose and OCT infiltration were accomplished by serially decreasing the volume of sucrose and increasing the volume of OCT through use of the following 20% sucrose:OCT ratio by volume solutions; 4:1, 2:1, 1:2, and 0:1. Samples were then embedded in OCT in a cryomold in dry ice and 95% ethanol to allow for quick freezing to prevent ice crystal formation. OCT samples were then sectioned at 10 μ m using a cryostat (LEICA Cryostat HM 355S), affixed to Superfrost Plus (VWR) glass slides. Cryosectioned samples were then fixed using acetone for 10 min at -20°C, rinsed

3 times with PBS for 5 minutes, and then blocked using 2% donkey serum in PBS for 45 min at room temperature. Next samples were rinsed twice in PBS for 5 min and then incubated with primary antibody (1:200) diluted in 2% donkey serum in PBS at 4°C overnight. Following primary incubation sections were rinsed 3 times in PBS for 5 minutes and then incubated with secondary antibody (1:500) and Hoechst (1:100) diluted in 2% donkey serum in PBS for 1 hr at room temperature. Samples were then rinsed in PBS 3 times, coverslipped using Flouregel Mounting media, and then imaged the following day using a Ziess 510 LSM Multiphoton confocal microscope.

Results

Embryoid Body Morphology

Following pre-conditioning (+/- shear), ESCs were further differentiated as EBs and treated either with (+VEGF) or without (-VEGF) soluble VEGF, with microparticles loaded with VEGF (+VEGF MPs), or unloaded microparticles (-VEGF MPs). During EB differentiation of soluble and microparticle VEGF treatment elicited vastly different EB morphologies between PC Static and PC Shear EB groups. At day 2, EBs which did not contain microparticles (Fig. 5.1 A, B, E, F) and were more homogeneous in shape and size in comparison to EBs which contained microparticles (Fig. 5.1 C,D, G, H). Following 4 days of EB differentiation, PC Shear -VEGF EBs (Fig. 5.1 I) developed large dark regions which were not observed in PC Shear +VEGF EBs (Fig. 5.1 N). Day 4 PC Static +VEGF MPs EB (Fig. 5.1K) appeared larger in size compared to all other EB groups. By day 4 EBs which did contain microparticles no longer exhibited uniform shape and size (Fig. 5.1, I, J, M, N). On day 7, PC Static -VEGF (Fig. 5.1Q) and PC Static +VEGF (Fig. 5.1R) EBs displayed a similar morphology with very few EBs developing dark regions. As observed in previous studies, dark regions within day 7 PC Shear EBs were indicative of VE-cadherin positive cell clustering (Chapter 3). On the other hand, day 7 PC Static EBs + VEGF MPs (Fig. 5.1S) and -VEGF MPs (Fig. 5.1T) both developed variable-sized dark regions within the EB populations. In contrast to the PC static -VEGF EBs, PC Shear -VEGF EBs (Fig.. 4.1U) developed dark foci at the center of the EBs. However, after 7 days of soluble VEGF treatment of PC Shear EBs (Fig. 5.1 F), dark regions were not observed. PC Shear +VEGF MPs (Fig. 5.1G) and PC Shear -VEGF MPs (Fig. 5.1H) developed similar morphology to PC Static EBs treated

with MPs, as they contained optically opaque regions of varying sizes throughout the EB samples. Altogether, the distinct differences in EB morphologies between PC Static and PC Shear EBs induced by VEGF treatment (+/- VEGF) and VEGF treatment method (soluble vs. released from MPs) demonstrated that VEGF has an effect on EB morphology and morphogenesis. Moreover, soluble VEGF treatment elicited a different EB morphology in shear pre-conditioned ESCs compared to statically cultured ESCs.

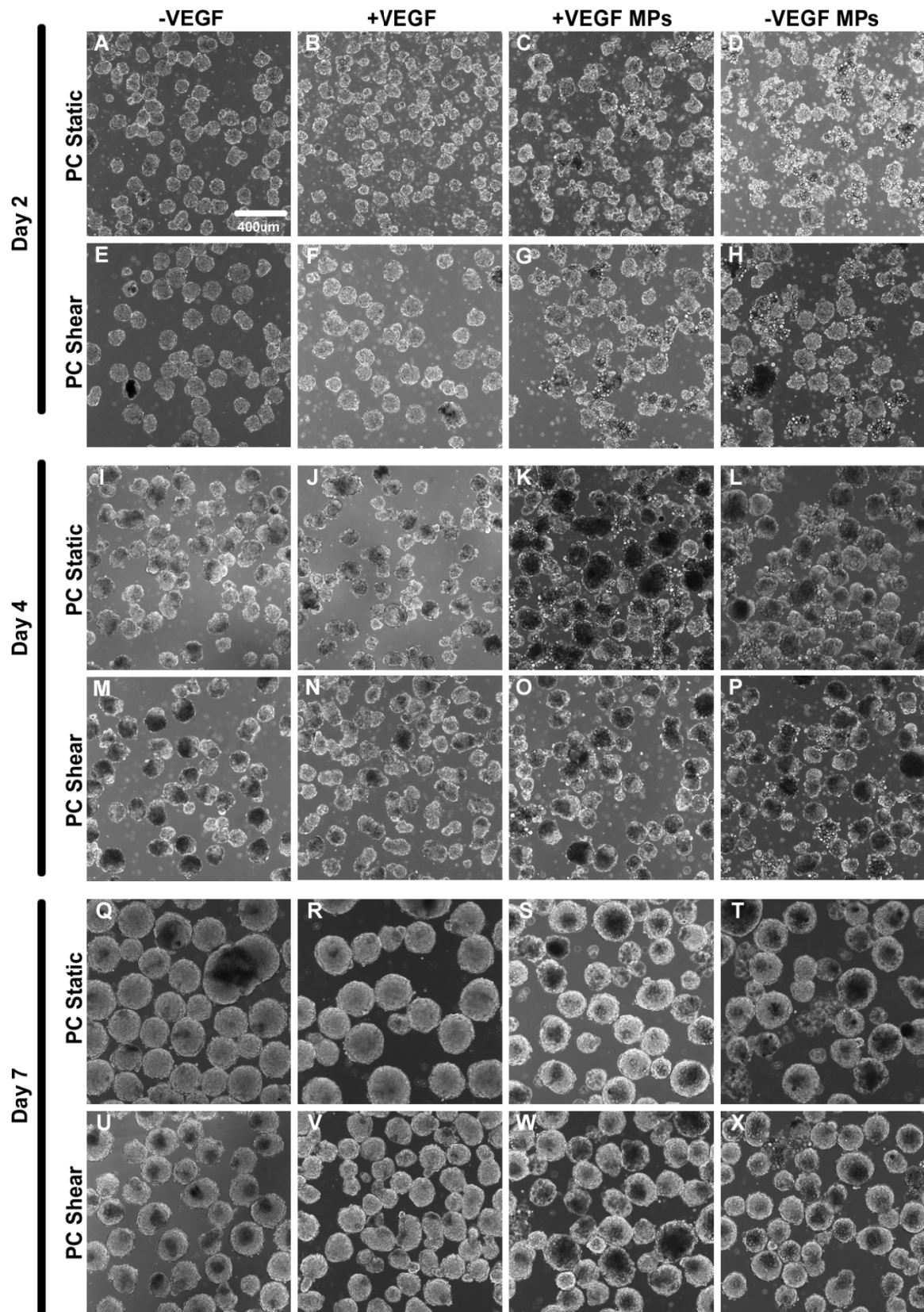


Figure 5.1: Embryoid Body Morphology. Following 2 days of EB culture EBs not containing microparticles (A, B, E, F) were more uniform than EBs which contained microparticles (C, D, G, H). At day 4 soluble VEGF treatment did not elicit different EB morphology in PC Static EBs (I, J). However, on day 4 PC Shear –VEGF EBs (M) contained dark regions which were not observed in PC Shear +VEGF EBs (N). By day 4 PC Static +VEGF MP EBs (K) appeared larger in sized compared to all other day 4 EB groups. Day 4 PC Static –VEGF MPs (L), PC Shear + VEGF MPs (O) and PC Shear –VEGF MPs appeared similar morphologically (P). At day 7, PC Static –VEGF EBs (Q) look similar in morphology to PC Static +VEGF EBs (R). However, PC Static +VEGF MPs (S) and PC Static –VEGF MPs (T) develop a distinctly different morphology with noticeable dark foci of varying sizes throughout the EB populations. PC Shear –VEGF EBs developed dark regions at the centroid (U). While dark regions were not observed in PC Shear +VEGF EBs (V), PC Shear +VEGF MPs (W) and PC Shear –VEGF MPs (X) develop dark regions of dissimilar sizes throughout the EB populations. (scale bar=400µm)

Endothelial Gene Expression

After 4 and 7 days of EB differentiation, PC Shear and PC Static EBs treated with VEGF were analyzed for expression of endothelial marker genes *Flk-1*, *Flt-1*, *VE-cadherin*, and *PECAM*. Gene expression was calculated as relative fold change by comparing all PC Static groups to PC Static –VEGF and all PC Shear groups to PC Shear –VEGF. Treatment with VEGF did not alter *Flk-1* expression in PC Static EB groups at day 4 or 7, however, PC Shear +VEGF EBs expressed the highest levels of *Flk-1* on day 4 and day 7 compared to any other EB group (Fig. 5.2A). Soluble or microparticle VEGF treatment of PC Static EBs did not alter *Flt-1* expression levels at any of the time points examined (Fig. 5.2B). However, PC Shear +VEGF expressed the highest levels of *Flt-1* when compared to all other EB groups. While, PC Shear +VEGF MPs and PC Shear –VEGF MPs expressed higher levels of *Flt-1* than PC Shear –VEGF, there were no differences in *Flt-1* expression between PC Shear +VEGF MPs and PC Shear –VEGF MPs (Fig. 5.2 B). *VE-cadherin* expression was highest in PC Shear +VEGF EBs at day 4 and 7. PC Shear +VEGF MPs and –VEGF MPs expressed comparable levels of *VE-cadherin* at day 4 (Fig. 5.2C). After 4 days of EB differentiation, PC Shear +VEGF EBs, PC Shear +VEGF MPs EBs, as well as PC Shear –VEGF MPs EBs expressed significantly higher levels of *PECAM* compared to PC Shear –VEGF EBs. However, by day 7 PC Shear +VEGF, PC Shear +VEGF MPs, and PC Shear –VEGF MPs EBs groups were significantly higher than PC Shear –VEGF and all PC Static EB groups but were not significantly different from one another (Fig. 5.2D). In general, VEGF treatment of EBs formed from statically cultured ESCs elicited no significant changes in *Flk-1*, *Flt-1*, *VE-cadherin*, or *PECAM* expression. However, VEGF treatment induced substantial

increases in *Flk-1*, *Flt-1*, *VE-cadherin*, and *PECAM* in EBs formed from shear pre-conditioned ESCs, with soluble VEGF treatment causing the largest increase in expression of endothelial marker genes. Even though *Flk-1* and *Flt-1* are VEGF receptors, *Flk-1* expression was only higher in EBs treated with soluble VEGF that were formed from shear pre-conditioned ESCs, while *Flt-1* expression was increased in VEGF treated EBs formed from shear pre-conditioned ESCs. Interestingly, addition of unloaded microparticles elicited increases in *Flt-1*, *VE-cadherin*, and *PECAM* in EBs formed from shear pre-conditioned ESCs. Overall, the results suggest that VEGF treatment enhanced the expression of endothelial marker genes only in EBs formed from shear pre-conditioned ESCs.

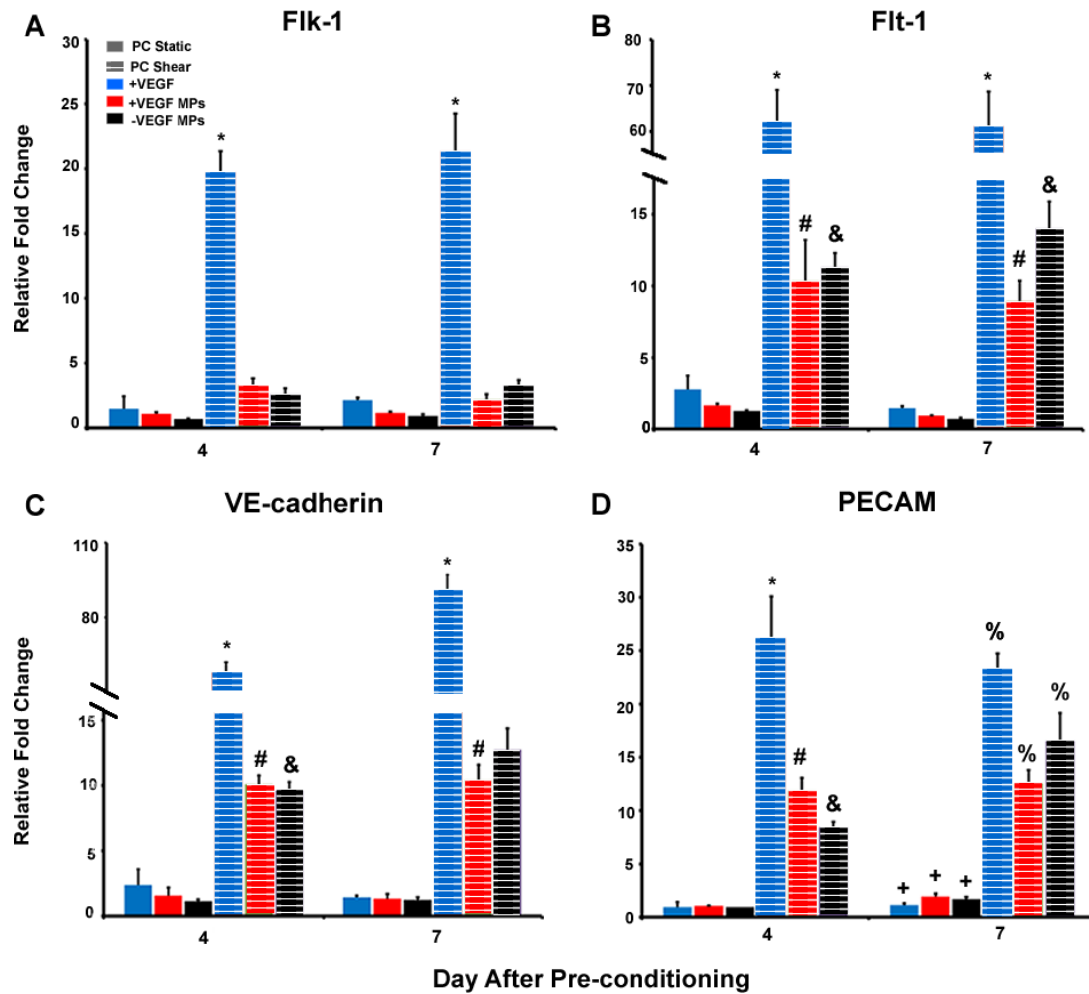


Figure 5.2: Endothelial marker gene expression of VEGF treated EBs. Gene expression is represented as relative fold change over untreated at similar time points (i.e. D4 PC Static +VEGF/ D4 PC Static –VEGF, D7 PC Shear +VEGF MPs/ D7 PC Shear –VEGF) *Flk-1* gene expression was highest in PC shear EBs treated with soluble VEGF at days 4 and 7 compared to all other treatment groups (A). *Flt-1* gene expression was not significantly altered in PC static EBs when treated with soluble VEGF or VEGF released from microparticles compared to untreated PC static EBs (B). PC shear EBs, irrespective of VEGF treatment method, expressed significantly higher levels of *VE-cadherin* than PC static EB samples (C). On day 4 *PECAM* gene expression was highest in PC shear EBs treated with soluble VEGF. However, by day 7 there was no difference in *VE-cadherin* gene expression in PC shear EBs treated with soluble VEGF and VEGF released from microparticles (D). (n=4-6, *=p<0.05 compared to all groups, #=p<0.05 significantly different from all groups except PC shear –VEGF MPs, &=p<0.05 significantly different from all groups except PC shear +VEGF MPs, +=p<0.05 compared to all PC shear groups, %=p<0.05 compared to PC shear -VEGF)

EB VE-cadherin Expression and Localization

EBs formed from pre-conditioned ESCs and treated with VEGF were examined for VE-cadherin protein expression and organization after 7 days of EB differentiation. PC Static –VEGF EBs displayed no detectable VE-cadherin expression (Fig. 5.3A). However, confocal images of PC Static +VEGF EBs suggested VE-cadherin expression was localized to the periphery of the EBs (Fig. 5.3B). Similar to PC Static –VEGF EBs, VE-cadherin⁺ cells were not detected in PC Static +VEGF MPs and –VEGF MPs (Fig. 5.3 C, D). VE-cadherin⁺ cells localized at the center of PC Shear –VEGF EBs (Fig. 5.3E), which is consistent with previous studies (Chapters 3). In contrast, VE-cadherin expression was confined to the periphery of PC Shear +VEGF EBs (Fig. 5.3F). PC Shear +VEGF MPs and –VEGF MPs EBs developed clusters of centrally located VE-cadherin⁺ cells (Fig. 5.3G,H) which is similar to VE-cadherin⁺ cellular organization observed in PC Shear –VEGF EBs. While confocal microscopy allows imaging within 3D structures, it artificially enhances fluorescence at the periphery of 3D structures. Therefore in order to better visualize and confirm VE-cadherin expression at the periphery of EBs, cryosections of EBs were assessed for VE-cadherin expression. While, VE-cadherin was not detected PC Static –VEGF EBs (Fig. 5.4A), low levels of VE-cadherin expression was detected in PC Static +VEGF, PC Static +VEGF MPs, and PC Static –VEGF MPs (Fig. 5.4B-D). The VE-cadherin expression observed in the cryosections and confocal images were similar in PC Static +VEGF EBs. Unlike PC Static –VEGF EBs, VE-cadherin expression was observed in PC Shear –VEGF EBs (Fig. 5.4 E). PC Shear +VEGF EBs contained a number of VE-cadherin⁺ cells localized to the periphery of the EB (Fig. 5.4F) which paralleled the VE-cadherin staining pattern observed in PC Shear +VEGF EBs. VE-cadherin was expressed at low levels in both PC

Shear +VEGF MPs and PC Shear –VEGF MPs (Fig. 5.4 G, H). Confocal images of PC Shear and PC Static EBs treated with or without VEGF demonstrated that VE-cadherin cellular organization and expression is modulated by method of VEGF delivery. In general, soluble delivery of VEGF induced VE-cadherin expression to localize to the periphery of EBs, while VEGF released from microparticles appeared to have no effect on VE-cadherin expression and cellular organization.

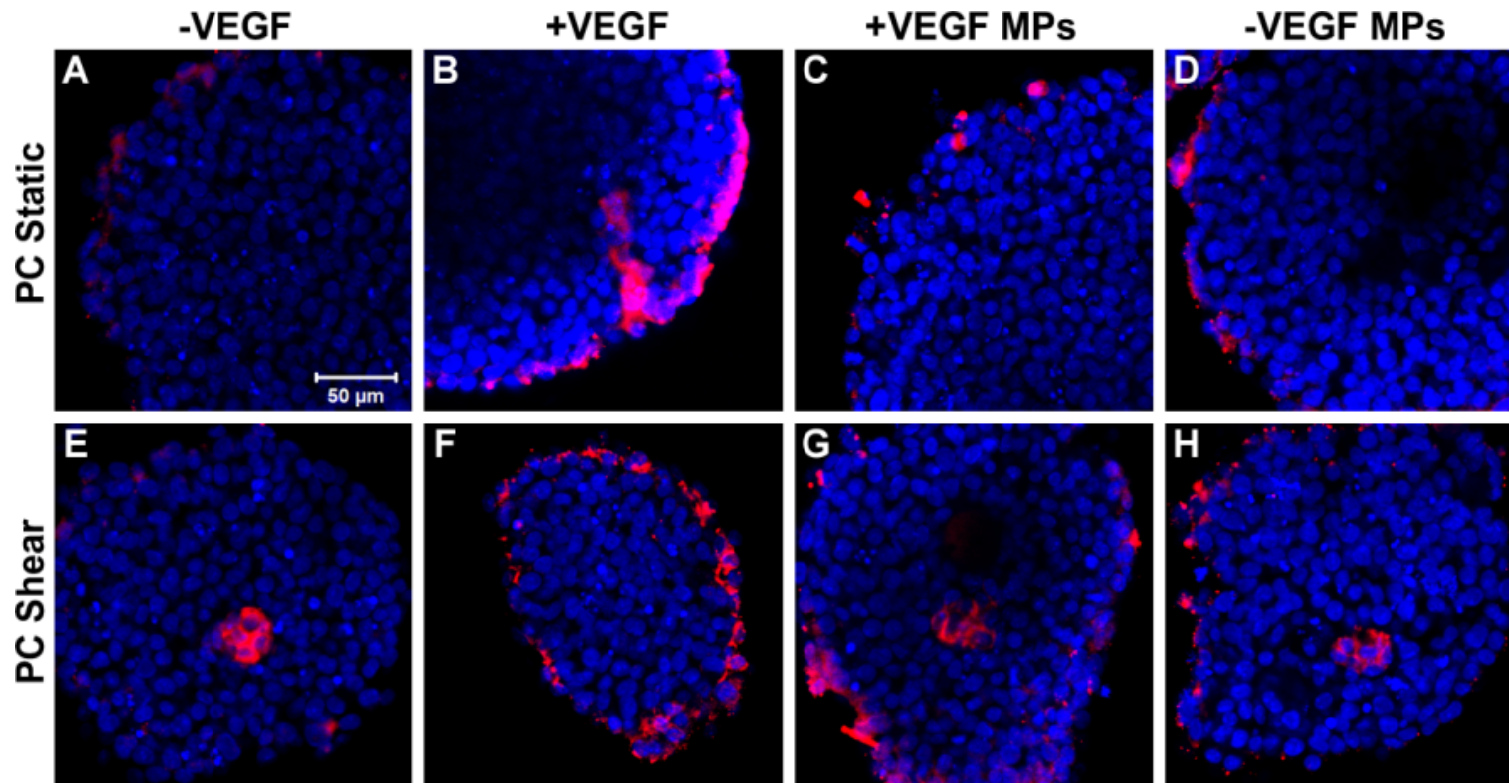


Figure 5.3: Confocal images of VE-cadherin protein expression in day 7 VEGF treated EBs. VE-cadherin expression was not observed in PC Static –VEGF EBs (A). However, VE-cadherin expression localized to the periphery of PC Static +VEGF EBs (B). Analogous to PC Static –VEGF EBs, VE-cadherin was not detected in PC Static +VEGF MPs and PC Static –VEGF MPs (C,D). PC Shear –VEGF EBs (E) developed a centroid of VE-cadherin+ cells. In contrast VE-cadherin expression was confined to the periphery of PC Shear +VEGF EBs (F). Comparable to PC Shear –VEGF EBs, PC Shear +VEGF MPs and PC Shear –VEGF MPs EBs developed clusters of VE-cadherin+ cells. (blue=nuclei, red=VE-cadherin, scale bar=50um)

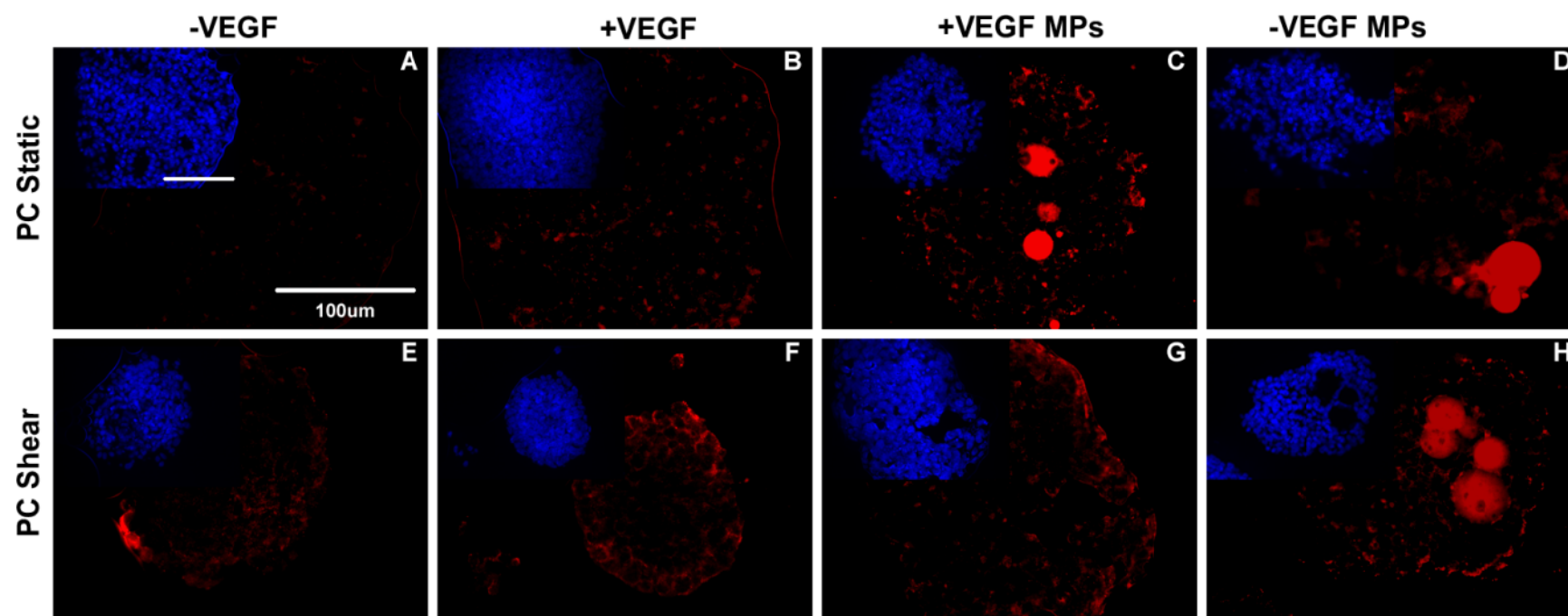


Figure 5.4: VE-cadherin Expression at the periphery day 7 VEGF treated EBs. Inset is hoescht stain of corresponding EB section. VE-cadherin was not detected in PC Static –VEGF EBs (A). However low levels of VE-cadherin was detected in PC Static –VEGF (B), PC Static +VEGF MPs (C), and PC Static –VEGF MPs (D). VE-cadherin was expressed at low levels in PC Shear –VEGF EBs (E). VE-cadherin was detected in a number of cells in PC Shear +VEGF EBs (F) while, VE-cadherin was detected at low levels in PC Shear +VEGF MPs (G) and PC Shear –VEGF MPs (H). Large circular red staining represents microparticles. (blue=nuclei, red=VE-cadherin, scale bars=100um)

pVE-cadherin GFP ESCs Embryoid Body Morphology

In order to track VE-cadherin expression in shear pre-conditioned ESCs during EB differentiation in response to VEGF treatment, ESCs were further differentiated as EBs and treated with (+VEGF) or without soluble VEGF (-VEGF) or with microparticles loaded with VEGF (+VEGF MPs) or unloaded microparticles (-VEGF MPs). After 7 days of EB differentiation treatment with VEGF, differences in EB morphology were observed. PC Static -VEGF EBs developed a rounded morphology and contained EBs of varying sizes (Fig. 5.5A). Similarly, PC Static +VEGF EBs were heterogeneous in size and shape (Fig. 5.5B). However, majority of PC Static +VEGF MPs (Fig. 5.5C) were rounded, but varied in size and appeared dark in contrast to PC static -VEGF and +VEGF EBs. PC Shear -VEGF EBs developed dark regions which protruded from the periphery of EBs (Fig. 5.5E). Comparable to PC Shear -VEGF EBs, PC Shear +VEGF EBs developed optically opaque dark protrusions (Fig. 5.5 F). PC Shear +VEGF MPs appeared smaller in size in comparison to PC Shear +VEGF EBs and had a more irregular morphology (Fig. 5.5G). PC Shear -VEGF MPs EBs (Fig. 5.5H) displayed similar morphology to PC Shear +VEGF MPs EBs. Similar to ESC EBs treated with VEGF, the VEGF delivery method modulated morphology of EBs formed from pre-conditioned VE-GFP ESCs.

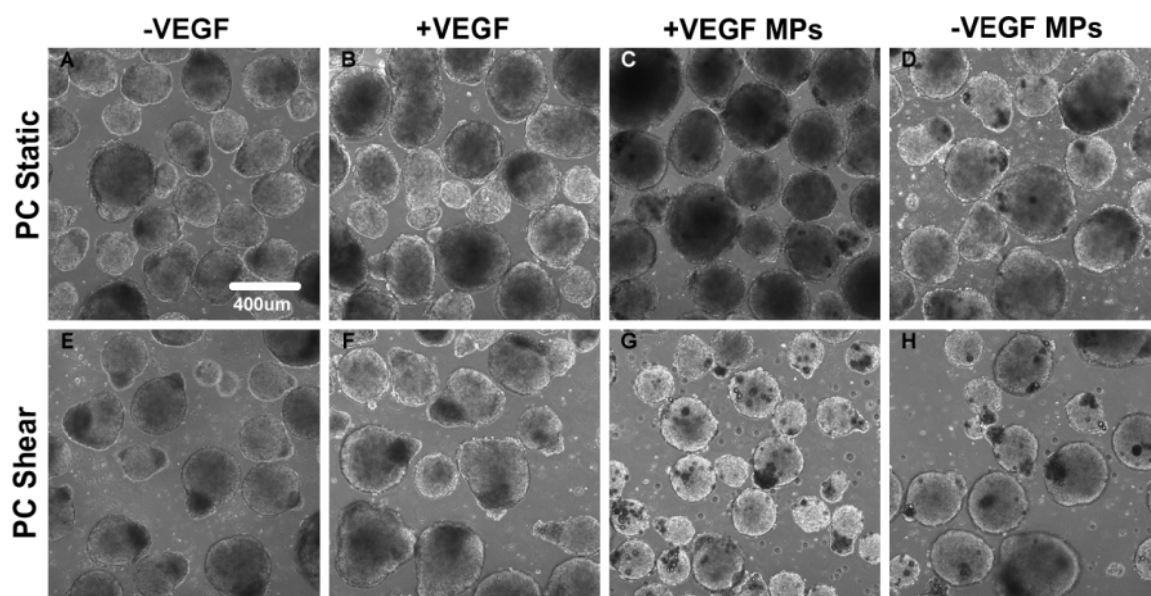


Figure 5.5: VEGF treated EBs formed from pre-conditioned VE-GFP ESCs. PC Static –VEGF EBs (A) varied in size, but had a uniform rounded morphology. PC Static +VEGF EBs (B) contained EBs with circular and elliptical morphology. PC Static +VEGF MPs (C) appeared darker in comparison to PC Static –VEGF, PC Static +VEGFMPs and PC Static –VEGF MPs. PC Shear –VEGF (E) and PC Shear +VEGF (F) EBs developed dark regions which protrude from the periphery of EBs. PC Shear +VEGF MPs EBs (G) appeared smaller than PC Shear –VEGF and PC Shear +VEGF EBs. While PC Shear –VEGF MPs EBs (H) appeared larger than PC Shear +VEGF MPs EBs they developed morphology which was comparable to PC Shear +VEGF MPs EBs.(scale bar=400um)

VE-cadherin Localization in pVE-cadherin GFP Embryoid Bodies

VE-cadherin expression and localization within EBs treated with VEGF was assessed at day 7 by examining GFP fluorescence in EBs formed from pVE-cadherin GFP ESCs (VE-GFP). Few GFP positive cells were detected in PC Static –VEGF EBs (Fig. 5.6 A). On the other hand, GFP positive cells were observed on the periphery of PC Static +VEGF EBs (Fig. 5.6 B). Small clusters of GFP positive cells emerged close to the periphery of PC Static +VEGF MPs and –VEGF MPs EBs (Fig. 5.5 C,D). In contrast to PC Static –VEGF EBs, large clusters of GFP+ cells protruded from the periphery of PC Shear –VEGF EBs (Fig. 5.6E). Similar GFP localization was observed in PC Shear +VEGF EBs with clusters of GFP+ cells close to the edge of the EB (Fig. 5.6F). Vastly different GFP expression was observed in PC Shear +VEGF MPs and PC Shear –VEGF MPs EBs with few GFP positive cells detected throughout the EB (Fig. 5.6 G,H). The localization of GFP expression in PC Shear +VEGF and PC Shear –VEGF EBs correlates with the localization of the dark regions observed in phase images of PC Shear +VEGF and PC Shear –VEGF EBs (Fig. 5.5 E,F). Altogether, VEGF treatment of EBs formed from statically cultured ESCs increased expression of VE-cadherin and modulated localization of endothelial-like cells. On the other hand, VEGF treatment of EBs formed from shear pre-conditioned ESCs appeared to have very little effect on localization of endothelial-like cells within EBs.

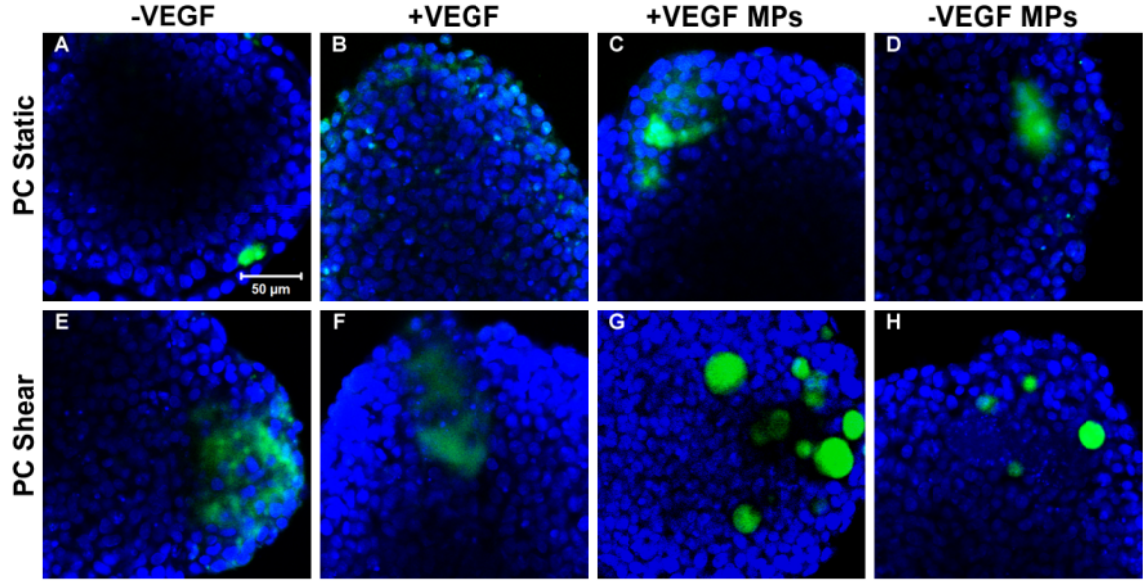


Figure 5.6: GFP localization in pVE-cadherin GFP EBs. PC Static –VEGF EBs (A) contained very few GFP positive cells, while GFP positive cells localized to the outer regions of PC Static +VEGF EBs (B). Both PC Static +VEGF MPs (C) and PC Static –VEGF MPs EBs (D) developed small clusters of GFP positive cells close to the periphery of the EB. In contrast PC Shear –VEGF (E) and PC Shear +VEGF EBs (F) developed large clusters of GFP+ cells which localized at the edge of the EB. Unlike PC Shear –VEGF and +VEGF EBs, PC Shear +VEGF MPs (G) and PC Shear –VEGF MPs EBs (H) did not develop clusters of GFP positive cells. Bright green circular staining denotes microparticles. (blue=nuclei, green=GFP, scale bar=50um)

GFP Expression Analysis of Single Cells from pVE-cadherin EBs

Throughout EB differentiation the percentage of cells which expressed VE-cadherin was tracked by analyzing GFP expression in cells dissociated from VE-GFP EBs treated with or without VEGF. GFP expression analysis of single cells provided a quantitative measure of VE-cadherin positive cells in contrast to confocal imaging which only reveals localization of the VE-cadherin positive cells within EBs. GFP expression was examined after 2, 4, and 7 days of EB culture. At day 2, PC Static –VEGF, PC Static +VEGF, PC Static +VEGF MPs, and PC Static –VEGF MPs contained approximately 2.5%, 2.1%, 3.4%, and 3.7% GFP positive cells, respectively (Fig. 5.7 A-D). However, by day 4 all PC Static EBs contained almost no GFP positive cells with all groups having less than 2% GFP positive cells (comparable to ESC control) (Fig. 5.7 E-H). By day 7, there was a drastic increase in the percentage of GFP positive cells in all PC Static groups. PC Static –VEGF, PC Static +VEGF, PC Static +VEGF MPs, and PC Static –VEGF MPs EBs contained 15.0%, 17.0%, 11.2%, and 11.3% GFP positive cells (Fig. 5.7 I-L). The percentage of GFP positive cells in PC Shear –VEGF, PC Shear +VEGF, PC Shear +VEGF MPs, and PC Shear –VEGF MPs was 2.2%, 1.7%, 3.7%, and 2.8%, respectively (Fig. 5.7 M-P). By day 4, no GFP+ cells were detected in any PC Shear EB groups (Fig. 5.7. Q-T). Similar to PC Static EB groups, by day 7 PC Shear EB groups displayed measurable increases in GFP positive cell percentages. PC Shear –VEGF, PC Shear +VEGF, PC Shear +VEGF MPs, and PC Shear –VEGF MPs EBs contained cell populations which were 10.9%, 12.0%, 9.3%, and 8.9% GFP positive, respectively (Fig. 5.7 U-X). Overall, GFP expression analysis of single cells from PC Static and PC Shear VE-GFP EBs suggests that treating EBs with soluble VEGF increased the percentage of

endothelial-like cells, while the presence of microparticles decreased the percentage of endothelial-like cells.

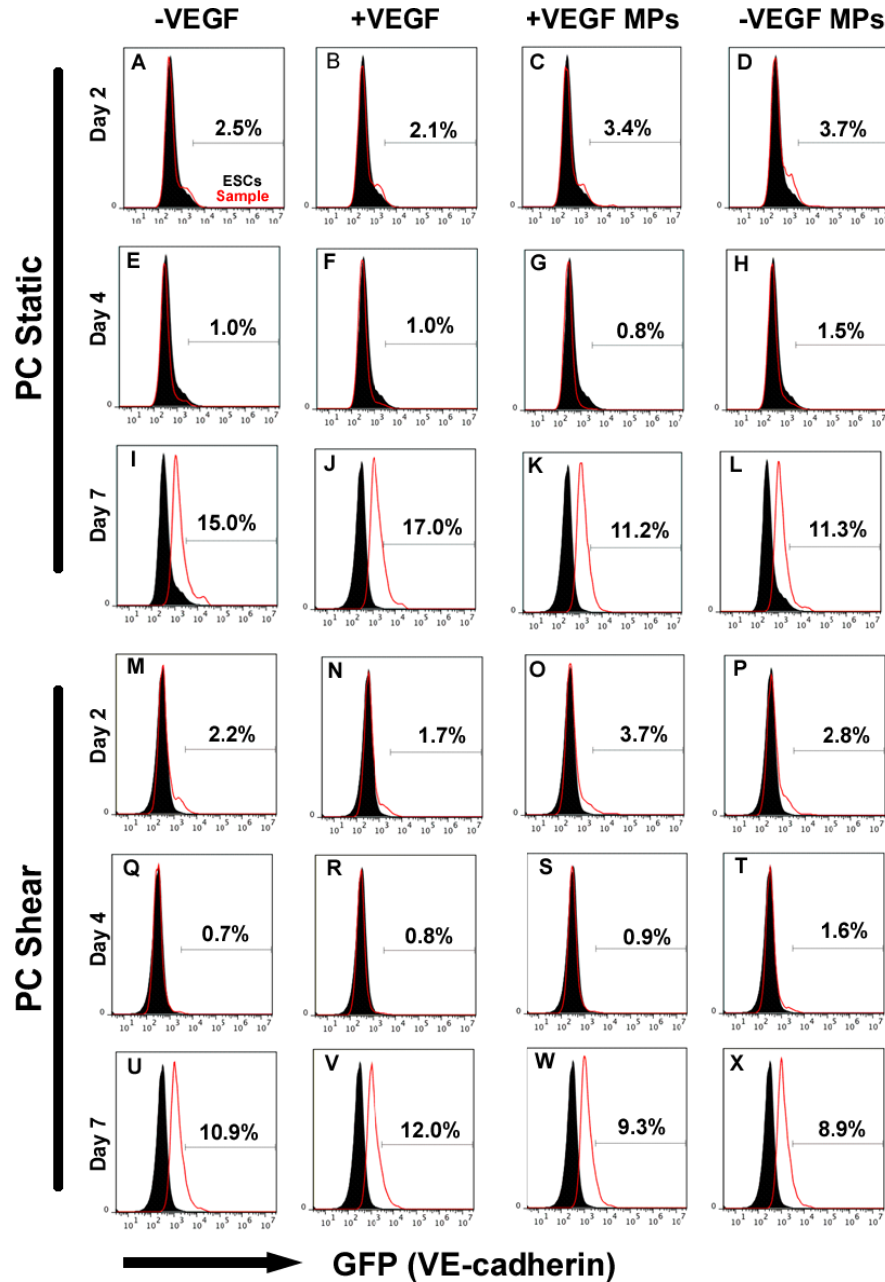


Figure 5.7: Single cell VE-cadherin expression in VEGF treated pVE-cadherin GFP EBs.. At day 2 PC Static EB groups have similarly low percentages of GFP positive cells (A-D). By day 4, PC Static -VEGF (E), PC Static +VEGF (F), PC Static +VEGF MPs(G) and PC Static -VEGF MPs (H) EBs contained less than 2% GFP positive cells. However by day 7, greater than 10% of the cells in all PC Static EB groups were GFP positive, with PC Static +VEGF EBs having the greatest percentage of GFP positive cells (I-L). Day 2 PC Shear -VEGF (M), PC Shear +VEGF (N), PC Shear +VEGF MPs (O), and PC Shear -VEGF MPs (P) EBs were all less than 4% GFP positive. By day 4, majority of PC Shear EB groups did not contain any GFP expressing cells (Q-T). In contrast, day 7 PC Shear EB groups contained GFP+ cells with PC Shear +VEGF EBs containing the greatest percentage (U-X).

Discussion

These studies revealed that VEGF treatment and delivery strategy (soluble or via microparticles) of EBs formed from pre-conditioned (+/- shear) ESCs modulates endothelial-like cell organization and endothelial differentiation. EBs formed from VE-cadherin GFP reporter ESCs were also treated with VEGF in order to directly assess the effects of VEGF on VE-cadherin expression and localization. Differences in EB morphology were observed in PC Static –VEGF EBs in comparison to PC Static +VEGF MPs and PC Static –VEGF MPs with the presence of variable sized dark regions. PC Static +VEGF MPs and PC Static –VEGF MPs displayed similar morphology, which suggests the presence of microparticles alone, irrespective of VEGF, induced different EB morphology. PC Shear –VEGF EBs developed morphology consistent with PC Shear EBs observed in chapter 4. However, when PC Shear EBs were treated with soluble VEGF for 7 days, optically opaque regions were no longer observed suggesting that VEGF modulated morphogenesis of shear pre-conditioned ESCs within the EBs. The dark regions observed in PC Shear +VEGF MPs and PC Shear –VEGF MPs EBs demonstrated that the presence of microparticles did not affect the EB morphology generally observed in EBs formed from shear pre-conditioned ESCs.

Evaluation of endothelial marker genes *Flk-1*, *Flt-1*, *VE-cadherin*, and *PECAM*, revealed large differences in VEGF effects on endothelial differentiation in PC Static EBs and PC Shear EBs. Treating PC Static EBs with VEGF did not stimulate significant differences in the 4 endothelial marker genes examined. However, VEGF soluble treatment of PC Shear EBs generated large increases in expression of all four endothelial genes. PC Shear +VEGF EBs displayed the most drastic increase in *Flk-1* compared to

PC Shear –VEGF EBs. PC Shear +VEGF EBs and PC Shear –VEGF EBs expressed significantly higher levels of *Flt-1*, *VE-cadherin*, and *PECAM* when compared to PC Shear –VEGF EBs. However, these genes were expressed at similar levels in both EB groups suggesting that the presence of the microparticles and not VEGF elicited the increase in gene expression. Studies that incorporated microparticles formed from different subtypes of extracellular matrices within EBs demonstrated differences in differentiation profile [177]. The disparity in changes in endothelial gene expression in response to VEGF stimulation between PC Static and PC Shear EB groups could be due to the variation in the number of cells that have VEGF receptors. Results from Chapter 3 as well as other published studies reveal that the expression of VEGF receptors, Flk-1 and Flt-1, is higher in ESCs pre-conditioned with shear in contrast to ESCs cultured under static conditions [81, 85, 148]. Differences in endothelial gene expression of PC Shear +VEGF EBs and PC Shear +VEGF MPs EBs could be due to the variance in VEGF concentrations delivered to the EBs. EBs were treated with 50 ng/ml VEGF every 2 days while microparticles released less than 5 ng/ml over 7 days. However, the majority of VEGF is released in the first 24 hours during initial EB formation (see Appendix C) [178]. Even though, 10 times less VEGF was delivered to PC Shear +VEGF EBs significant increases in endothelial marker genes were still observed.

VE-cadherin positive cellular localization within PC Shear EBs was altered by VEGF. VE-cadherin expression in PC Shear +VEGF EBs was localized to the outer edge of EBs while VE-cadherin expression in PC Shear –VEGF EBs localized to the center of the EB. Soluble growth factor diffusion within EBs is limited by the tight connections between cells on the outermost layer of the EB[175]. Therefore, VEGF is most likely

only stimulating endothelial differentiation in the outermost layer of the EB. Additionally, PC Shear +VEGF EBs are formed in the presence of VEGF which may also be affecting initial localization and aggregation of VE-cadherin positive cells. Cellular aggregation is mediated by the presence of soluble factors and cytokines as was demonstrated in hepatocytes exposed to soluble epidermal growth factor [179] and blood cells treated with a combination of cytokines including erythropoietin, thrombopoietin, and stem cell factor [180]. The VEGF released from microparticles did not alter VE-cadherin positive cellular organization within PC Shear EBs. Additionally, the comparable VE-cadherin cell patterning in PC Shear –VEGF, PC Shear +VEGF MPs, and PC Shear –VEGF MPs suggests that the quantity of VEGF released from the microparticles was not sufficient to induce any unique VE-cadherin cellular organization.

In order to directly measure VE-cadherin expression and observe VE-cadherin cellular organization in response to VEGF within PC Shear and PC Static EBs and confirm the results observed using ESCs, an ESC VE-cad GFP reporter cell line was used for similar studies. In this study, PC Shear VEGFP –VEGF EBs developed dark regions that protruded from the edge of the EBs unlike PC Shear –VEGF EBs in wildtype D3 ESCs, which developed dark foci at the center of the EBs. Soluble VEGF treatment had different effects on VE-cadherin cellular organization within PC Shear +VEGF EBs and PC Shear +VEGF VE-GFP EBs. PC Shear VEGFP + VEGF EBs maintained a similar VE-cadherin expression pattern compared to PC Shear VEGFP –VEGF EBs. While VE-cadherin⁺ cells were not observed in confocal images of PC Static +VEGF, PC Static +VEGF MPs, and PC Static –VEGF MPs, VE-cadherin⁺ cells were observed in all PC Static VE-GFP EB groups. In general, GFP expression analysis of all PC Static VEGFP

and PC Shear VEGFP EB groups revealed that on day 2 all samples contained some endothelial-like cells. However, by day 4 few endothelial-like cells were detected and by day 7 greater than 8% of the cells were endothelial-like. These results taken together with confocal images of day 7 VE-GFP EBs suggest that VE-cadherin⁺ cells within PC Static VEGFP EBs were dispersed throughout the EB unlike the clustering of VE-cadherin⁺ cells observed in PC Shear -VEGF VE-GFP EBs and PC Shear +VEGF VE-GFP EBs. Altogether, this suggests that soluble VEGF treatment elicited increases VE-cadherin expression, while the presence of microparticles decreased VE-cadherin expression. The results of the VE-GFP ESC studies do not confirm the results obtained in the ESC studies.

In this study, 50 ng/ml of VEGF was used to treat EBs because established protocols that derive endothelial cells from ESCs generally use similar VEGF concentrations of 50 ng/ml over a 3 week culture period [54, 56]. However, soluble diffusion of growth factors within EBs has been demonstrated and reported to be limited by the outer cell layer [175]. Therefore, these studies explored another method of delivering VEGF by incorporating gelatin microparticles, which can release VEGF within the EB microenvironment. This strategy of VEGF delivery overcomes the challenges of molecule diffusion through the outer layer of the EB and allows for control of local release of VEGF to cells within the EB. While gelatin microparticles have been utilized as a delivery vehicle for several factors such as BMP2, TGF- β , and IGF [178, 181-183], few studies have delivered factors to stem cell aggregates via microparticles [174, 183]. The similarities in the increases of endothelial marker gene expression in VEGF loaded and VEGF unloaded treated EBs formed from shear pre-conditioned

suggested that the VEGF released from the microparticles had less of an effect on differentiation than the mere presence of microparticles within the EB. Incorporation of unloaded microparticles formed from different materials within pluripotent stem cell aggregates elicited different differentiation profiles [177] compared to pluripotent stem cell aggregates not containing microparticles. Recent studies have demonstrated that ESCs produce factors that can enhance somatic cell survival, increase neovascularization, and promote endothelial differentiation [184-186]. The significant increase in endothelial gene expression in PC Shear -VEGF MPs EBs compared to PC Shear –VEGF EBs may be due to the presence of microparticles as well as differences in growth factor production between EB populations.

Conclusion

Soluble VEGF treatment of EBs formed from shear pre-conditioned ESCs elicited changes in endothelial marker gene expression, organization, and EB morphology. The mere presence of gelatin microparticles in shear pre-conditioned EBs promoted endothelial differentiation but has little effect on endothelial cellular organization and morphogenesis. The quantities of VEGF delivered via microparticles may not have been sufficient to promote endothelial differentiation to the extent of the VEGF quantities used for soluble VEGF treatment. Priming ESCs with fluid shear prior to EB differentiation mediated ESC responses to VEGF stimulation. However, treating EBs formed from shear pre-conditioned ESCs with VEGF did not substantially enhance the number of endothelial-like cells within the EBs. These studies suggest that the soluble factor delivery strategy to EBs modulates stem cell organization and differentiation potential.

Furthermore, physical forces can be used to modulate stem cell response to growth factors.

CHAPTER 6

HYPOXIA EFFECTS ON VASCULOGENESIS OF FLUID SHEAR STRESS PRE-CONDITIONED EMBRYONIC STEM CELLS

Introduction

Low oxygen or hypoxic conditions are present throughout many physiological environments, disease pathologies, and during embryonic development [19, 104-107]. While cells are generally maintained and cultured at 21% oxygen (normoxic) in vitro, in vivo cells develop and function at oxygen levels generally ranging from 1-10% (hypoxic) [19]. Oxygen levels play a very important role in many cellular processes including but not limited to metabolism, differentiation, proliferation, and tissue morphogenesis, [19, 108-110]. More specifically oxygen levels play a critical role in vascular development and differentiation during embryogenesis[19, 24, 111].

Prior to the development of the circulatory system embryonic oxygen levels are approximately 3% O₂ [114, 121]. Low oxygen tension is imperative for proper morphogenesis and function of the cardiovascular system in the early embryo [122]. Oxygen constitutes an integral micronvironmental cue which is critical for endothelial and vascular development [122, 125]. Oxygen levels within the embryo range from 1-3% [114, 121] indicating that embryogenesis occurs in a hypoxic environment. During development, oxygen gradients develop across embryos which are responsible for patterning and formation of the cardiovascular system [19, 122]. Additionally, oxygen modulates cellular VEGF production in vivo [123, 124] as well as in vitro [187]. In vitro, hypoxia has been utilized to differentiate stem cells into, cardiac [188] and vascular

progenitors [189]. Low oxygen may provide instructive cues for endothelial differentiation and vasculogenesis within EB microenvironments.

Fluid shear stress also plays an important role in the development of the cardiovascular system, which is the first functioning physiological system to be established within the embryo [16, 17]. Gene and protein expression patterns which develop in the embryonic cardiovascular system are regulated by fluid shear stress, and disruption of fluid flow can lead to abnormal cardiogenesis [17, 20]. Even though the initial embryonic vascular networks, yolk sac and trunk axial vessels, develop prior to the onset of blood flow, fluid shear stress imparted by blood flow is vital to the maturation and stabilization of the primitive embryonic vasculature [21]. In vivo, fluid shear stress is vital for the proper development of the cardiac, vascular, and hematopoietic system, demonstrating the instructive potential of this physical force to promote vasculogenesis in vitro.

Based on the results from chapters 3 and 4 in which fluid shear stress pre-conditioned ESCs from EBs develop a core of endothelial like-cells (VE-cadherin+), this study aimed to use hypoxia to modulate endothelial differentiation and vasculogenesis in EBs formed from shear pre-conditioned ESCs. EBs formed from (+/- shear) pre-conditioned ESCs were cultured under normoxia (21%) or hypoxia (3%) for 7 days and then assessed for morphology, endothelial gene and protein expression, VEGF gene and protein production, as well as hypoxia inducible factor A gene and protein expression during EB differentiation. This study indicates that fluid shear and hypoxia modulate primitive vascular formation as well as angiogenic factor production within EBs.

Therefore, providing a new strategy to pre-vascularize stem cell based constructs which can be utilized as a template for a multitude of tissue engineered products.

Methods

ESC and EB Culture

D3 and D3 pVE-cadherin GFP murine embryonic stem cells were cultured using methods previously described in Chapter 3. EBs were cultured as previously described in Chapter 3 under normoxic (21% O₂, 5% CO₂) or hypoxic (3% O₂, 5% CO₂) conditions.

LIVE/DEAD Cell Viability Assay

Following 2, 4, and 7 days of EB differentiation, cell viability was assessed using LIVE/DEAD staining (Invitrogen). EBs were incubated under gentle agitation in phenol red- free, serum-free medium containing 1uM calcein AM and 2uM ethidiumhomodimer I at room temperature for 30min. EBs were then washed three times with PBS (w/o Ca²⁺ and Mg⁺) and immediately imaged using a Ziess LSM 510Multiphoton confocal microscope.

Total Protein Quantification Assays

The total protein content of day 7 EBs was determined using a bicinchonic assay (BCA, Thermo). EBs were lysed using 200 µL TPER buffer (Thermo) with rotation for 30 min at room temperature followed by 5 minutes of centrifugation at 14,000 RPM to remove particulate. Total protein content was analyzed using a bicinchoninic acid (BCA) assay kit (Pierce). 25 µl of sample was incubated with BCA solution for 30 minutes. Bovine serum albumin diluted in TPER was used as to generate a standard curve (0 µg/mL - 2,000 µg/mL). Absorbance readings were taken at 562 nm using a SpectraMax

M2e plate reader. The absorbance readings of the EB lysate samples were compared against the standard to calculate absolute protein concentrations.

VEGF Quantity Protein Analysis

Enzyme-linked immunosorbent assay (ELISA) kits (DuoSet, R&D Systems) were used to quantify the amount of VEGFA produced day 7 EBs. EBs were lysed using 200 μ L TPER buffer (Thermo) with rotation for 30 min at room temperature followed by 5 minutes of centrifugation at 14,000 RPM to remove particulate. Briefly, capture antibody was adsorbed onto a MaxiSorp™ Immuno 96-well plate (Nunc), followed by a blocking step, incubation with 100 μ L sample, and binding of analyte to a biotinylated detection antibody. The concentrations of capture and detection antibodies used were dictated by the DuoSet protocol for each protein: 400 ng/mL and 100 ng/mL. TPER buffer was used as the diluent for the standard curve samples. The amount of analyte was assessed using the colorimetric reaction of peroxidase and tetramethylbenzidine (TMB) with an absorbance reading at 450 nm. The absorbances for each sample were compared to the standard curve to establish the protein analyte content, which was normalized to the total protein in the EB lysate determined from the total protein quantification assay.

SDS-PAGE and Western Blotting

Sample protein concentration was determined using the aforementioned BCA Protein Quantification kit (Pierce); equal amounts of protein (\approx 80 μ g) per sample were mixed with loading buffer (0.1 M Tris-HCl containing SDS, glycerol, biomophenol blue, and 2-mercaptoethanol), heated at 95°C for 5 minutes, and loaded in 7.5% Tris-HCl

polyacrylamide precast gels (Bio-Rad). Vertical electrophoresis was performed using a Mini-PROTEAN Tetra Cell system with SDS/PAGE running buffer (Tris base/glycine/SDS solution) run at 100V for 1 hour to separate the protein samples by molecular weight. A protein ladder (Precision Plus Protein Kaleidoscope, 10-250kD, Bio-Rad) was loaded into each gel as a reference for protein products.

Following SDS PAGE separation, gels were removed from the electrophoresis tank and loaded into transfer cassettes. Gels were placed directly beside a PVDF membrane (Fisher Scientific) and sandwiched between filter paper within the cassettes to allow for protein transfer from the gel onto the PVDF membrane. Protein transfer was run in transfer buffer overnight at 4°C with 30V. Once protein transfer was complete, membranes were removed and equilibrated in PBS prior to immunostaining. Blots were stained using the Snap ID system (Bio-Rad). Membranes were placed in Snap ID staining wells, and IR blocking medium (30 mL per well, Rockland) was pulled through the well by vacuum. Membranes were then incubated with primary antibodies for HIF1 α (1:100), and anti- β -actin (loading control, 1:300) over night at 4°C. Primary antibody incubation was followed by continuous vacuum rinse with 0.01% Tween-20/PBS solution, and membranes were incubated with IR secondary antibodies (680 anti-goat and 800 anti-rabbit, 1:5000, LiCor), followed by continuous vacuum rinse with 30 mL PBS/0.1% Tween-20 solution. Stained membranes were removed from the staining wells and rinsed 2 more times in PBS with gentle rocking for 10 minutes at room temperature. Blots were imaged using the LiCor Odyssey Infrared imager for dual secondary visualization.

Results

Embryoid Body Morphology

EBs were formed from (+/- shear) pre-conditioned ESCs and cultured under normoxic (21%) or hypoxic (3%) conditions for 7 days and assessed for viability. During EB differentiation EBs formed from statically cultured ESCs displayed similar morphology under both oxygen conditions at day 4 (Fig. 6.1A, B). Day 4 EBs formed from shear pre-conditioned ESCs cultured under hypoxia and normoxia appeared dark, however, PC Shear hypoxia EBs appeared larger in size compared to PC Shear normoxia EBs (Fig. 6.1C,D). PC shear hypoxic EBs appeared larger in size and developed optically opaque dark regions which covered approximately 70% of the EB. By day 7, PC static normoxia and PC static hypoxia EBs exhibited similar morphology (Fig. 6.1E, F). However, after 7 days of EB differentiation distinct differences in PC shear normoxia and PC shear hypoxia morphology were apparent with dark regions present at the center of PC shear normoxia EBs (Fig. 6.1G). PC shear hypoxia EBs contained dark regions as well however, unlike the dark regions in PC Shear normoxia EBs, these dark regions varied in size, optical opaqueness, and did not localize to the center of EBs (Fig. 6.1H). After 7 days of EB culture distinct differences in cell death were not observed between hypoxic and normoxia EB groups (Fig. 6.1-L). Overall the data suggested that hypoxia elicited unique morphology within EBs formed from ESCs pre-conditioned with shear.

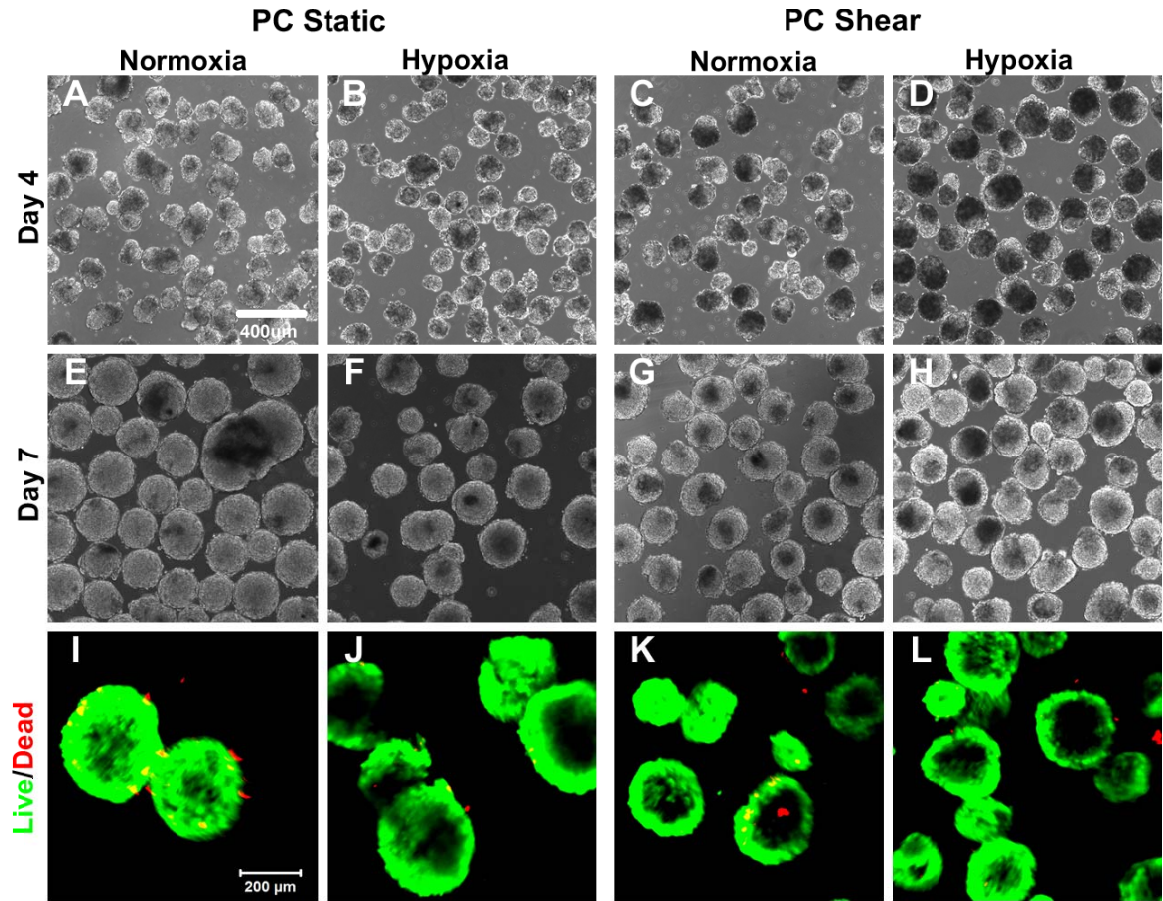


Figure 6.1: Embryoid Body Differentiation under Hypoxic conditions. PC static normoxia and PC static hypoxia EBs appeared similar morphologically by day 4 (A, B). However, PC shear normoxia EBs (C) appeared smaller than PC shear hypoxia EBs (D), develop dark regions which cover more than 50% of the EB. By day 7 PC static normoxia (E) and PC static hypoxia EBs (F) did not display any significant morphological differences (scale bar= 400µm). Day 7 PC shear normoxia EBs (G) developed centrally located optically opaque circular regions, while day 7 PC shear hypoxia EBs (H) develop larger dark regions which are not centrally located within the EB. Live/Dead staining revealed no differences in cell death between EB groups (I-L). (Scale bar=200µm, Green=live cells, Red=dead cells).

Endothelial Gene Expression

Endothelial differentiation of EBs was assessed by examining *Flk-1*, *Flt-1*, *VE-cadherin*, and *PECAM* gene expression after 4 and 7 days of hypoxia culture. *Flk-1* gene expression was similar in normoxia and hypoxia EB samples at day 4, however on day 7 *Flk-1* was higher in both PC static hypoxia and PC shear hypoxia EBs as compared to PC static normoxia and PC shear normoxia EBs, respectively (Fig. 6.2A). Similarly, *Flt-1* expression levels were not significantly altered on day 4, but by day 7 when PC static hypoxia EBs expressed higher levels of *Flt-1* than PC static normoxia EBs and PC shear hypoxia EBs expressed higher levels of *Flt-1* than PC shear normoxia EBs (Fig. 6.2B). *VE-cadherin* was also expressed at similar levels in normoxia and hypoxia EB groups on day 4. At day 7, EBs cultured under hypoxic conditions expressed higher levels of *VE-cadherin* than EBs cultured under normoxia (Fig. 6.3C). *PECAM* gene expression was only increased under hypoxia in D7 PC static EBs (Fig. 6.3D). The increased expression of endothelial genes *Flt-1*, *Flk-1*, and *VE-cadherin* at day 7 in EBs cultured under hypoxia suggested that hypoxia promoted endothelial differentiation in EBs. Additionally, long term culture under hypoxia is required to promote endothelial differentiation within EBs.

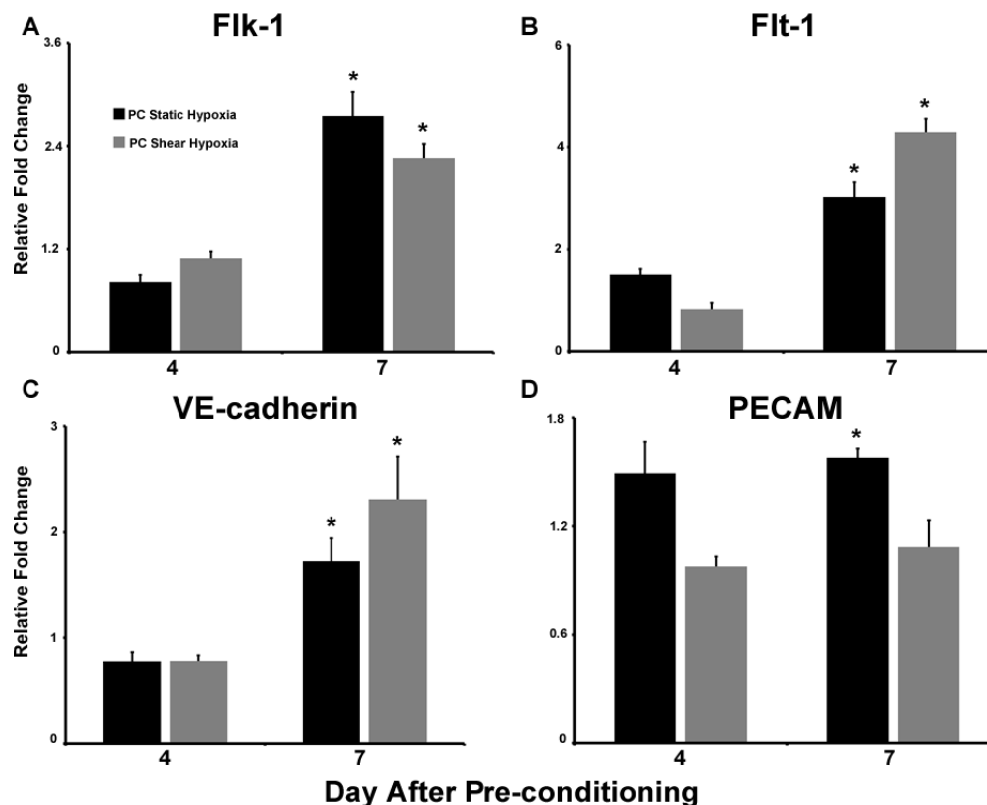


Figure 6.2: Embryoid body endothelial marker gene expression under hypoxia. *Flk-1* relative fold change (D4 PC static hypoxia/D4 PC static normoxia, D7 PC shear hypoxia/D7 PC shear normoxia) was not altered by day 4, however at day 7 PC Static and PC Shear hypoxia EBs expressed higher levels of *Flk-1* than PC Static and PC Shear normoxia EBs respectively (A). Similarly, *Flt-1* expression was not altered by hypoxia at day 4, while PC Static Hypoxia and PC Shear Hypoxia EBs expressed increased levels of *Flt-1* by day 7(B). VE-cadherin expression levels were higher in hypoxia samples when compared to normoxia samples only at day 7 (C). *PECAM* expression was only significantly different in PC Static Hypoxia EBs when compared to PC Static NormoxiaEBs (D). (n=3-5, *=p<0.05 compared to normoxia EBs pre-conditioned similarly)

VE-cadherin Protein Expression

Endothelial cell organization was analyzed by assessing VE-cadherin expression and patterning in normoxic and hypoxic EBs formed from pre-conditioned (+/- shear) ESCs. After 2 days of EB formation VE-cadherin⁺ cells were not detected in PC static normoxia EBs (Fig. 6.3A), PC static hypoxia EBs (Fig. 6.3B) or PC shear hypoxia EBs (Fig. 6.3D). However, VE-cadherin was detected in PC shear normoxia EBs (Fig. 6.3C). By day 4, only for PC static normoxia EBs were negative for VE-cadherin (Fig. 6.3E). PC static hypoxia, PC shear normoxia, and PC shear hypoxia EBs developed clusters of VE-cadherin⁺ cells at the interior of the EB. By day 7 each EB group developed markedly different VE-cadherin cellular organization. PC static normoxia EBs remained negative for VE-cadherin (Fig. 6.3I) while the VE-cadherin expression is not only found in the center but also close to the periphery of the PC static hypoxia EBs (Fig. 6.3J). Day 7 PC shear EBs under normoxia and hypoxia develop significantly different VE-cadherin⁺ cell organization (Fig. 6.3 K, L). VE-cadherin⁺ cells remain at the center of PC shear normoxia EBs, while VE-cadherin⁺ cells organize into primitive networks which radiated from the center of PC shear hypoxia EBs. The VE-cadherin⁺ cellular organization observed at day 7 in hypoxia EBs correlated with increased expression of endothelial genes Flk-1, Flt-1, and VE-cadherin. Altogether, these results demonstrate that hypoxia and fluid shear stress pre-conditioning played a role in endothelial-like cell organization within EBs.

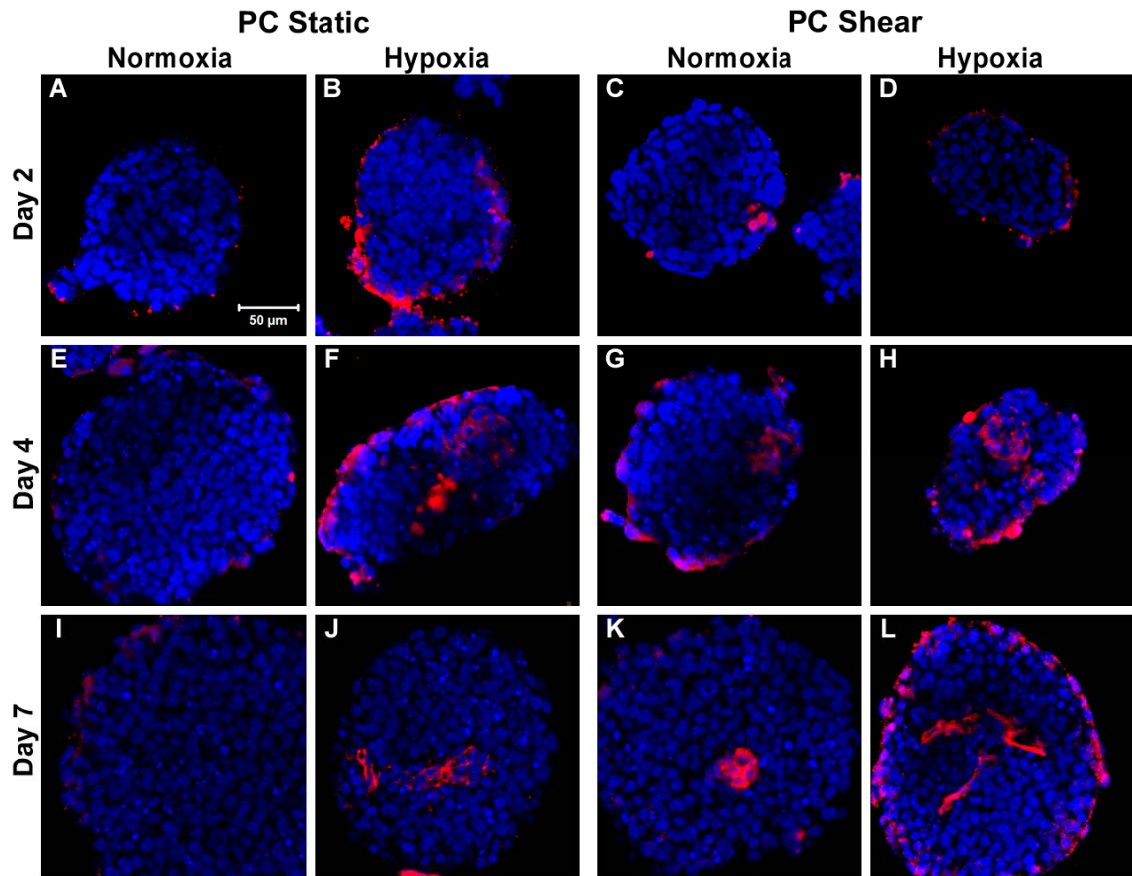


Figure 6.3: Embryoid body endothelial morphogenesis. Day 2 PC static normoxia EBs (B) and PC static hypoxia EBs were negative for VE-cadherin (B). Additionally, day 2 PC shear normoxia EBs(C) were positive for VE-cadherin while PC shear hypoxia EBs (D) were negative for VE-cadherin. By day 4 PC static normoxia EBs(E) remained negative for VE-cadherin, however PC static hypoxia(F), PC shear normoxia (G), and PC shear hypoxia EBs(H) are contained clusters of VE-cadherin+ cells. After 7 days of EB differentiation PC static normoxia EBs (I) did not contain VE-cadherin+ cells, while VE-cadherin+ cells differentially organized within PC static hypoxia (J), PC shear normoxia (K), and PC shear hypoxia (L) EBs.

Hypoxia Inducible Factor A Expression

HIF1 α gene and protein expression were examined in EBs formed from (+/- shear) pre-conditioned ESCs cultured under normoxic or hypoxic conditions. Following 4 days of EB differentiation PC static normoxia EBs expressed less *HIF1 α* than PC static hypoxia EBs (Fig. 6.4A). In contrast, D4 PC shear normoxia EBs had a significantly higher expression of *HIF1 α* than D4 PC shear hypoxia EBs (Fig. 6.4A). By day 7 PC static normoxia EBs expressed higher levels of *HIF1 α* than PC static hypoxia EBs (Fig. 6.4A). Interestingly, in day 7 shear normoxia EBs *HIF1 α* was not detected in majority of samples, however in day 7 shear hypoxia EBs *HIF1 α* expression levels were similarly low in all samples (Fig. 6.4A). Analysis of relative fold change of *HIF1 α* expression through qRT-PCR did not display drastic changes in PC Static hypoxia or PC Shear hypoxia EBs at days 4 and 7 (Fig. 6.4B). HIF1 α protein expression is highest in day 7 PC static hypoxia EBs compared to all other EB groups (Fig. 6.4C). The *HIF1 α* gene and protein expression results suggest that under normoxia *HIF1 α* EB expression was variable and transient. However, long term exposure to hypoxia elicited uniform *HIF1 α* expression in EB populations.

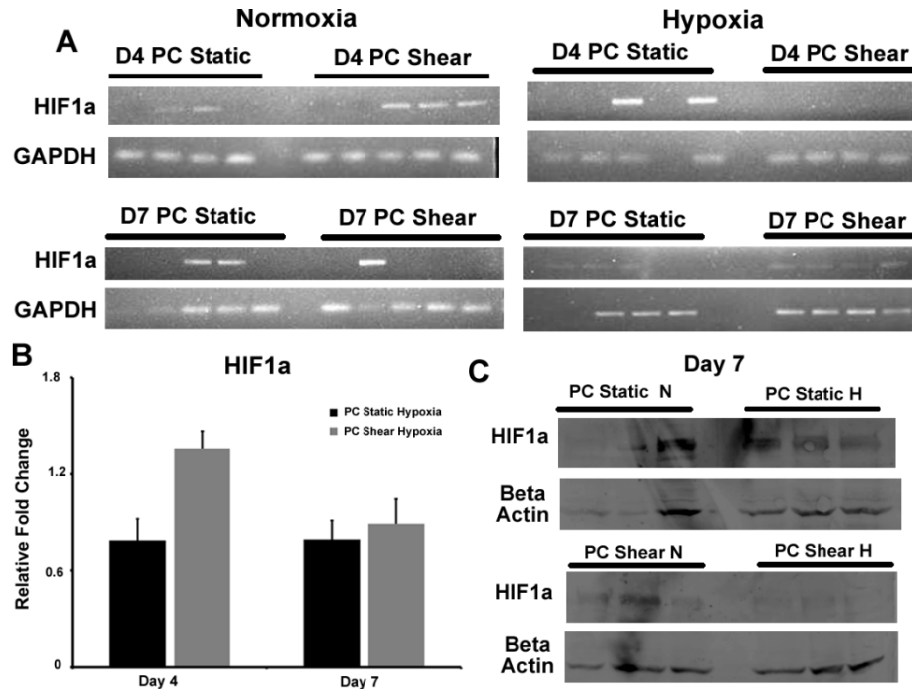


Figure 6.4: Hypoxia Inducible Factor A Gene and protein expression. D4 PC static normoxia EBs express less *HIF1α* compared to D4 PC static hypoxia EBs. D4 PC shear EBs expressed higher levels of *HIF1α* compared to D4 PC shear EBs, in which *HIF1α* was not detected in any samples. By day 7 *HIF1α* was detected at high levels in PC static normoxia and PC shear normoxia EBs, while *HIF1α* was expressed at similarly low levels in PC static hypoxia and PC shear hypoxia EBs (RT-PCR)(A). qRT-PCR analysis of *HIF1α* gene expression revealed no differences between normoxia and hypoxia EB samples. Results indicated are mean \pm standard error (qRT-PCR) (B). *HIF1α* protein was detected in some D7 PC static normoxia and PC shear normoxia EB samples. However, *HIF1α* was detected in all D7 PC static hypoxia EB samples but not detected in D7 PC shear hypoxia EBs (Western Blot) (C).

VEGFA Gene and Protein Expression

VEGFA gene expression was analyzed in D4 and D7 PC static/shear normoxia/hypoxia EBs. *VEGFA* protein expression in D7 PC static/shear normoxia/hypoxia EBs was also evaluated. After 4 days of EB differentiation, *VEGFA* gene expression did not change significantly compared to EBs cultured under hypoxic conditions compared to EBs cultured under normoxia (Fig. 6.5A). However, by day 7, PC static hypoxia EBs and PC shear hypoxia EBs expressed significantly higher levels of *VEGFA* than PC static normoxia EBs and PC shear normoxia EBs, respectively (Fig. 6.5A). Additionally, by day 7, PC shear hypoxia EBs expressed higher levels of *VEGFA* protein compared to PC static hypoxia and PC shear normoxia EBs (Fig. 6.5B). No *VEGFA* protein was detected in the EB conditioned media for any of the groups studied. Altogether this suggests that *VEGFA* produced by EBs was retained within the EB microenvironment. *VEGFA* gene and protein expression results suggest that hypoxia modulated *VEGFA* gene expression and *VEGFA* EB production.

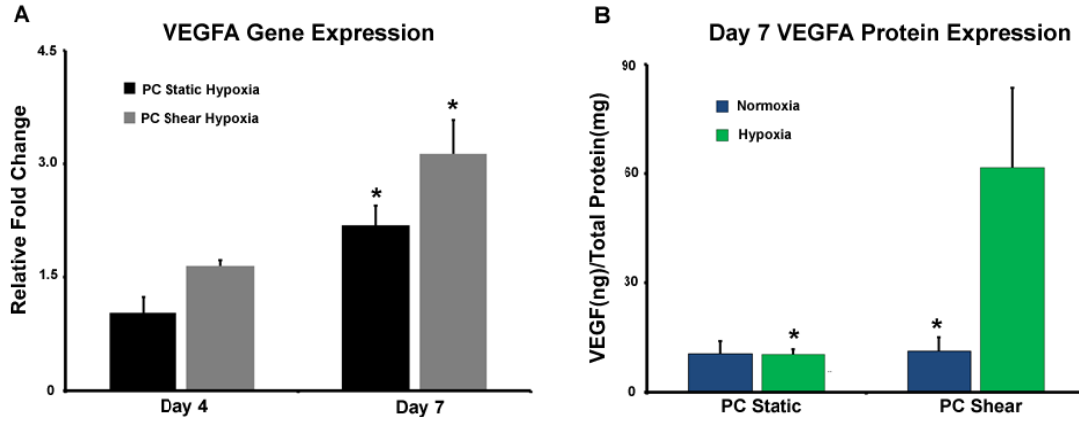


FIGURE 6.5: Hypoxia modulates VEGF-A gene and protein expression. VEGF-A relative fold change (i.e. D4 PC static hypoxia/D4 PC static normoxia, D7 PC shear hypoxia/D7 PC shear normoxia) was highest in EB samples at day 7. Results indicated are mean \pm standard error (n=3-5, \ast =p<0.05, compared to D7 normoxia EBs) (A). PC shear hypoxia EBs produced more VEGFA than PC static hypoxia and PC shear normoxia EBs (B). Results indicated are mean \pm standard error. (n=3-4, \ast =p<0.05, compared to PC shear hypoxia).

VE-cadherin GFP Embryoid Bodies

Endothelial differentiation was examined during hypoxia culture of EBs by pre-conditioning VE-cadherin GFP reporter ESCs and then assessing their GFP fluorescence at day 2, 4, and 7 of EB differentiation. Following 2 days of EB culture, the observed mean GFP fluorescence intensity was highest in PC Shear normoxia EBs compared to all other EB groups. However, by day 4 the mean GFP fluorescence was not different in cells from PC Static normoxia and PC Shear normoxia EBs. At day 4, the mean fluorescence intensity of cells in PC Static hypoxia EBs and PC Shear hypoxic EBs was less than PC Static normoxia EBs and PC Shear normoxia EBs, respectively. Following 7 days of EB culture, the mean fluorescence intensity of cells in PC Static hypoxia EBs was markedly higher than cells from PC Static normoxia and PC Shear normoxia EBs (Fig. 6.6A). Percentage of VE-cadherin cells within EB populations was also assessed throughout EB differentiation. Similar to the GFP mean fluorescence intensity, on day 2 PC Shear normoxia EBs had the highest percentage of VE-cadherin positive cells in comparison to all other EB groups (Fig. 6.6B-F). By day 4, $5.7 \pm 2.8\%$ and $7.0 \pm 0.8\%$ of the cells were VE-cadherin positive in PC Static normoxia and PC Shear normoxia EBs, respectively (Fig. 6.6 G,I). In contrast, EBs exposed to PC Static hypoxia and PC Shear hypoxia EBs had less than 2% of the cells that were positive for VE-cadherin (Fig. 6.6 H, J). However, after 7 days of EB culture $58.0 \pm 9.7\%$ and $10.7 \pm 2.5\%$ of the cells were VE-cadherin positive in PC Static hypoxia EBs and PC Shear hypoxia EBs, respectively (Fig. 6.6B, K-N). Altogether the results suggest that oxygen modulated VE-cadherin expression differently in EBs formed from statically cultured ESCs and shear pre-conditioned ESCs. Additionally, these results indicate that long term culture under

low oxygen elicited higher expression of endothelial marker genes compared to short term culture under low oxygen.

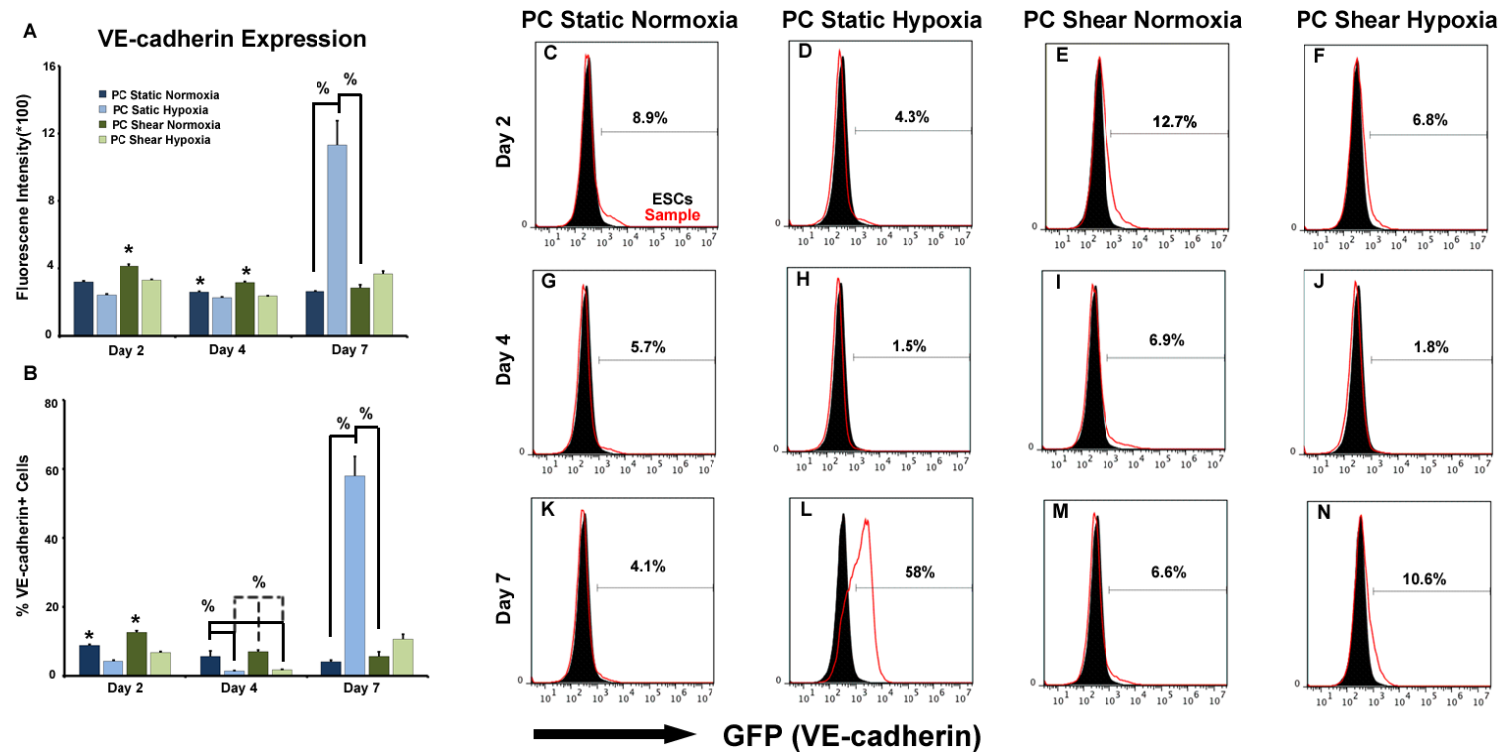


Figure 6.6: VE-cadherin expression in VE-GFP EBs cultured under hypoxia. Differences in mean fluorescence intensity VE-GFP ESCs dissociated from day 2, 4, and 7 EBs cultured under normoxia or hypoxia were observed throughout EB differentiation (A). Black histograms represent undifferentiated VE-GFP ESCs and red histograms represent cells dissociated from VEGFP EB samples. Oxygen environment modulates percentage of VE-cadherin+ cells in shear pre-conditioned VE-GFP EBs (B) ($n=3$, $*=p<0.05$ compared to samples at same time point, $\%=p<0.05$ compared to linked samples). Histograms representative of 3 samples per group and per time point of dissociated VE-GFP ESCs from pre-conditioned EBs (C-N). After 2 days of EB culture PC Shear Normoxia EBs (E) contain the highest percentage of VE-cadherin positive cells. Day 4 PC Static Normoxia (G) and PC Shear Normoxia EBs (I) contain similar percentages of VE-cadherin positive cells which was higher than the percentage of VE-cadherin positive cells in PC Static Hypoxia (H) and PC Shear Hypoxia EBs (J), respectively. However, at day 7 of EB culture PC Static Hypoxia EBs (L) and PC Shear Hypoxia EBs (N) give rise to higher percentages of VE-cadherin positive cells than similar EBs cultured under normoxia (K, M).

Discussion

This study demonstrated that hypoxia microenvironments promoted endothelial differentiation and vasculogenic events as well as enhanced ESC VEGFA production. EBs formed from fluid shear stress pre-conditioned ESCs developed primitive vascular networks when cultured under low oxygen. Additionally, the combination of fluid shear pre-conditioning and low oxygen induced EBs to produce increased levels of VEGF compared to EBs formed from ESCs cultured statically and under hypoxic conditions. In general, hypoxic microenvironments promoted vascular differentiation within EBs.

The morphological differences observed between EB groups cultured under hypoxia and normoxia at day 7 correlate with the differences in VE-cadherin⁺ cell patterning and organization observed at similar time points. PC static normoxia EBs did not develop any dark regions as well as any detectable VE-cadherin⁺ cell staining and a subset of PC static hypoxia EBs developed dark regions as well as some organization of VE-cadherin⁺ cells. On the other hand, PC shear normoxia EBs developed dark regions at the centroid of the EB similar to the morphology observed in chapters 3 and 4 as well as centrally located clusters of VE-cadherin⁺ cells. Most interestingly, PC shear hypoxia EBs developed optically opaque regions markedly larger than the optically opaque regions observed in PC shear normoxia EBs which correlated with the organization of VE-cadherin⁺ cells in complex networks. While both PC shear and PC static EBs cultured under hypoxic conditions contained populations of vascular cells, the formation of primitive vasculature within PC shear hypoxia EBs may be due to the enhanced production of the angiogenic factor VEGF. VEGF stimulates endothelial differentiation

and vasculogenesis and is a critical molecule for vasculogenesis during embryonic development [92, 93].

Comparing live/dead staining of normoxia and hypoxia EBs indicated no detrimental effects of low oxygen on ESC viability within EBs. This observation parallels other research suggesting that hypoxia promotes expression of pro-survival genes and proteins to prevent cellular death [127, 190]. Furthermore, while 3% oxygen was a significantly lower oxygen level than 21%, 3% oxygen is more representative of the oxygen environment ESCs would experience in vivo [19].

Endothelial gene expression was significantly increased in both PC static and PC shear hypoxia EBs suggesting that hypoxia, irrespective of pre-treatment of ESCs prior to EB formation, has significant effects on endothelial differentiation. However, these effects were not pronounced until day 7 suggesting that long term culture under hypoxia is necessary to modulate vascular differentiation and vasculogenesis. Other studies examine effects of hypoxia on EB differentiation culture EBs at oxygen levels ranging from 1-10% for periods of 7-16 days [24, 191, 192]. However while these studies demonstrate increased EB endothelial differentiation and vasculogenesis through endothelial gene and protein expression and angiogenic sprouting assays [24, 191], the studies presented here are unique as they illustrate primitive vascular formation in EBs cultured under hypoxia.

HIF1 α , a transcription factor stabilized under hypoxic conditions which regulates numerous genes responsible for cellular adaptive responses to low oxygen [193-195], was expressed at some level in all EB groups in both normoxia and hypoxia. The presence of HIF1 α in EB groups under normoxic conditions suggests that oxygen gradients exist in

the EB microenvironment [196, 197]. These oxygen gradients may be due in part to EB size causing lower oxygen levels at the center of larger EBs [197]. Stem cell aggregate size regulates differentiation potential [198-201] because differentiation is influenced by temporal and spatial cell-cell interactions. After 4 days of hypoxia culture EBs formed from shear pre-conditioned ESCs were noticeably larger in size compared to all other EB groups. This increase in EB size may have played a role in endothelial-like cell network formation as well as increased VEGF production only observed in this EB groups at day 7. Studies have reported that HIF1 α is responsible for upregulation of VEGF receptors (Flk-1 and Flt-1) and is important for initiation and stabilization of vasculature during embryonic development [121, 122]. Furthermore, HIF1 α regulates production of VEGF under hypoxic conditions by binding to its promoter region thereby increasing VEGF expression [114, 121]. The HIF1 α signaling pathway played a role in increased VEGF production in trophoblastic cells cultured under hypoxia [187]. Overall, the increased expression of endothelial genes and primitive vascular network formation in PC shear hypoxia EBs demonstrated the critical role of hypoxia, HIF1 α , VEGF receptors, and VEGF in vasculogenesis within EBs.

PC Shear hypoxia EBs produced VEGFA at magnitudes similar to the quantities typically used in protocols to derive ECS from ESCs [45, 56, 149]. Hypoxic conditions have mediated increase in VEGF production in a number of cells including vascular smooth muscle cells[202], hepatic cells[203]and fibroblasts [204]. The coincident increase in VEGFA production with expression of HIF1 α parallels other studies which demonstrated that HIF1 α activation VEGF is mediated by HIF1 α stabilization via hypoxia[114]. This study revealed that exposing stem cells to 7 days of low oxygen can

result in over 50% of the cells expressing VE-cadherin and parallels a previous study which reported increases in stem cell vascular differentiation efficiency when cultured at low oxygen [189]. The results of this study suggest that exposing ESCs to hypoxic microenvironments can be used as an alternative to supplementing ESCs with VEGF in order to promote vascular differentiation.

Conclusion

Overall, this study demonstrates that hypoxia microenvironments modulate EB morphogenesis, VE-cadherin positive cell patterning, endothelial differentiation, HIF1 α expression, and angiogenic factor production. Moreover, in combination with fluid shear stress pre-conditioning, hypoxia elicited primitive vascular network formation and increased production of angiogenic factor, VEGF. Priming ESCs with fluid shear stress prior to EB differentiation under hypoxic conditions yielded EBs which recapitulate aspects of embryonic vasculogenesis. Interestingly, hypoxia elicited similar endothelial marker gene expression profiles in EBs formed from statically cultured ESCs and shear pre-conditioned ESCs suggesting that priming ESCs with fluid shear does not modulate ESC endothelial differentiation under hypoxic conditions but demonstrates that oxygen levels are an instructive cue for endothelial differentiation within EBs.

CHAPTER 7

FUTURE CONSIDERATIONS

This body of work examined the subsequent effects of fluid shear stress preconditioning on embryonic stem cell (ESC) endothelial and vascular differentiation within embryoid bodies (EBs). Additionally, these studies investigated the effects of vasculogenic cues, fluid shear stress, vascular endothelial growth factor (VEGF) and hypoxia on EB vascular differentiation. Fluid shear stress has been established as a method to initiate endothelial differentiation in many stem cell populations; however, this work determined the role of fluid shear stress in endothelial differentiation commitment of ESCs long after cells have been subjected to this mechanical stimulation. In vivo fluid shear stress, hypoxia, and VEGF play critical roles in establishing the vascular system within the developing embryo; however few studies have examined these cues in combination in vitro in the EB model.

Fluid shear stress has been proposed as a new means to generate endothelial cells from ESCs because of the number of studies demonstrating its ability to promote an endothelial cell (EC) phenotype in ESCs [81, 148, 205]. In order to definitively determine if fluid shear stress is a better method derived ECs from ESCs compared to standard protocols, direct comparisons of the quantities and quality of the ECs generated by fluid shear stress and established protocols which use a myriad of growth factors and cell sorting procedures need to be made [45, 55, 56, 86]. Additionally, the mechanism by which ESCs respond to fluid shear stress which leads to changes in phenotype need to be better characterized and well understood. The studies presented in this thesis

demonstrate that while applying fluid shear stress to an entire monolayer of ESCs only a subset of ESCs develop an EC phenotype. Furthermore, similar studies have demonstrated that approximately 30-40% develop an EC phenotype [148]. On the other hand, more recent studies have claimed that fluid shear stress also leads to self renewal of ESCs rather than increased differentiation towards a vascular cell type [206]. Examining how ESCs respond to fluid shear stress and how this physical stimulation switches the ESC fate to differentiate or self renew needs to be elucidated.

The aforementioned studies focused on shearing ESCs on collagen type IV coated glass slides. While different shear magnitudes were examined, different extracellular matrices and substrates were not investigated. In the vasculature endothelial cells are exposed to collagen type IV; however the mechanical properties of the vasculature are drastically different from glass. In order to better recapitulate the vascular microenvironment, biomaterials which have comparable mechanical properties (i.e. elastic modulus) need to be explored. Research examining the effects of varying mechanical properties such as elastic modulus on stem cell behavior and differentiation is expanding while also receiving some controversial debate [207-210]. Biomaterials which allow for tuning of mechanical properties present some challenges because they rely on the use of synthetic biomaterials which use harsh crosslinking agents [211] or yield materials which require extensive chemical modification to ensure adsorption of extracellular matrices and proper cell attachment.

The patterning of endothelial-like cells within EBs following shear preconditioning suggests that mechanical stimulation of ESCs prior to EB formation may be used as a method to control cellular patterning and organization within 3D cell

aggregates. Patterning of cells on 2D substrates has been well studied using extracellular matrices, biomaterials, chemokines, growth factors, and/or cytokines [206, 212]. However, few in depth studies on patterning stem cell populations in 3D structures have been performed due to challenges of controlling the presentation of growth factors or extracellular matrices in a more complex structure. Using physical forces which mimic physiological forces can potentially overcome these challenges. For examples, strain has been reported to promote stem cells to differentiate into smooth muscles cells [213]. Additionally, low magnitudes of fluid shear stress promote hematopoietic differentiation [89]. Subjecting different populations of stem cells to prescribed physical stimulation and then forming 3D cellular aggregates (strained stem cells=smooth muscle cells and sheared stem cells=endothelial cells) may lead to enhanced morphogenic events which mimic in vivo morphogenic processes.

During embryogenesis fluid shear stress plays a critical role in the development of vasculature and differentiation of endothelial cells. While VE-cadherin positive cells developed a more mature endothelial phenotype with expression of vWF, imparting shear stress to these cells within the embryoid body may have further increase maturation, expansion and proliferation of these endothelial-like cells, or organization into primitive vasculature. Typically, standard EB suspension culture systems generally only impart fluid shear stresses to the periphery of the EBs [76, 214], therefore only cells on the outermost layer are experiencing fluid shear stresses. Perfusion culture could be utilized in order to impart fluid shear stress within the EB. Novel technologies such as microfluidic chambers and flow systems [215, 216] could be employed to impart fluid shear stress through the interior of the EB.

Cadherins ensure that cells within tissues bind to one another and mediate selective cell adhesions. Like cadherins only bind like cadherins giving rise to specific cadherin expression in each tissue [163, 217]. For example E-cadherin is only expressed in epithelial tissues, N-cadherin is specific to neurons, and M-cadherin is restricted to myotubes. This cadherin specificity can be used to pattern in vitro 3D stem cell aggregates which better mimic tissue organization and morphogenesis observed during embryogenesis. Pre-conditioning stem cells with different growth factors, culturing them in microenvironments, or stimulating them with physical forces to promote specific cadherin expression and then forming 3D aggregates may be a potential method to generate in vitro stem cell aggregates which better recapitulate embryogenesis.

VEGF delivery within EBs through the use of gelatin microparticles increased endothelial gene expression. Surprisingly, incorporation of empty gelatin microparticles also increased endothelial gene expression of EBs to similar levels. These results indicated that the VEGF released from the gelatin microparticles had no effect on endothelial differentiation of EBs. During incorporation of microparticles within EBs, the microparticles were being agitated due to the rotary suspension culture used to form EBs. This agitation could have stimulated the release of VEGF. Additionally, the interaction of VEGF and the gelatin microparticles may have been weak because VEGF absorption to gelatin microparticles occurs via electrostatics since VEGF is positively charged and gelatin is negatively charged. Therefore, similar results observed for VEGF loaded microparticles and empty microparticles could be due to the rotary agitation as well as weak interactions between the VEGF and the gelatin. In order to overcome these challenges allowing microparticles to incorporate within EBs in the absence of rotary

suspension could be performed by utilizing forced aggregation. This method forces cells and miroparticles to form individual aggregates using centrifugation [199, 218]. On the other hand, VEGF and gelatin interaction and release could be better controlled by adding a binding motif to mediate enhanced binding of VEGF to gelatin; one such binding motif is heparin [219-221]. Delivering VEGF bound to heparin stimulates VEGF receptor activity [222].

Use of a pVE-cadherin GFP reporter ESC cell line allowed for direct and real time assessment of VE-cadherin expression and ESC endothelial differentiation during embryoid body culture. Additionally, the GFP reporter cell line provided confirmation of the observations and results of similar studies performed using ESCs. While GFP reporter cell lines are useful in confirming results observed when using traditional cell lines, when initially performing differentiation experiments in which one is screening for general differentiation of ESCs towards the 3 germ layers a specific GFP reporter cell line may not be as useful. Reporter cell lines that have been transduced with 2 or 3 plasmids which incorporates multiple promoters associated with different color fluorescence proteins, such as pFlk-1 GFP (mesoderm), pPax6 RFP (ectoderm), and pAFP YFP (endoderm) may be more useful in quickly assessing differentiation towards multiple cell lineages. Moreover, when looking at differentiated cells which come from similar pre-cursors such as endothelial cells and hematopoietic cells or endothelial cells and smooth muscle cells this technology would be very beneficial and lead to the design of more efficient and sophisticated experiments.

In chapter 5 the effects of exogenous VEGF on EBs formed from pre-conditioned ESCs was examined, while in chapter 6 hypoxic effects on endogenous VEGF production

in EBs formed from pre-conditioned ESCs were analyzed. These studies demonstrated that exogenous effects of VEGF and endogenous production of VEGF is modulated by pre-treatment of ESCs, respectively. 50 ng/ml of soluble VEGF was delivered to EBs, which is the typical quantity used in protocols to differentiate ESCs in monolayers to ECs [55, 86]. On the other hand, EBs cultured under normoxic conditions produced on the order of 11ng of VEGF per mg of total proteins within the EBs. Unexpectedly, ESCs pre-conditioned with shear stress produced approximately 60 ng of VEGF per mg of total proteins produced within the EBs. This indicates that EBs under hypoxia have the ability to produce growth factors such as VEGF on the orders of magnitudes comparable to amounts used for differentiation protocols. In the aforementioned studies, VEGF was the only growth factor analyzed, however other growth factors relevant to endothelial differentiation and angiogenesis (pro or anti) need to be examined such as IGF, FGF, ephrin, TGF- β 1, Ang1, and PDGF.

The hypoxia studies presented in this work cultured EBs at 3% oxygen for 7 days. At day 7 formation of primitive vascular structures were observed suggesting that long term culture under low oxygen is needed for endothelial network formation. It still remains to be shown whether these structures within the EBs are maintained, become more complex or regress after 7 days of hypoxic culture. Additionally, if these EBs were to be cultured at normoxic condition following 7 days of hypoxia culture how would the endothelial like cells organize within the EB. Moreover, if these EBs were allowed to aggregate would the primitive vascular structures in each EB connect with other networks in surrounding EBs to develop into an intricate complex vascular network.

EBs formed from shear pre-conditioned ESCs cultured under hypoxia provide an ideal pre-vascularized tissue for numerous tissues. The ESCs surrounding the primitive vascular network can be treated with a prescribed cocktail of growth factors and cytokines to yield cardiomyocytes to produce a vascularized cardiac patch. The presence of primitive vasculature may enhance the success of in vivo implantation and efficacy when used in an in vivo myocardial infarction model. On the other hand, these EBs can also be implanted into a hind limb ischemia model in order to stimulate angiogenesis.

Drug screening is typically performed on cells in monolayer prior to testing in animal models [223, 224]. However, cells in monolayer are not an accurate representation of the in vivo 3D tissue structure. In order to screen or test drugs more accurately 3D cellular aggregates are more representative of in vivo microenvironment. Specifically in understanding how different drugs may affect embryogenesis or tissue development EBs better represent the embryonic environment compared to ESCs in monolayer. The EBs formed from ESCs pre-conditioned with shear cultured under normoxia and under hypoxia would be ideal for screening drugs which have implications in vascular formation, angiogenesis, vascular defects and cardiovascular diseases.

All experiments performed in this work used mESCs. While mESCs are a good cell line to use for proof of principle and for initial investigations, similar experiments should be performed using hESCs because many differences have been observed between human and mouse ESCs[225-227]. Published studies have generally looked at the self-renewal properties of hESCs in the presence of low shear stresses [228, 229]. Using hESCs will provide more insight into feasibility for potential use of fluid shear pre-conditioning and hypoxia as a method to generate pre-vascularized tissues for

regenerative medicine applications. Generating quantities of hESCs required to perform these experiments is a key challenge, which has been hindered by the labor intensive culturing methods and lengthy expansion periods for hESCs

In conclusion, this work has contributed to developing new methods to control endothelial differentiation and vasculogenesis within EBs, as well as strategies to generate ECs from ESCs. Fluid shear stress and hypoxic culture represent bioprocessing methods which can generate vasculogenic EBs. Overall, the insights gained from this work provide a platform to explore a number of avenues including but not limited to EB growth factor production under hypoxia, pre-vascularized stem cell constructs, and 3D vasculogenic models for drug screening.

APPENDIX A

EMBRYOID BODIES FORMED FROM EMBRYONIC STEM CELLS

CULTURED ON DIFFERENT MATRICES

Embryoid bodies (EBs) were formed from ESCs cultured on gelatin (control) and ESCs cultured on collagen type IV (static) and cultured for 7 days on a 40 RPM rotary. EB morphology (Fig.A1. A-F), EB yields (Fig.A1.G) and cross sectional area (Fig. A1.H) were examined. Additionally, endothelial marker genes Flk-1, Flt-1, VE-cadherin, and PECAM expression was analyzed during EB differentiation. EB morphology was similar between control and static EB groups at all time points examined (Fig.A1. A-F). On day 2, ESCs cultured on gelatin and collagen IV formed similar amounts of EBs (Fig. A1.G). Furthermore, by day 2 the EB cross sectional area distribution of both EB groups were comparable (Fig. A1.H). Analysis of Flk-1 gene expression revealed control EBs expressed similar levels of Flk-1 throughout EB differentiation, while static EBs expressed varying levels of Flk-1 throughout EB differentiation (Fig. A1.I). Flt-1 gene expression progressively increased from from day 2 to day 7 in control EBs, while Flt-1 expression in static EBs was variable throughout EB differentiation (Fig. A1.J). Control EBs expressed similar levels of VE-cadherin throughout EB differentiation. VE-cadherin expression levels were altered throughout EB differentiation, levels of expression reached a maximum at day 4 (Fig. A1.K). PECAM expression in both control EBs and static EBs was variable throughout EB differentiation (Fig. A1.L). Altogether, these preliminary results suggested that culturing ESCs on different matrices prior to EB differentiation had little effect on EB morphology. However, endothelial marker gene expression analysis

revealed that the matrix ESCs were cultured on prior to EB differentiation affects endothelial differentiation profile.

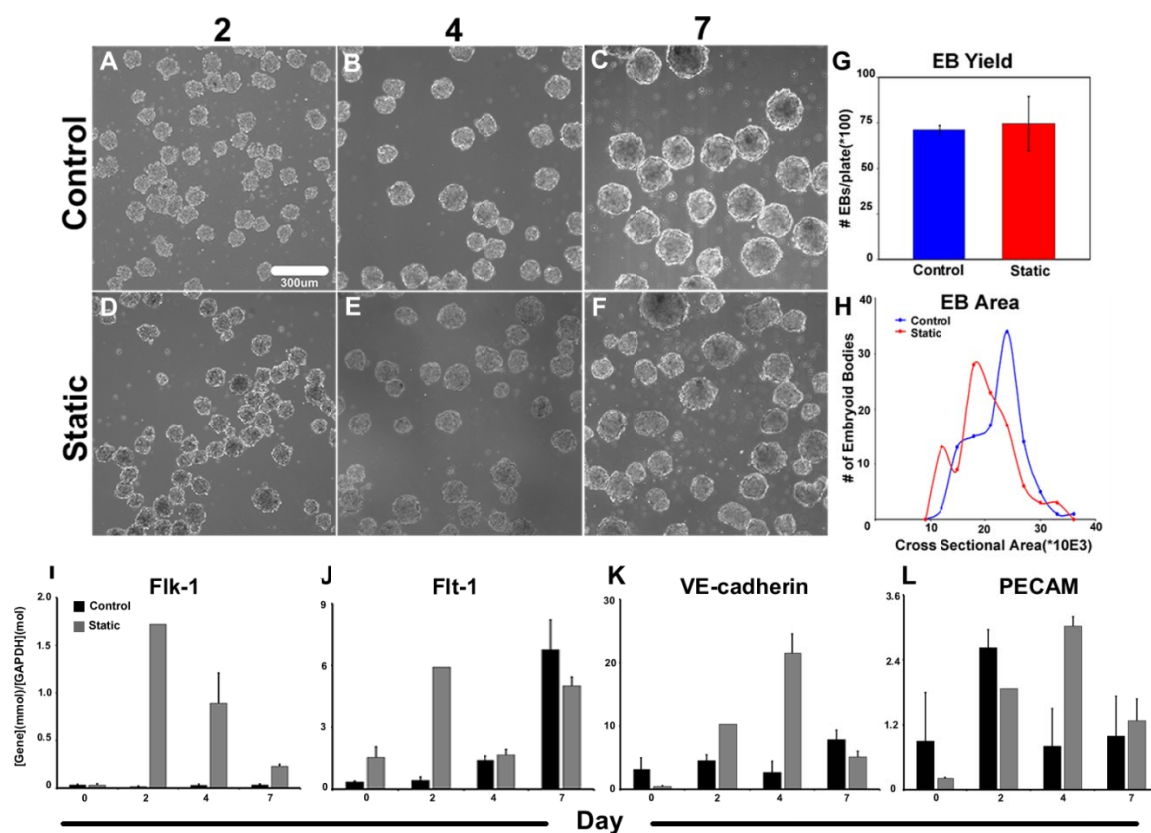


Figure A1: EB Morphology and Endothelial Marker Gene Expression. Control EBs were formed from ESCs cultured on gelatin (day 2, 4, and 7) (A-C). Static EBs were formed from ESC cultured on collagen IV (day 2, 4, and 7) (D-F). Day 2 EB Yield and EB cross sectional area revealed no differences in EB quantities and distribution in cross sectional are between control and static EB groups, respectively (G,H). Flk-1 (I), Flt-1(J), and VE-cadherin (K), and PECAM (L) gene expression analysis of control EBs and static (EBs). (mean \pm standard deviation)

APPENDIX B

E-CADHERIN AND VE-CADHERIN EXPRESSION IN EMBRYOID BODIES FORMED FROM PRE-CONDITIONED EMBRYONIC STEM CELLS

E-cadherin and VE-cadherin expression in day 7 EBs formed from pre-conditioned (static or shear 5 dyn/cm²) ESCs was examined using immunofluorescence and confocal imaging. E-cadherin is expressed by undifferentiated ESCs, while VE-cadherin is expressed in vascular endothelial cells. PC Static EBs were negative for VE-cadherin, but contained many cells that were E-cadherin positive (Fig. B1.A). Additionally, phase images of the same EBs revealed no optically opaque regions within the EB (Fig. B1.B). PC Shear 5 EBs contained a few VE-cadherin positive cells which localized to the center of the EB and were not positive for E-cadherin (Fig. B1.C). A phase image of the same EB reveals localization of E-cadherin negative cells in dark areas of the EB (Fig. B1.D). These results suggest that dark areas of EBs formed from shear pre-conditioned ESCs contain differentiating ESCs while endothelial-like cells remain localized to the center of PC Shear 5 EBs.

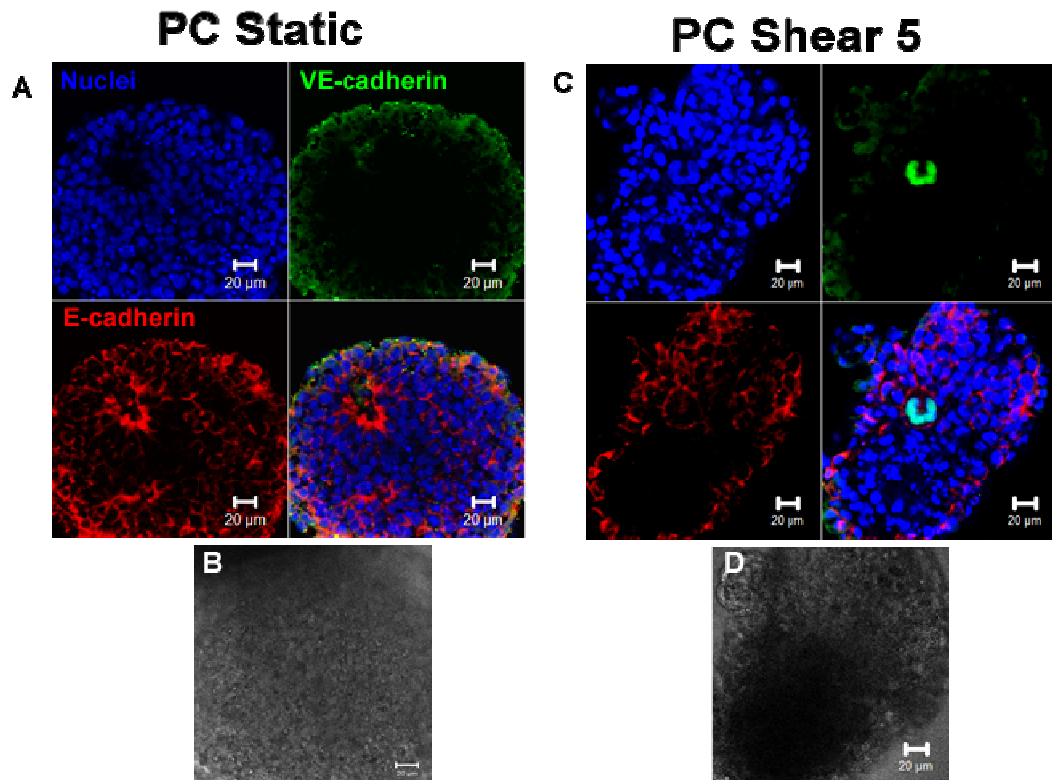


Figure B1: Embryoid Body VE-cadherin and E-cadherin Expression. Day 7 PC Static EBs were negative for VE-cadherin but contained many cells that were E-cadherin positive (A). A Phase image of the same PC Static EB displayed no areas of dark contrast within the EB. Day 7 PC Shear 5 EB contained a few VE-cadherin positive cells at the center of the EB which were not E-cadherin positive (C). Corresponding phase image of the same EB revealed a large dark region which corresponds with the region of the EB which is negative for E-cadherin (D).

APPENDIX C

VASCULAR ENDOTHELIAL GROWTH FACTOR RELEASE FROM GELATIN MICROPARTICLES

Vascular endothelial growth factor (VEGF) release kinetics from gelatin microparticles was analyzed in a cell free basal media using an ELISA assay. Lyophilized Gelatin microparticles (MPs) (3mg, 2.5E6 /mg) were loaded with VEGF (50ng VEGF/ mg of mps, 15ul) in a 1.5ml tube and incubated overnight at 4°C. Following overnight incubation MPs were resuspended in 750ul of 1% BSA in basal media (DMEM). Next MPs were centrifuged for 1.5 minutes and then 300 µl of supernatant was collected immediately to measure initial VEGF quantities released (0 hr). MPs were resuspended by adding 300 µl of 1% BSA solution followed by incubation at 37°C with constant gentle agitation. For each time point assessed 300 µl was collected from the MPs suspension followed by resuspension of MP solution by adding 300 µl of 1% BSA solution. Collected supernatants were stored at -20°C until VEGF ELISA (Chapter 6 Methods) was performed. Gelatin MPs were on average 5 µm in diameter (Fig. C1.A). There was a bolus release of majority of the VEGF loaded within MPs within the first 24 hours. However, VEGF release plateaued for the next 6 days (Fig. C1.B)

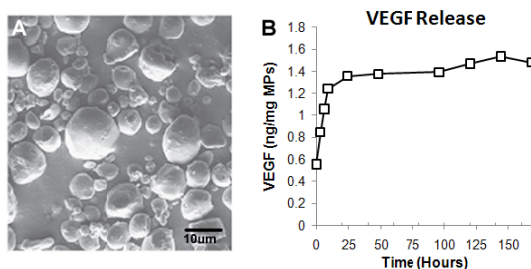


Figure C1. VEGF Release from Gelatin Microparticles. Gelatin MPs were round with an average diameter of 5µm (A). Majority of VEGF loaded in gelatin MPs was released in the first 24hours (B).

APPENDIX D

MONOLAYER AND EMBRYOID BODY DIFFERENTIATION OF FLUID SHEAR STRESS PRE-CONDITIONED EMBRYONIC STEM CELLS

Following pre-conditioning at either 0 dyn/cm² (PC static) or 15 dyn/cm² (PC Shear 15), ESCs were cultured as monolayers or as EBs for 4 days. Pre-conditioned ESCs were culture in monolayer on gelatin or as EBs on a 40 RPM rotary orbital shaker. Monolayer cultures were initiated by seeding 250,000 cells in 100 mm Petri dish. EB cultures were initiated by seeding 2E6 cells in 100 mm petric dishes. Cultures were maintained for 4 days which is the time point at which monolayer cultures reached confluency. Phase images of monolayers displayed no distinct differences in cell morphology between pre-conditioning regimens (Fig. D1. A, B). Embryoid body morphology was also similiar between groups (Fig. D1. C, D). Analysis of endothelial marker genes Flk-1, Flt-1, VE-cadherin, and PECAM revealed differing gene expression patterns in monolayer and EB differentiation of pre-conditioned ESCs.

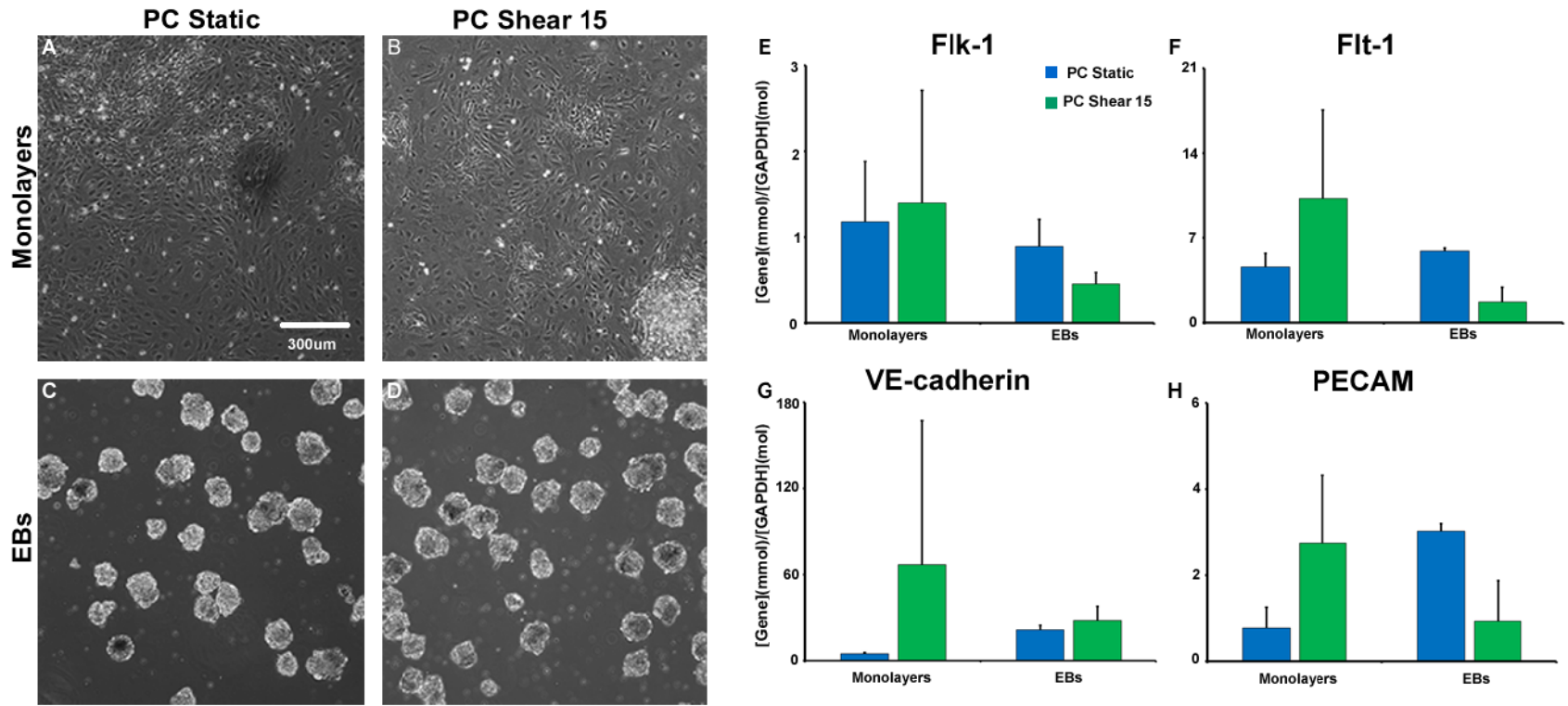


Figure D1. Monolayer and EB Differentiation of Pre-conditioned ESCs. Day 4 phase images of ESCs pre-conditioned at 0 dyn/cm² (A) and ESCs pre-conditioned at 15 dyn/cm² (B) cultured in monolayers. Day 4 phase images of EBs formed from ESCs pre-conditioned at 0 dyn/cm² (C) and ESCs pre-conditioned at 15 dyn/cm² (D). Day 4 Flk-1 (E), Flt-1 (F), VE-cadherin (G), and PECAM (H) gene expression of PC Static monolayers, PC Static EBs, PC Shear 15 monolayers, and PC Shear 15 EBs. (mean \pm standard deviation).

REFERENCES

1. Sarig, U. and M. Machluf, Engineering cell platforms for myocardial regeneration. *Expert Opin Biol Ther*, 2011. **11**;8: 1055-77.
2. Godier-Furnemont, A.F., T.P. Martens, M.S. Koeckert, L. Wan, J. Parks, K. Arai, et al., Composite scaffold provides a cell delivery platform for cardiovascular repair. *Proc Natl Acad Sci U S A*, 2011. **108**;19: 7974-9.
3. Rauch, M.F., S.R. Hynes, J. Bertram, A. Redmond, R. Robinson, C. Williams, et al., Engineering angiogenesis following spinal cord injury: a coculture of neural progenitor and endothelial cells in a degradable polymer implant leads to an increase in vessel density and formation of the blood-spinal cord barrier. *Eur J Neurosci*, 2009. **29**;1: 132-45.
4. Veriter, S., N. Aouassar, P.Y. Adnet, M.S. Paridaens, C. Stuckman, B. Jordan, et al., The impact of hyperglycemia and the presence of encapsulated islets on oxygenation within a bioartificial pancreas in the presence of mesenchymal stem cells in a diabetic Wistar rat model. *Biomaterials*, 2011. **32**;26: 5945-56.
5. Streit, M. and L.R. Braathen, Apligraf--a living human skin equivalent for the treatment of chronic wounds. *Int J Artif Organs*, 2000. **23**;12: 831-3.
6. Fedorovich, N.E., R.T. Haverslag, W.J. Dhert, and J. Alblas, The role of endothelial progenitor cells in prevascularized bone tissue engineering: development of heterogeneous constructs. *Tissue Eng Part A*, 2010. **16**;7: 2355-67.
7. Ramirez, E., S.G. Burillo, C. Barrera-Diaz, G. Roa, and B. Bilyeu, Use of pH-sensitive polymer hydrogels in lead removal from aqueous solution. *J Hazard Mater*, 2011. **192**;2: 432-9.
8. Dvir, T., A. Kedem, E. Ruvinov, O. Levy, I. Freeman, N. Landa, et al., Prevascularization of cardiac patch on the omentum improves its therapeutic outcome. *Proc Natl Acad Sci U S A*, 2009. **106**;35: 14990-5.
9. Sakurai, T., A. Satake, S. Sumi, K. Inoue, N. Nagata, Y. Tabata, and J. Miyakoshi, The efficient prevascularization induced by fibroblast growth factor 2 with a collagen-coated device improves the cell survival of a bioartificial pancreas. *Pancreas*, 2004. **28**;3: e70-9.
10. Sakakibara, Y., K. Nishimura, K. Tambara, M. Yamamoto, F. Lu, Y. Tabata, and M. Komeda, Prevascularization with gelatin microspheres containing basic fibroblast growth factor enhances the benefits of cardiomyocyte transplantation. *J Thorac Cardiovasc Surg*, 2002. **124**;1: 50-6.

11. Chen, X., A.S. Aledia, C.M. Ghajar, C.K. Griffith, A.J. Putnam, C.C. Hughes, and S.C. George, Prevascularization of a fibrin-based tissue construct accelerates the formation of functional anastomosis with host vasculature. *Tissue Eng Part A*, 2009. **15**;6: 1363-71.
12. Griffith, C.K. and S.C. George, The effect of hypoxia on in vitro prevascularization of a thick soft tissue. *Tissue Eng Part A*, 2009. **15**;9: 2423-34.
13. Asakawa, N., T. Shimizu, Y. Tsuda, S. Sekiya, T. Sasagawa, M. Yamato, et al., Pre-vascularization of in vitro three-dimensional tissues created by cell sheet engineering. *Biomaterials*, 2010. **31**;14: 3903-9.
14. Griffith, C.K., C. Miller, R.C. Sainson, J.W. Calvert, N.L. Jeon, C.C. Hughes, and S.C. George, Diffusion limits of an in vitro thick prevascularized tissue. *Tissue Eng*, 2005. **11**;1-2: 257-66.
15. Bekhite, M.M., A. Finkensieper, S. Binas, J. Muller, R. Wetzker, H.R. Figulla, et al., VEGF-mediated PI3K class IA and PKC signaling in cardiomyogenesis and vasculogenesis of mouse embryonic stem cells. *J Cell Sci*, 2011. **124**;Pt 11: 1819-30.
16. Bagatto, B. and W. Burggren, A three-dimensional functional assessment of heart and vessel development in the larva of the zebrafish (*Danio rerio*). *Physiol Biochem Zool*, 2006. **79**;1: 194-201.
17. Hove, J.R., R.W. Koster, A.S. Forouhar, G. Acevedo-Bolton, S.E. Fraser, and M. Gharib, Intracardiac fluid forces are an essential epigenetic factor for embryonic cardiogenesis. *Nature*, 2003. **421**;6919: 172-7.
18. Semenza, G.L., Regulation of mammalian O₂ homeostasis by hypoxia-inducible factor 1. *Annu Rev Cell Dev Biol*, 1999. **15**: 551-78.
19. Simon, M.C. and B. Keith, The role of oxygen availability in embryonic development and stem cell function. *Nat Rev Mol Cell Biol*, 2008. **9**;4: 285-96.
20. Groenendijk, B.C., B.P. Hierck, J. Vrolijk, M. Baiker, M.J. Pourquie, A.C. Gittenberger-de Groot, and R.E. Poelmann, Changes in shear stress-related gene expression after experimentally altered venous return in the chicken embryo. *Circ Res*, 2005. **96**;12: 1291-8.
21. Weinstein, B.M., What guides early embryonic blood vessel formation? *Developmental Dynamics*, 1999. **215**;1: 2-11.
22. le Noble, F., D. Moyon, L. Pardanaud, L. Yuan, V. Djonov, R. Matthijsen, et al., Flow regulates arterial-venous differentiation in the chick embryo yolk sac. *Development*, 2004. **131**;2: 361-75.

23. Jones, E.A., M.H. Baron, S.E. Fraser, and M.E. Dickinson, Measuring hemodynamic changes during mammalian development. *Am J Physiol Heart Circ Physiol*, 2004. **287**;4: H1561-9.
24. Han, Y., S.Z. Kuang, A. Gomer, and D.L. Ramirez-Bergeron, Hypoxia influences the vascular expansion and differentiation of embryonic stem cell cultures through the temporal expression of vascular endothelial growth factor receptors in an ARNT-dependent manner. *Stem Cells*, 2010. **28**;4: 799-809.
25. Ramirez-Bergeron, D.L. and M.C. Simon, Hypoxia-inducible factor and the development of stem cells of the cardiovascular system. *Stem Cells*, 2001. **19**;4: 279-86.
26. Itskovitz-Eldor, J., M. Schuldiner, D. Karsenti, A. Eden, O. Yanuka, M. Amit, et al., Differentiation of human embryonic stem cells into embryoid bodies compromising the three embryonic germ layers. *Mol Med*, 2000. **6**;2: 88-95.
27. Keller, G.M., In vitro differentiation of embryonic stem cells. *Curr Opin Cell Biol*, 1995. **7**;6: 862-9.
28. Martin, G.R., Isolation of a pluripotent cell line from early mouse embryos cultured in medium conditioned by teratocarcinoma stem cells. *Proc Natl Acad Sci U S A*, 1981. **78**;12: 7634-8.
29. Wobus, A.M., H. Holzhausen, P. Jakel, and J. Schoneich, Characterization of a pluripotent stem cell line derived from a mouse embryo. *Exp Cell Res*, 1984. **152**;1: 212-9.
30. Wang, R., R. Clark, and V.L. Bautch, Embryonic stem cell-derived cystic embryoid bodies form vascular channels: an in vitro model of blood vessel development. *Development*, 1992. **114**;2: 303-16.
31. Nikolova-Krstevski, V., M. Bhasin, H.H. Otu, T. Libermann, and P. Oettgen, Gene expression analysis of embryonic stem cells expressing VE-cadherin (CD144) during endothelial differentiation. *BMC Genomics*, 2008. **9**: 240.
32. Desbaillets, I., U. Ziegler, P. Groscurth, and M. Gassmann, Embryoid bodies: an in vitro model of mouse embryogenesis. *Exp Physiol*, 2000. **85**;6: 645-51.
33. Siminovitch, L., E.A. McCulloch, and J.E. Till, The Distribution of Colony-Forming Cells among Spleen Colonies. *J Cell Physiol*, 1963. **62**: 327-36.
34. Becker, A.J., C.E. Mc, and J.E. Till, Cytological demonstration of the clonal nature of spleen colonies derived from transplanted mouse marrow cells. *Nature*, 1963. **197**: 452-4.
35. Lewis, P.D., Mitotic activity in the primate subependymal layer and the genesis of gliomas. *Nature*, 1968. **217**;5132: 974-5.

36. Altman, J. and G.D. Das, Autoradiographic and histological evidence of postnatal hippocampal neurogenesis in rats. *J Comp Neurol*, 1965. **124**;3: 319-35.
37. Zuk, P.A., M. Zhu, P. Ashjian, D.A. De Ugarte, J.I. Huang, H. Mizuno, et al., Human adipose tissue is a source of multipotent stem cells. *Mol Biol Cell*, 2002. **13**;12: 4279-95.
38. Sacco, A., R. Doyonnas, P. Kraft, S. Vitorovic, and H.M. Blau, Self-renewal and expansion of single transplanted muscle stem cells. *Nature*, 2008. **456**;7221: 502-6.
39. Toma, J.G., M. Akhavan, K.J. Fernandes, F. Barnabe-Heider, A. Sadikot, D.R. Kaplan, and F.D. Miller, Isolation of multipotent adult stem cells from the dermis of mammalian skin. *Nat Cell Biol*, 2001. **3**;9: 778-84.
40. Stemple, D.L. and D.J. Anderson, Isolation of a stem cell for neurons and glia from the mammalian neural crest. *Cell*, 1992. **71**;6: 973-85.
41. De Coppi, P., G. Bartsch, Jr., M.M. Siddiqui, T. Xu, C.C. Santos, L. Perin, et al., Isolation of amniotic stem cell lines with potential for therapy. *Nat Biotechnol*, 2007. **25**;1: 100-6.
42. Evans, M.J. and M.H. Kaufman, Establishment in culture of pluripotential cells from mouse embryos. *Nature*, 1981. **292**;5819: 154-6.
43. Thomson, J.A., J. Itskovitz-Eldor, S.S. Shapiro, M.A. Waknitz, J.J. Swiergiel, V.S. Marshall, and J.M. Jones, Embryonic stem cell lines derived from human blastocysts. *Science*, 1998. **282**;5391: 1145-7.
44. Walter, G., A. Intek, A.M. Wobus, and J. Schoneich, Serological characterization of a pluripotent mouse embryonal stem cell line, two transformed derivatives, and an endoderm-like cell line. *Cell Differ*, 1984. **15**;2-4: 147-51.
45. Levenberg, S., J.S. Golub, M. Amit, J. Itskovitz-Eldor, and R. Langer, Endothelial cells derived from human embryonic stem cells. *Proc Natl Acad Sci U S A*, 2002. **99**;7: 4391-6.
46. Fijnvandraat, A.C., A.C. van Ginneken, C.A. Schumacher, K.R. Boheler, R.H. Lekanne Deprez, V.M. Christoffels, and A.F. Moorman, Cardiomyocytes purified from differentiated embryonic stem cells exhibit characteristics of early chamber myocardium. *J Mol Cell Cardiol*, 2003. **35**;12: 1461-72.
47. Okabe, S., K. Forsberg-Nilsson, A.C. Spiro, M. Segal, and R.D. McKay, Development of neuronal precursor cells and functional postmitotic neurons from embryonic stem cells in vitro. *Mech Dev*, 1996. **59**;1: 89-102.
48. Colman, A., Making new beta cells from stem cells. *Semin Cell Dev Biol*, 2004. **15**;3: 337-45.

49. Keller, G., M. Kennedy, T. Papayannopoulou, and M.V. Wiles, Hematopoietic commitment during embryonic stem cell differentiation in culture. *Mol Cell Biol*, 1993. **13**;1: 473-86.
50. Hirashima, M., M. Ogawa, S. Nishikawa, K. Matsumura, K. Kawasaki, and M. Shibuya, A chemically defined culture of VEGFR2⁺ cells derived from embryonic stem cells reveals the role of VEGFR1 in tuning the threshold for VEGF in developing endothelial cells. *Blood*, 2003. **101**;6: 2261-7.
51. Battista, S., D. Guarnieri, C. Borselli, S. Zeppetelli, A. Borzacchiello, L. Mayol, et al., The effect of matrix composition of 3D constructs on embryonic stem cell differentiation. *Biomaterials*, 2005. **26**;31: 6194-207.
52. Williams, R.L., D.J. Hilton, S. Pease, T.A. Willson, C.L. Stewart, D.P. Gearing, et al., Myeloid leukaemia inhibitory factor maintains the developmental potential of embryonic stem cells. *Nature*, 1988. **336**;6200: 684-7.
53. Schuldiner, M., O. Yanuka, J. Itskovitz-Eldor, D.A. Melton, and N. Benvenisty, Effects of eight growth factors on the differentiation of cells derived from human embryonic stem cells. *Proc Natl Acad Sci U S A*, 2000. **97**;21: 11307-12.
54. McCloskey, K.E., I. Lyons, R.R. Rao, S.L. Stice, and R.M. Nerem, Purified and proliferating endothelial cells derived and expanded in vitro from embryonic stem cells. *Endothelium*, 2003. **10**;6: 329-36.
55. Vittet, D., M.H. Prandini, R. Berthier, A. Schweitzer, H. Martin-Sisteron, G. Uzan, and E. Dejana, Embryonic stem cells differentiate in vitro to endothelial cells through successive maturation steps. *Blood*, 1996. **88**;9: 3424-31.
56. Blancas, A.A., N.E. Lauer, and K.E. McCloskey, Endothelial differentiation of embryonic stem cells. *Curr Protoc Stem Cell Biol*, 2008. **Chapter 1**: Unit 1F 5.
57. Hirashima, M., H. Kataoka, S. Nishikawa, and N. Matsuyoshi, Maturation of embryonic stem cells into endothelial cells in an in vitro model of vasculogenesis. *Blood*, 1999. **93**;4: 1253-63.
58. Risau, W., H. Sariola, H.G. Zerwes, J. Sasse, P. Ekblom, R. Kemler, and T. Doetschman, Vasculogenesis and angiogenesis in embryonic-stem-cell-derived embryoid bodies. *Development*, 1988. **102**;3: 471-8.
59. Choi, K., M. Kennedy, A. Kazarov, J.C. Papadimitriou, and G. Keller, A common precursor for hematopoietic and endothelial cells. *Development*, 1998. **125**;4: 725-32.
60. Loges, S., B. Fehse, M.A. Brockmann, K. Lamszus, M. Butzal, M. Guckenberg, et al., Identification of the adult human hemangioblast. *Stem Cells Dev*, 2004. **13**;3: 229-42.

61. Chung, Y.S., W.J. Zhang, E. Arentson, P.D. Kingsley, J. Palis, and K. Choi, Lineage analysis of the hemangioblast as defined by FLK1 and SCL expression. *Development*, 2002. **129**;23: 5511-20.
62. Lugus, J.J., C. Park, and K. Choi, Developmental relationship between hematopoietic and endothelial cells. *Immunol Res*, 2005. **32**;1-3: 57-74.
63. Sabin, F.R., Studies on the origin of blood-vessels and of red blood-corpuscles as seen in the living blastoderm of chicks during the second day of incubation. *Contributions to Embryology*, 1920. **9**;27/46: 215-U56.
64. Drake, C.J. and P.A. Fleming, Vasculogenesis in the day 6.5 to 9.5 mouse embryo. *Blood*, 2000. **95**;5: 1671-9.
65. Mikkola, H.K., Y. Fujiwara, T.M. Schlaeger, D. Traver, and S.H. Orkin, Expression of CD41 marks the initiation of definitive hematopoiesis in the mouse embryo. *Blood*, 2003. **101**;2: 508-16.
66. Davies, P.F., Hemodynamic shear stress and the endothelium in cardiovascular pathophysiology. *Nat Clin Pract Cardiovasc Med*, 2009. **6**;1: 16-26.
67. Levesque, M.J., R.M. Nerem, and E.A. Sprague, Vascular endothelial cell proliferation in culture and the influence of flow. *Biomaterials*, 1990. **11**;9: 702-707.
68. Hierck, B.P., K. Van der Heiden, F.E. Alkemade, S. Van de Pas, J.V. Van Thienen, B.C. Groenendijk, et al., Primary cilia sensitize endothelial cells for fluid shear stress. *Dev Dyn*, 2008. **237**;3: 725-35.
69. Helmke, B.P., Choosing sides in polarized endothelial adaptation to shear stress. *Circ Res*, 2008. **103**;2: 122-4.
70. Huang, J., R. Roth, J.E. Heuser, and J.E. Sadler, Integrin alpha(v)beta(3) on human endothelial cells binds von Willebrand factor strings under fluid shear stress. *Blood*, 2009. **113**;7: 1589-97.
71. Levesque, M.J. and R.M. Nerem, The Elongation and Orientation of Cultured Endothelial Cells in Response to Shear Stress. *Journal of Biomechanical Engineering*, 1985. **107**;4: 341-347.
72. Nauli, S.M., Y. Kawanabe, J.J. Kaminski, W.J. Pearce, D.E. Ingber, and J. Zhou, Endothelial cilia are fluid shear sensors that regulate calcium signaling and nitric oxide production through polycystin-1. *Circulation*, 2008. **117**;9: 1161-71.
73. Walsh, T.G., R.P. Murphy, P. Fitzpatrick, K.D. Rochfort, A.F. Guinan, A. Murphy, and P.M. Cummins, Stabilization of brain microvascular endothelial barrier function by shear stress involves VE-cadherin signaling leading to modulation of pTyr-occludin levels. *J Cell Physiol*, 2011. **226**;11: 3053-63.

74. Goettsch, C., W. Goettsch, M. Brux, C. Haschke, C. Brunssen, G. Muller, et al., Arterial flow reduces oxidative stress via an antioxidant response element and Oct-1 binding site within the NADPH oxidase 4 promoter in endothelial cells. *Basic Res Cardiol*, 2011. **106**;4: 551-61.
75. Dang, S.M., S. Gerecht-Nir, J. Chen, J. Itskovitz-Eldor, and P.W. Zandstra, Controlled, scalable embryonic stem cell differentiation culture. *Stem Cells*, 2004. **22**;3: 275-82.
76. Sargent, C.Y., G.Y. Berguig, M.A. Kinney, L.A. Hiatt, R.L. Carpenedo, R.E. Berson, and T.C. McDevitt, Hydrodynamic modulation of embryonic stem cell differentiation by rotary orbital suspension culture. *Biotechnol Bioeng*, 2009.
77. Carpenedo, R.L., C.Y. Sargent, and T.C. McDevitt, Rotary suspension culture enhances the efficiency, yield, and homogeneity of embryoid body differentiation. *Stem Cells*, 2007. **25**;9: 2224-34.
78. Cameron, C.M., W.S. Hu, and D.S. Kaufman, Improved development of human embryonic stem cell-derived embryoid bodies by stirred vessel cultivation. *Biotechnol Bioeng*, 2006. **94**;5: 938-48.
79. Chung, C.A., M.R. Tzou, and R.W. Ho, Oscillatory flow in a cone-and-plate bioreactor. *J Biomech Eng*, 2005. **127**;4: 601-10.
80. Stolberg, S. and K.E. McCloskey, Can shear stress direct stem cell fate? *Biotechnol Prog*, 2009. **25**;1: 10-9.
81. Yamamoto, K., T. Sokabe, T. Watabe, K. Miyazono, J.K. Yamashita, S. Obi, et al., Fluid shear stress induces differentiation of Flk-1-positive embryonic stem cells into vascular endothelial cells in vitro. *Am J Physiol Heart Circ Physiol*, 2005. **288**;4: H1915-24.
82. Zeng, C., X. Wang, X. Hu, J. Chen, and L. Wang, Autologous endothelial progenitor cells transplantation for the therapy of primary pulmonary hypertension. *Med Hypotheses*, 2007. **68**;6: 1292-5.
83. Illi, B., A. Scopece, S. Nanni, A. Farsetti, L. Morgante, P. Biglioli, et al., Epigenetic histone modification and cardiovascular lineage programming in mouse embryonic stem cells exposed to laminar shear stress. *Circ Res*, 2005. **96**;5: 501-8.
84. Huang, H., Y. Nakayama, K. Qin, K. Yamamoto, J. Ando, J. Yamashita, et al., Differentiation from embryonic stem cells to vascular wall cells under in vitro pulsatile flow loading. *J Artif Organs*, 2005. **8**;2: 110-8.
85. Zeng, L., Q. Xiao, A. Margariti, Z. Zhang, A. Zampetaki, S. Patel, et al., HDAC3 is crucial in shear- and VEGF-induced stem cell differentiation toward endothelial cells. *J Cell Biol*, 2006. **174**;7: 1059-69.

86. McCloskey, K.E., D.A. Smith, H. Jo, and R.M. Nerem, Embryonic stem cell-derived endothelial cells may lack complete functional maturation in vitro. *J Vasc Res*, 2006. **43**;5: 411-21.
87. Metallo, C.M., M.A. Vodyanik, J.J. de Pablo, Slukvin, II, and S.P. Palecek, The response of human embryonic stem cell-derived endothelial cells to shear stress. *Biotechnol Bioeng*, 2008. **100**;4: 830-7.
88. Obi, S., K. Yamamoto, N. Shimizu, S. Kumagaya, T. Masumura, T. Sokabe, et al., Fluid shear stress induces arterial differentiation of endothelial progenitor cells. *J Appl Physiol*, 2009. **106**;1: 203-11.
89. Adamo, L., O. Naveiras, P.L. Wenzel, S. McKinney-Freeman, P.J. Mack, J. Gracia-Sancho, et al., Biomechanical forces promote embryonic haematopoiesis. *Nature*, 2009. **459**;7250: 1131-5.
90. Ferrara, N., Role of vascular endothelial growth factor in physiologic and pathologic angiogenesis: therapeutic implications. *Semin Oncol*, 2002. **29**;6 Suppl 16: 10-4.
91. Machein, M.R. and K.H. Plate, Role of VEGF in developmental angiogenesis and in tumor angiogenesis in the brain. *Cancer Treat Res*, 2004. **117**: 191-218.
92. Nourse, M.B., D.E. Halpin, M. Scatena, D.J. Mortisen, N.L. Tulloch, K.D. Hauch, et al., VEGF induces differentiation of functional endothelium from human embryonic stem cells: implications for tissue engineering. *Arterioscler Thromb Vasc Biol*, 2010. **30**;1: 80-9.
93. Gu, A., W. Tsark, K.V. Holmes, and J.E. Shively, Role of Ceacam1 in VEGF induced vasculogenesis of murine embryonic stem cell-derived embryoid bodies in 3D culture. *Exp Cell Res*, 2009. **315**;10: 1668-82.
94. Ferrara, N., Vascular endothelial growth factor. *Eur J Cancer*, 1996. **32A**;14: 2413-22.
95. Ferrara, N. and S. Bunting, Vascular endothelial growth factor, a specific regulator of angiogenesis. *Curr Opin Nephrol Hypertens*, 1996. **5**;1: 35-44.
96. Bieri, M., M. Oroszlan, A. Farkas, N. Ligeti, J. Bieri, and P. Mohacsi, Anti-HLA I antibodies induce VEGF production by endothelial cells, which increases proliferation and paracellular permeability. *Int J Biochem Cell Biol*, 2009. **41**;12: 2422-30.
97. Herzog, B., C. Pellet-Many, G. Britton, B. Hartzoulakis, and I.C. Zachary, VEGF binding to NRP1 is essential for VEGF stimulation of endothelial cell migration, complex formation between NRP1 and VEGFR2, and signaling via FAK Tyr407 phosphorylation. *Mol Biol Cell*, 2011. **22**;15: 2766-76.

98. Wang, Y., M. Nakayama, M.E. Pitulescu, T.S. Schmidt, M.L. Bochenek, A. Sakakibara, et al., Ephrin-B2 controls VEGF-induced angiogenesis and lymphangiogenesis. *Nature*, 2010. **465**;7297: 483-6.
99. Franco, M., P. Roswall, E. Cortez, D. Hanahan, and K. Pietras, Pericytes promote endothelial cell survival through induction of autocrine VEGF-A signaling and Bcl-w expression. *Blood*, 2011. **118**;10: 2906-17.
100. Cerdan, C., A. Rouleau, and M. Bhatia, VEGF-A165 augments erythropoietic development from human embryonic stem cells. *Blood*, 2004. **103**;7: 2504-12.
101. Purpura, K.A., J. Morin, and P.W. Zandstra, Analysis of the temporal and concentration-dependent effects of BMP-4, VEGF, and TPO on development of embryonic stem cell-derived mesoderm and blood progenitors in a defined, serum-free media. *Exp Hematol*, 2008. **36**;9: 1186-98.
102. Takayama, N., H. Nishikii, J. Usui, H. Tsukui, A. Sawaguchi, T. Hiroyama, et al., Generation of functional platelets from human embryonic stem cells in vitro via ES-sacs, VEGF-promoted structures that concentrate hematopoietic progenitors. *Blood*, 2008. **111**;11: 5298-306.
103. Gerber, H.P., A.K. Malik, G.P. Solar, D. Sherman, X.H. Liang, G. Meng, et al., VEGF regulates haematopoietic stem cell survival by an internal autocrine loop mechanism. *Nature*, 2002. **417**;6892: 954-8.
104. Eckardt, K.U., W.M. Bernhardt, A. Weidemann, C. Warnecke, C. Rosenberger, M.S. Wiesener, and C. Willam, Role of hypoxia in the pathogenesis of renal disease. *Kidney Int Suppl*, 2005;99: S46-51.
105. Peers, C., H.A. Pearson, and J.P. Boyle, Hypoxia and Alzheimer's disease. *Essays Biochem*, 2007. **43**: 153-64.
106. Eliasson, P. and J.I. Jonsson, The hematopoietic stem cell niche: low in oxygen but a nice place to be. *J Cell Physiol*, 2010. **222**;1: 17-22.
107. Eltzschig, H.K. and P. Carmeliet, Hypoxia and inflammation. *N Engl J Med*, 2011. **364**;7: 656-65.
108. Whelan, K.A. and M.J. Reginato, Surviving without oxygen: hypoxia regulation of mammary morphogenesis and anoikis. *Cell Cycle*, 2011. **10**;14: 2287-94.
109. Wheaton, W.W. and N.S. Chandel, Hypoxia. 2. Hypoxia regulates cellular metabolism. *Am J Physiol Cell Physiol*, 2011. **300**;3: C385-93.
110. Lee, H.J., C.H. Jeong, J.H. Cha, and K.W. Kim, PKC-delta inhibitors sustain self-renewal of mouse embryonic stem cells under hypoxia in vitro. *Exp Mol Med*, 2010. **42**;4: 294-301.

111. Prado-Lopez, S., A. Conesa, A. Arminan, M. Martinez-Losa, C. Escobedo-Lucea, C. Gandia, et al., Hypoxia promotes efficient differentiation of human embryonic stem cells to functional endothelium. *Stem Cells*, 2010. **28**;3: 407-18.
112. Semenza, G.L., Hypoxia-inducible factor 1: oxygen homeostasis and disease pathophysiology. *Trends Mol Med*, 2001. **7**;8: 345-50.
113. Wouters, B.G., T. van den Beucken, M.G. Magagnin, M. Koritzinsky, D. Fels, and C. Koumenis, Control of the hypoxic response through regulation of mRNA translation. *Semin Cell Dev Biol*, 2005. **16**;4-5: 487-501.
114. Forsythe, J.A., B.H. Jiang, N.V. Iyer, F. Agani, S.W. Leung, R.D. Koos, and G.L. Semenza, Activation of vascular endothelial growth factor gene transcription by hypoxia-inducible factor 1. *Mol Cell Biol*, 1996. **16**;9: 4604-13.
115. Jiang, B.H., E. Rue, G.L. Wang, R. Roe, and G.L. Semenza, Dimerization, DNA binding, and transactivation properties of hypoxia-inducible factor 1. *J Biol Chem*, 1996. **271**;30: 17771-8.
116. Maxwell, P.H., Hypoxia-inducible factor as a physiological regulator. *Exp Physiol*, 2005. **90**;6: 791-7.
117. Holmquist-Mengelbier, L., E. Fredlund, T. Lofstedt, R. Noguera, S. Navarro, H. Nilsson, et al., Recruitment of HIF-1alpha and HIF-2alpha to common target genes is differentially regulated in neuroblastoma: HIF-2alpha promotes an aggressive phenotype. *Cancer Cell*, 2006. **10**;5: 413-23.
118. Wiesener, M.S., J.S. Jurgensen, C. Rosenberger, C.K. Scholze, J.H. Horstrup, C. Warnecke, et al., Widespread hypoxia-inducible expression of HIF-2alpha in distinct cell populations of different organs. *FASEB J*, 2003. **17**;2: 271-3.
119. Forristal, C.E., K.L. Wright, N.A. Hanley, R.O. Oreffo, and F.D. Houghton, Hypoxia inducible factors regulate pluripotency and proliferation in human embryonic stem cells cultured at reduced oxygen tensions. *Reproduction*, 2010. **139**;1: 85-97.
120. Covello, K.L., J. Kehler, H. Yu, J.D. Gordan, A.M. Arsham, C.J. Hu, et al., HIF-2alpha regulates Oct-4: effects of hypoxia on stem cell function, embryonic development, and tumor growth. *Genes Dev*, 2006. **20**;5: 557-70.
121. Shweiki, D., A. Itin, D. Soffer, and E. Keshet, Vascular endothelial growth factor induced by hypoxia may mediate hypoxia-initiated angiogenesis. *Nature*, 1992. **359**;6398: 843-5.
122. Sharma, S.K., J.L. Lucitti, C. Nordman, J.P. Tinney, K. Tobita, and B.B. Keller, Impact of hypoxia on early chick embryo growth and cardiovascular function. *Pediatr Res*, 2006. **59**;1: 116-20.

123. Mitchell, J.A. and J.M. Yochim, Intrauterine oxygen tension during the estrous cycle in the rat: its relation to uterine respiration and vascular activity. *Endocrinology*, 1968. **83**;4: 701-5.
124. Rodesch, F., P. Simon, C. Donner, and E. Jauniaux, Oxygen measurements in endometrial and trophoblastic tissues during early pregnancy. *Obstet Gynecol*, 1992. **80**;2: 283-5.
125. Lee, Y.M., C.H. Jeong, S.Y. Koo, M.J. Son, H.S. Song, S.K. Bae, et al., Determination of hypoxic region by hypoxia marker in developing mouse embryos in vivo: a possible signal for vessel development. *Dev Dyn*, 2001. **220**;2: 175-86.
126. Hu, C.J., S. Iyer, A. Sataur, K.L. Covello, L.A. Chodosh, and M.C. Simon, Differential regulation of the transcriptional activities of hypoxia-inducible factor 1 alpha (HIF-1alpha) and HIF-2alpha in stem cells. *Mol Cell Biol*, 2006. **26**;9: 3514-26.
127. Hu, X., S.P. Yu, J.L. Fraser, Z. Lu, M.E. Ogle, J.A. Wang, and L. Wei, Transplantation of hypoxia-preconditioned mesenchymal stem cells improves infarcted heart function via enhanced survival of implanted cells and angiogenesis. *J Thorac Cardiovasc Surg*, 2008. **135**;4: 799-808.
128. Ohnishi, S., T. Yasuda, S. Kitamura, and N. Nagaya, Effect of hypoxia on gene expression of bone marrow-derived mesenchymal stem cells and mononuclear cells. *Stem Cells*, 2007. **25**;5: 1166-77.
129. Grayson, W.L., F. Zhao, B. Bunnell, and T. Ma, Hypoxia enhances proliferation and tissue formation of human mesenchymal stem cells. *Biochem Biophys Res Commun*, 2007. **358**;3: 948-53.
130. Li, Z., S. Bao, Q. Wu, H. Wang, C. Eyler, S. Sathornsumetee, et al., Hypoxia-inducible factors regulate tumorigenic capacity of glioma stem cells. *Cancer Cell*, 2009. **15**;6: 501-13.
131. Yoshida, Y., K. Takahashi, K. Okita, T. Ichisaka, and S. Yamanaka, Hypoxia enhances the generation of induced pluripotent stem cells. *Cell Stem Cell*, 2009. **5**;3: 237-41.
132. Theus, M.H., L. Wei, L. Cui, K. Francis, X. Hu, C. Keogh, and S.P. Yu, In vitro hypoxic preconditioning of embryonic stem cells as a strategy of promoting cell survival and functional benefits after transplantation into the ischemic rat brain. *Exp Neurol*, 2008. **210**;2: 656-70.
133. Bell, E., H.P. Ehrlich, D.J. Buttle, and T. Nakatsuji, Living tissue formed in vitro and accepted as skin-equivalent tissue of full thickness. *Science*, 1981. **211**;4486: 1052-4.

134. Bell, E., H. Moore, C. Mitchie, S. Sher, and H. Coon, Reconstruction of a thyroid gland equivalent from cells and matrix materials. *J Exp Zool*, 1984. **232**;2: 277-85.
135. Langer, R. and J.P. Vacanti, Tissue engineering. *Science*, 1993. **260**;5110: 920-6.
136. Vacanti, J.P. and R. Langer, Tissue engineering: the design and fabrication of living replacement devices for surgical reconstruction and transplantation. *Lancet*, 1999. **354 Suppl 1**: SI32-4.
137. Bell, E., ed. *Tissue Engineering in perspective*. 2000, Academic Press: NY.
138. Langer, R.S. and J.P. Vacanti, Tissue engineering: the challenges ahead. *Sci Am*, 1999. **280**;4: 86-9.
139. L'Heureux, N., S. Paquet, R. Labbe, L. Germain, and F.A. Auger, A completely biological tissue-engineered human blood vessel. *FASEB J*, 1998. **12**;1: 47-56.
140. L'Heureux, N., T.N. McAllister, and L.M. de la Fuente, Tissue-engineered blood vessel for adult arterial revascularization. *N Engl J Med*, 2007. **357**;14: 1451-3.
141. Du, Y., E. Lo, S. Ali, and A. Khademhosseini, Directed assembly of cell-laden microgels for fabrication of 3D tissue constructs. *Proc Natl Acad Sci U S A*, 2008. **105**;28: 9522-7.
142. McGuigan, A.P., B. Leung, and M.V. Sefton, Fabrication of cell-containing gel modules to assemble modular tissue-engineered constructs [corrected]. *Nat Protoc*, 2006. **1**;6: 2963-9.
143. McGuigan, A.P. and M.V. Sefton, Design and fabrication of sub-mm-sized modules containing encapsulated cells for modular tissue engineering. *Tissue Eng*, 2007. **13**;5: 1069-78.
144. McGuigan, A.P. and M.V. Sefton, Vascularized organoid engineered by modular assembly enables blood perfusion. *Proc Natl Acad Sci U S A*, 2006. **103**;31: 11461-6.
145. McGuigan, A.P. and M.V. Sefton, The thrombogenicity of human umbilical vein endothelial cell seeded collagen modules. *Biomaterials*, 2008. **29**;16: 2453-63.
146. Rosines, E., K. Johkura, X. Zhang, H.J. Schmidt, M. Decambre, K.T. Bush, and S.K. Nigam, Constructing kidney-like tissues from cells based on programs for organ development: toward a method of in vitro tissue engineering of the kidney. *Tissue Eng Part A*, 2010. **16**;8: 2441-55.
147. MacKay, S.M., A.J. Funke, D.A. Buffington, and H.D. Humes, Tissue engineering of a bioartificial renal tubule. *ASAIO J*, 1998. **44**;3: 179-83.

148. Ahsan, T. and R.M. Nerem, Fluid Shear Stress Promotes an Endothelial-Like Phenotype During the Early Differentiation of Embryonic Stem Cells. *Tissue Eng Part A*.
149. Nishikawa, S.I., S. Nishikawa, M. Hirashima, N. Matsuyoshi, and H. Kodama, Progressive lineage analysis by cell sorting and culture identifies FLK1+VE-cadherin+ cells at a diverging point of endothelial and hemopoietic lineages. *Development*, 1998. **125**;9: 1747-57.
150. Pfaffl, M.W., A new mathematical model for relative quantification in real-time RT-PCR. *Nucleic Acids Res*, 2001. **29**;9: e45.
151. Toh, Y.C. and J. Voldman, Fluid shear stress primes mouse embryonic stem cells for differentiation in a self-renewing environment via heparan sulfate proteoglycans transduction. *FASEB J*, 2011. **25**;4: 1208-17.
152. Sargent, C.Y., G.Y. Berguig, M.A. Kinney, L.A. Hiatt, R.L. Carpenedo, R.E. Berson, and T.C. McDevitt, Hydrodynamic modulation of embryonic stem cell differentiation by rotary orbital suspension culture. *Biotechnol Bioeng*, 2010. **105**;3: 611-26.
153. Fok, E.Y.L. and P.W. Zandstra, Shear-controlled single-step mouse embryonic stem cell expansion and embryoid body-based differentiation. *Stem Cells*, 2005. **23**;9: 1333-1342.
154. Niebruegge, S., A. Nehring, H. Bar, M. Schroeder, R. Zweigerdt, and J. Lehmann, Cardiomyocyte Production in Mass Suspension Culture: Embryonic Stem Cells as a Source for Great Amounts of Functional Cardiomyocytes. *Tissue Engineering Part A*, 2008. **14**;10: 1591-1601.
155. Discher, D.E., D.J. Mooney, and P.W. Zandstra, Growth factors, matrices, and forces combine and control stem cells. *Science*, 2009. **324**;5935: 1673-7.
156. Kennedy, M., S.L. D'Souza, M. Lynch-Kattman, S. Schwantz, and G. Keller, Development of the hemangioblast defines the onset of hematopoiesis in human ES cell differentiation cultures. *Blood*, 2007. **109**;7: 2679-87.
157. Medvinsky, A. and E. Dzierzak, Definitive hematopoiesis is autonomously initiated by the AGM region. *Cell*, 1996. **86**;6: 897-906.
158. Bautch, V.L., W.L. Stanford, R. Rapoport, S. Russell, R.S. Byrum, and T.A. Futch, Blood island formation in attached cultures of murine embryonic stem cells. *Developmental Dynamics*, 1996. **205**;1: 1-12.
159. Palis, J. and M.C. Yoder, Yolk-sac hematopoiesis: the first blood cells of mouse and man. *Exp Hematol*, 2001. **29**;8: 927-36.

160. Vischer, U.M., von Willebrand factor, endothelial dysfunction, and cardiovascular disease. *J Thromb Haemost*, 2006. **4**;6: 1186-93.
161. Nose, A. and M. Takeichi, A novel cadherin cell adhesion molecule: its expression patterns associated with implantation and organogenesis of mouse embryos. *J Cell Biol*, 1986. **103**;6 Pt 2: 2649-58.
162. Takeichi, M., Functional correlation between cell adhesive properties and some cell surface proteins. *J Cell Biol*, 1977. **75**;2 Pt 1: 464-74.
163. Weiss, P. and A.C. Taylor, Reconstitution of Complete Organs from Single-Cell Suspensions of Chick Embryos in Advanced Stages of Differentiation. *Proc Natl Acad Sci U S A*, 1960. **46**;9: 1177-85.
164. Lampugnani, M.G., M. Resnati, M. Raiteri, R. Pigott, A. Pisacane, G. Houen, et al., A novel endothelial-specific membrane protein is a marker of cell-cell contacts. *J Cell Biol*, 1992. **118**;6: 1511-22.
165. Gory-Faure, S., M.H. Prandini, H. Pointu, V. Roullot, I. Pignot-Paintrand, M. Vernet, and P. Huber, Role of vascular endothelial-cadherin in vascular morphogenesis. *Development*, 1999. **126**;10: 2093-102.
166. Breier, G., F. Breviario, L. Caveda, R. Berthier, H. Schnurch, U. Gotsch, et al., Molecular cloning and expression of murine vascular endothelial-cadherin in early stage development of cardiovascular system. *Blood*, 1996. **87**;2: 630-41.
167. Gerecht-Nir, S., S. Cohen, and J. Itskovitz-Eldor, Bioreactor cultivation enhances the efficiency of human embryoid body (hEB) formation and differentiation. *Biotechnol Bioeng*, 2004. **86**;5: 493-502.
168. Takeichi, M., T. Atsumi, C. Yoshida, K. Uno, and T.S. Okada, Selective adhesion of embryonal carcinoma cells and differentiated cells by Ca²⁺-dependent sites. *Dev Biol*, 1981. **87**;2: 340-50.
169. Duguay, D., R.A. Foty, and M.S. Steinberg, Cadherin-mediated cell adhesion and tissue segregation: qualitative and quantitative determinants. *Dev Biol*, 2003. **253**;2: 309-23.
170. Kawamoto, A., M. Ii, and T. Asahara, *Vascular Regeneration: Endothelial Progenitor Cell Therapy for Ischemic Diseases* *Regenerative Medicine*, G. Steinhoff, Editor. 2011, Springer Netherlands. p. 731-744.
171. Briguori, C., U. Testa, R. Riccioni, A. Colombo, E. Petrucci, G. Condorelli, et al., Correlations between progression of coronary artery disease and circulating endothelial progenitor cells. *FASEB J*, 2010. **24**;6: 1981-8.

172. Wang, H., G.M. Riha, S. Yan, M. Li, H. Chai, H. Yang, et al., Shear stress induces endothelial differentiation from a murine embryonic mesenchymal progenitor cell line. *Arterioscler Thromb Vasc Biol*, 2005. **25**;9: 1817-23.
173. Liersch, R., F. Nay, L. Lu, and M. Detmar, Induction of lymphatic endothelial cell differentiation in embryoid bodies. *Blood*, 2006. **107**;3: 1214-6.
174. Carpenedo, R.L., A.M. Bratt-Leal, R.A. Marklein, S.A. Seaman, N.J. Bowen, J.F. McDonald, and T.C. McDevitt, Homogeneous and organized differentiation within embryoid bodies induced by microsphere-mediated delivery of small molecules. *Biomaterials*, 2009. **30**;13: 2507-15.
175. Sachlos, E. and D.T. Auguste, Embryoid body morphology influences diffusive transport of inductive biochemicals: a strategy for stem cell differentiation. *Biomaterials*, 2008. **29**;34: 4471-80.
176. Tabata, Y., S. Hijikata, M. Muniruzzaman, and Y. Ikada, Neovascularization effect of biodegradable gelatin microspheres incorporating basic fibroblast growth factor. *J Biomater Sci Polym Ed*, 1999. **10**;1: 79-94.
177. Bratt-Leal, A.M., R.L. Carpenedo, M.D. Ungrin, P.W. Zandstra, and T.C. McDevitt, Incorporation of biomaterials in multicellular aggregates modulates pluripotent stem cell differentiation. *Biomaterials*, 2011. **32**;1: 48-56.
178. Patel, Z.S., H. Ueda, M. Yamamoto, Y. Tabata, and A.G. Mikos, In vitro and in vivo release of vascular endothelial growth factor from gelatin microparticles and biodegradable composite scaffolds. *Pharm Res*, 2008. **25**;10: 2370-8.
179. Mehta, G., C.M. Williams, L. Alvarez, M. Lesniewski, R.D. Kamm, and L.G. Griffith, Synergistic effects of tethered growth factors and adhesion ligands on DNA synthesis and function of primary hepatocytes cultured on soft synthetic hydrogels. *Biomaterials*, 2010. **31**;17: 4657-71.
180. Morgan, D.A., R. Class, G. Violetta, and G. Soslau, Cytokine mediated proliferation of cultured sea turtle blood cells: morphologic and functional comparison to human blood cells. *Tissue Cell*, 2009. **41**;4: 299-309.
181. Patel, Z.S., M. Yamamoto, H. Ueda, Y. Tabata, and A.G. Mikos, Biodegradable gelatin microparticles as delivery systems for the controlled release of bone morphogenetic protein-2. *Acta Biomater*, 2008. **4**;5: 1126-38.
182. Link, D.P., J. van den Dolder, J.J. van den Beucken, J.G. Wolke, A.G. Mikos, and J.A. Jansen, Bone response and mechanical strength of rabbit femoral defects filled with injectable CaP cements containing TGF-beta 1 loaded gelatin microparticles. *Biomaterials*, 2008. **29**;6: 675-82.
183. Park, H., J.S. Temenoff, Y. Tabata, A.I. Caplan, R.M. Raphael, J.A. Jansen, and A.G. Mikos, Effect of dual growth factor delivery on chondrogenic differentiation

- of rabbit marrow mesenchymal stem cells encapsulated in injectable hydrogel composites. *J Biomed Mater Res A*, 2009. **88**;4: 889-97.
184. Fatma, S., D.E. Selby, R.D. Singla, and D.K. Singla, Factors Released from Embryonic Stem Cells Stimulate c-kit-FLK-1(+ve) Progenitor Cells and Enhance Neovascularization. *Antioxid Redox Signal*, 2010. **13**;12: 1857-65.
 185. Singla, D.K., R.D. Singla, and D.E. McDonald, Factors released from embryonic stem cells inhibit apoptosis in H9c2 cells through PI3K/Akt but not ERK pathway. *Am J Physiol Heart Circ Physiol*, 2008. **295**;2: H907-13.
 186. Singla, D.K., R.D. Singla, S. Lamm, and C. Glass, TGF-beta2 treatment enhances cytoprotective factors released from embryonic stem cells and inhibits apoptosis in infarcted myocardium. *Am J Physiol Heart Circ Physiol*, 2011. **300**;4: H1442-50.
 187. Fujita, D., A. Tanabe, T. Sekijima, H. Soen, K. Narahara, Y. Yamashita, et al., Role of extracellular signal-regulated kinase and AKT cascades in regulating hypoxia-induced angiogenic factors produced by a trophoblast-derived cell line. *J Endocrinol*, 2010. **206**;1: 131-40.
 188. Niebruegge, S., A. Nehring, H. Bar, M. Schroeder, R. Zweigerdt, and J. Lehmann, Cardiomyocyte production in mass suspension culture: embryonic stem cells as a source for great amounts of functional cardiomyocytes. *Tissue Eng Part A*, 2008. **14**;10: 1591-601.
 189. Shin, J.M., J. Kim, H.E. Kim, M.J. Lee, K.I. Lee, E.G. Yoo, et al., Enhancement of differentiation efficiency of hESCs into vascular lineage cells in hypoxia via a paracrine mechanism. *Stem Cell Res*, 2011. **7**;3: 173-85.
 190. Lian Jin, H., W.A. Pennant, M. Hyung Lee, S. Su, H. Ah Kim, M. Lu Liu, et al., Neural stem cells modified by a hypoxia-inducible VEGF gene expression system improve cell viability under hypoxic conditions and spinal cord injury. *Spine (Phila Pa 1976)*, 2011. **36**;11: 857-64.
 191. Cameron, C.M., F. Harding, W.S. Hu, and D.S. Kaufman, Activation of hypoxic response in human embryonic stem cell-derived embryoid bodies. *Exp Biol Med (Maywood)*, 2008. **233**;8: 1044-57.
 192. Niebruegge, S., C.L. Bauwens, R. Peerani, N. Thavandiran, S. Masse, E. Sevaptisidis, et al., Generation of human embryonic stem cell-derived mesoderm and cardiac cells using size-specified aggregates in an oxygen-controlled bioreactor. *Biotechnol Bioeng*, 2009. **102**;2: 493-507.
 193. Wang, G.L., B.H. Jiang, E.A. Rue, and G.L. Semenza, Hypoxia-inducible factor 1 is a basic-helix-loop-helix-PAS heterodimer regulated by cellular O₂ tension. *Proc Natl Acad Sci U S A*, 1995. **92**;12: 5510-4.

194. Wang, G.L. and G.L. Semenza, Characterization of hypoxia-inducible factor 1 and regulation of DNA binding activity by hypoxia. *J Biol Chem*, 1993. **268**;29: 21513-8.
195. Smith, T.G., P.A. Robbins, and P.J. Ratcliffe, The human side of hypoxia-inducible factor. *Br J Haematol*, 2008. **141**;3: 325-34.
196. Wartenberg, M., F. Donmez, F.C. Ling, H. Acker, J. Hescheler, and H. Sauer, Tumor-induced angiogenesis studied in confrontation cultures of multicellular tumor spheroids and embryoid bodies grown from pluripotent embryonic stem cells. *FASEB J*, 2001. **15**;6: 995-1005.
197. Gassmann, M., J. Fandrey, S. Bichet, M. Wartenberg, H.H. Marti, C. Bauer, et al., Oxygen supply and oxygen-dependent gene expression in differentiating embryonic stem cells. *Proc Natl Acad Sci U S A*, 1996. **93**;7: 2867-72.
198. Mohr, J.C., J. Zhang, S.M. Azarin, A.G. Soerens, J.J. de Pablo, J.A. Thomson, et al., The microwell control of embryoid body size in order to regulate cardiac differentiation of human embryonic stem cells. *Biomaterials*, 2010. **31**;7: 1885-93.
199. Ungrin, M.D., C. Joshi, A. Nica, C. Bauwens, and P.W. Zandstra, Reproducible, ultra high-throughput formation of multicellular organization from single cell suspension-derived human embryonic stem cell aggregates. *PLoS One*, 2008. **3**;2: e1565.
200. Ng, E.S., R.P. Davis, L. Azzola, E.G. Stanley, and A.G. Elefanty, Forced aggregation of defined numbers of human embryonic stem cells into embryoid bodies fosters robust, reproducible hematopoietic differentiation. *Blood*, 2005. **106**;5: 1601-3.
201. Bauwens, C.L., R. Peerani, S. Niebruegge, K.A. Woodhouse, E. Kumacheva, M. Husain, and P.W. Zandstra, Control of human embryonic stem cell colony and aggregate size heterogeneity influences differentiation trajectories. *Stem Cells*, 2008. **26**;9: 2300-10.
202. Okuda, Y., K. Tsurumaru, S. Suzuki, T. Miyauchi, M. Asano, Y. Hong, et al., Hypoxia and endothelin-1 induce VEGF production in human vascular smooth muscle cells. *Life Sci*, 1998. **63**;6: 477-84.
203. Wang, Y.Q., J.M. Luk, K. Ikeda, K. Man, A.C. Chu, K. Kaneda, and S.T. Fan, Regulatory role of vHL/HIF-1 α in hypoxia-induced VEGF production in hepatic stellate cells. *Biochem Biophys Res Commun*, 2004. **317**;2: 358-62.
204. Steinbrech, D.S., B.J. Mehrara, D. Chau, N.M. Rowe, G. Chin, T. Lee, et al., Hypoxia upregulates VEGF production in keloid fibroblasts. *Ann Plast Surg*, 1999. **42**;5: 514-9; discussion 519-20.

205. Isogai, S., N.D. Lawson, S. Torrealday, M. Horiguchi, and B.M. Weinstein, Angiogenic network formation in the developing vertebrate trunk. *Development*, 2003. **130**;21: 5281-90.
206. Toh, Y.C., K. Blagovic, H. Yu, and J. Voldman, Spatially organized in vitro models instruct asymmetric stem cell differentiation. *Integr Biol (Camb)*, 2011.
207. Engler, A.J., M.A. Griffin, S. Sen, C.G. Bonnemann, H.L. Sweeney, and D.E. Discher, Myotubes differentiate optimally on substrates with tissue-like stiffness: pathological implications for soft or stiff microenvironments. *J Cell Biol*, 2004. **166**;6: 877-87.
208. Engler, A.J., S. Sen, H.L. Sweeney, and D.E. Discher, Matrix elasticity directs stem cell lineage specification. *Cell*, 2006. **126**;4: 677-89.
209. Evans, N.D., C. Minelli, E. Gentleman, V. LaPointe, S.N. Patankar, M. Kallivretaki, et al., Substrate stiffness affects early differentiation events in embryonic stem cells. *Eur Cell Mater*, 2009. **18**: 1-13; discussion 13-4.
210. Even-Ram, S., V. Artym, and K.M. Yamada, Matrix control of stem cell fate. *Cell*, 2006. **126**;4: 645-7.
211. Wang, Y.L. and R.J. Pelham, Jr., Preparation of a flexible, porous polyacrylamide substrate for mechanical studies of cultured cells. *Methods Enzymol*, 1998. **298**: 489-96.
212. Roth, E.A., T. Xu, M. Das, C. Gregory, J.J. Hickman, and T. Boland, Inkjet printing for high-throughput cell patterning. *Biomaterials*, 2004. **25**;17: 3707-15.
213. Shimizu, N., K. Yamamoto, S. Obi, S. Kumagaya, T. Masumura, Y. Shimano, et al., Cyclic strain induces mouse embryonic stem cell differentiation into vascular smooth muscle cells by activating PDGF receptor beta. *J Appl Physiol*, 2008. **104**;3: 766-72.
214. Sucosky, P., D.F. Osorio, J.B. Brown, and G.P. Neitzel, Fluid mechanics of a spinner-flask bioreactor. *Biotechnol Bioeng*, 2004. **85**;1: 34-46.
215. Toh, Y.C., C. Zhang, J. Zhang, Y.M. Khong, S. Chang, V.D. Samper, et al., A novel 3D mammalian cell perfusion-culture system in microfluidic channels. *Lab Chip*, 2007. **7**;3: 302-9.
216. Ong, S.M., C. Zhang, Y.C. Toh, S.H. Kim, H.L. Foo, C.H. Tan, et al., A gel-free 3D microfluidic cell culture system. *Biomaterials*, 2008. **29**;22: 3237-44.
217. Takeichi, M., Cadherins: key molecules for selective cell-cell adhesion. *IARC Sci Publ*, 1988;92: 76-9.

218. Bratt-Leal, A.M., R.L. Carpenedo, and T.C. McDevitt, Engineering the embryoid body microenvironment to direct embryonic stem cell differentiation. *Biotechnol Prog*, 2009. **25**;1: 43-51.
219. Cohen, T., H. Gitay-Goren, R. Sharon, M. Shibuya, R. Halaban, B.Z. Levi, and G. Neufeld, VEGF121, a vascular endothelial growth factor (VEGF) isoform lacking heparin binding ability, requires cell-surface heparan sulfates for efficient binding to the VEGF receptors of human melanoma cells. *J Biol Chem*, 1995. **270**;19: 11322-6.
220. Galambos, C., Y.S. Ng, A. Ali, A. Noguchi, S. Lovejoy, P.A. D'Amore, and D.E. DeMello, Defective pulmonary development in the absence of heparin-binding vascular endothelial growth factor isoforms. *Am J Respir Cell Mol Biol*, 2002. **27**;2: 194-203.
221. Dougher, A.M., H. Wasserstrom, L. Torley, L. Shridaran, P. Westdock, R.E. Hileman, et al., Identification of a heparin binding peptide on the extracellular domain of the KDR VEGF receptor. *Growth Factors*, 1997. **14**;4: 257-68.
222. Ito, N. and L. Claesson-Welsh, Dual effects of heparin on VEGF binding to VEGF receptor-1 and transduction of biological responses. *Angiogenesis*, 1999. **3**;2: 159-66.
223. Holbeck, S.L., J.M. Collins, and J.H. Doroshow, Analysis of Food and Drug Administration-approved anticancer agents in the NCI60 panel of human tumor cell lines. *Mol Cancer Ther*, 2010. **9**;5: 1451-60.
224. Sharma, S.V., D.A. Haber, and J. Settleman, Cell line-based platforms to evaluate the therapeutic efficacy of candidate anticancer agents. *Nat Rev Cancer*, 2010. **10**;4: 241-53.
225. Ginis, I., Y. Luo, T. Miura, S. Thies, R. Brandenberger, S. Gerecht-Nir, et al., Differences between human and mouse embryonic stem cells. *Dev Biol*, 2004. **269**;2: 360-80.
226. Greber, B., G. Wu, C. Bernemann, J.Y. Joo, D.W. Han, K. Ko, et al., Conserved and divergent roles of FGF signaling in mouse epiblast stem cells and human embryonic stem cells. *Cell Stem Cell*, 2010. **6**;3: 215-26.
227. Xie, C.Q., Y. Jeong, M. Fu, A.L. Bookout, M.T. Garcia-Barrio, T. Sun, et al., Expression profiling of nuclear receptors in human and mouse embryonic stem cells. *Mol Endocrinol*, 2009. **23**;5: 724-33.
228. Villa-Diaz, L.G., Y.S. Torisawa, T. Uchida, J. Ding, N.C. Nogueira-de-Souza, K.S. O'Shea, et al., Microfluidic culture of single human embryonic stem cell colonies. *Lab Chip*, 2009. **9**;12: 1749-55.

229. Yirme, G., M. Amit, I. Laevsky, S. Osenberg, and J. Itskovitz-Eldor, Establishing a dynamic process for the formation, propagation, and differentiation of human embryoid bodies. *Stem Cells Dev*, 2008. **17**;6: 1227-41.